Earth-Science Reviews 237 (2023) 104331

Contents lists available at ScienceDirect

Earth-Science Reviews

journal homepage: www.elsevier.com/locate/earscirev

Basic structural geology of Venus: A review of the gaps and how to bridge them

Simon Hanmer *

42 Bower St, Ottawa, Ontario K1S 0K3, Canada

ARTICLE INFO

Keywords:
Venus
Structural geology
Inner solar system
Extension
Shortening
Strike slip
Shear zones

ABSTRACT

The next decade will see new geological mapping of the surface of Venus spurred by multiple new science missions. Planetary scientists must be cognisant of gaps in our understanding of the geology of the second planet in order to plan and maximise the scientific value of these new missions. While our current knowledge of major aspects of volcanology and broad-scale tectonic features on Venus is reasonably advanced, within the limitations of available data. However, the same cannot be said of the basic structural geology of venusian extensional and shortening, and strike-slip features. Published interpretations of distributed extensional tectonic features on Venus do not account for the absence of associated regional strain localisation. Models of shortening tectonic features on Venus are based on structural geological analogies with potentially similar features elsewhere in the inner Solar System. However, the purported analogues on Mercury, Mars and the Moon, as well as commonly invoked terrestrial analogues, have their own issues, which have not been acknowledged or treated in the literature. In addition, empirical application of terrestrial map patterns as analogues for identifying and analysing strike-slip shearing on Venus has not taken account of the established Earth-based determinants of crustal-scale shear zone development. Application of the current state of basic structural geology on Venus to provide constraints on models of planet-scale tectonic behaviour, and their potential extension to the early Earth, is premature. Accordingly, it is both appropriate and timely to critically review the current state of basic structural geological understanding of Venus, with reference to the inner Solar System as a whole. Strategies are proposed for addressing some of the fundamental gaps in our understanding of the basic structural geology of Venus using both analogue modelling and currently available remotely-sensed data while awaiting the results of the planned new science missions in the mid-2030s.

1. Introduction

The next decade will see multiple new science missions sent to Venus, some of which will include mandates to map the planetary surface.[1] Maximising the scientific returns for such mandates will require that planetary scientists[2] be cognisant of gaps in our understanding of the geology of the second planet. Our current knowledge of major aspects of volcanology and broad-scale tectonic features on Venus is reasonably advanced, within the limitations of the Magellan mission data (e.g. Ernst et al., 1995, 2001, 2003, 2007; Ivanov and Head, 2011, 2013, 2015, and references therein). However, the same cannot be said of basic venusian structural geology (distributed shortening and extension, plus shearing; e.g. Hanmer, 2020). Nonetheless, models of the global planetary structure and tectonic behaviour of Venus have been proposed, based on basic structural geological observations and interpretations derived from 1990 to 1994 vintage Magellan data[3] (e.g. Ford et al., 1993; Sandwell et al., 1997; Bilotti and Suppe, 1999; Hansen, 2006; Byrne et al., 2021), with hypothetical implications for the tectonic behaviour of Earth's early lithosphere (e.g. Hansen, 2007, 2018; Harris and Bédard, 2014a, 2014b; Byrne et al., 2021).

The basic structural geology of Venus addressed in this contribution refers to simple, regularly- to periodically-spaced, extensional and

* Corresponding author.
E-mail address: simon.hanmer@bell.net.

[1] https://www.nasa.gov/feature/goddard/2021/nasa-to-explore-divergent-fate-of-earth-s-mysterious-twin-with-goddard-s-davinci; https://www.esa.int/Science_Exploration/Space_Science/ESA_selects_revolutionary_Venus_mission_EnVision

[2] All references in this contribution to planetary science, planetary scientists and the planetary science community are limited to the inner Solar System.

[3] https://solarsystem.nasa.gov/magellan/

https://doi.org/10.1016/j.earscirev.2023.104331
Received 20 October 2022; Received in revised form 18 January 2023; Accepted 18 January 2023
Available online 24 January 2023

shortening tectonic features, and to purported crustal-scale strike-slip shear zones. Graben, folds and thrust/reverse faults, distributed over vast regional- to planet-scale areas, each have their own specific structural geological issues. First, distributed xtensional features show a noteable absence of regional-scale strain localisation, apparently specific to Venus (see Hanmer, 2020). Second, distributed shortening features have been interpreted based on proposed analogues elsewhere in the inner Solar System (e.g. Squyres et al., 1992; McGill, 1993; Kreslavsky and Basilevsky, 1998; Bilotti and Suppe, 1999; Ghail, 2002; Young and Hansen, 2005; see also Supplemental 1). However, the application of purportedly analogous features on Mercury, Mars and the Moon, as well as commonly invoked terrestrial analogues, has its own issues that have not been generally acknowledged or treated in the literature. Third, the purported crustal-scale strike-slip shear zones reported for Venus were identified and interpreted by analogies drawn with terrestrial examples (e.g. Koenig and Aydin, 1998; Kumar, 2005; Romeo et al., 2005; Fernández et al., 2010). Furthermore, some have been extrapolated to support of a model of planet-scale, semi-mobile *"jostling"* lid tectonics, with hypothetical implications for the tectonic behaviour of Earth's early lithosphere (Byrne et al., 2021). However, consideration of well-established Earth-based determinants of shear zone development calls into question the very existence of the proposed crustal-scale strike-slip features on Venus.

This paper will address these gaps in our understanding of the basic structural geology of Venus. After a brief summary of the principal structural and tectonic features of the second planet (Section 2):

- Sections 3 through 5 examine gaps in our structural geological understanding of distributed extensional and shortening features, in that order, with emphasis on the local scale. Previous studies of shortening features commonly invoked analogies with potentially similar features elsewhere in the inner Solar System. Hence, it is necessary to include an examination of the basic structural geology of Mercury, Mars and the Moon here.
- Sections 3.3 and 6 extend the examination of distributed extensional and shortening features to the regional and planet scales, and address issues related to stress transmission and the absence of strain localisation at such scales.
- Section 7 is a critical review of the terrestrial analogues that have been commonly invoked in the literature to support interpretation of shortening features throughout the inner Solar System, and thereby on Venus.
- Section 8 presents an brief overview of the established determinants of shear zone development in general, and critically reviews the published reports of crustal-scale strike-slip shear zones specific to Venus.
- Section 9, the Discussion, includes suggestions for future studies of the basic structural geology of Venus.
- An Appendix critically reviews reported relationships between structural features and impact craters that are commonly used to identify and analyse thrust/reverse faults throughout the inner Solar System, with implications for analogues invoked for Venus.

2. Venus

There are multiple observational hurdles specific to Venus. Given that it is shrouded by an opaque atmosphere, its surface cannot be observed optically, and the available Magellan mission radar data are not of the resolution of data from the more recent orbital missions to Mercury,[4] Mars[5] and the Moon.[6] Most importantly, interpreting radar images is very different from visible light imagery. The reflection of the outgoing signal is principally a function of the angle of incidence, and of surface roughness down to the sub-metre scale (e.g. Solomon et al., 1991; Suppe and Connors, 1992; Ford et al., 1993; Hansen and Willis, 1996; Pettengill et al., 1997; Ghent and Hansen, 1999).Note that the early geological history of the planet is apparently not preserved. Impact crater statistics point to a volcanic resurfacing (catastrophic or progressive) of the planet, potentially during the past ~1 Ga, that has veiled the preceding ~3.6 Ga of geological history (Basilevsky and Head, 1998; Hansen and Young, 2007; Hansen and López, 2010, 2018; Bjonnes et al., 2012; Romeo, 2013; Kreslavsky et al., 2015; Ivanov and Head, 2015).

Ivanov and Head (2015) recognised five tectonized units, mostly unique to Venus. These were generally interpreted in terms of extension or shortening and, in some cases, potentially modified by contemporaneous or later shearing. In relative chronological order, they are (i) tessera terrains (7.3% of the planetary surface), (ii) lineated plains (1.6%), (iii) ridged plains and ridge belts (2.4%), (iv) fracture belts (also called groove belts; 8.1%) and (v) rift zones (5.0%), for a total of ~20% of the planetary surface. Vast areas of the rest of the planet are characterised by (vi) a variety of extensive, younger, regional volcanic plains that also display tectonic features related to extension, shortening and purported strike-slip shearing. These volcanic plains, likely basaltic in composition (e.g. Solomon et al., 1991, 1992; Squyres et al., 1992; Basilevsky and Head, 1998, 2003; DeShon et al., 2000; Ivanov and Head, 2011, 2013), surround and embay inliers of *"tessera terrain";* i.e. relatively high-standing, potentially cratonic plateaux whose origins and evolution are poorly understood (e.g. Bindschadler and Head, 1991; Ivanov and Head, 1996, 2011, 2015; Hansen and Willis, 1996, 1998; Hansen, 2006, 2018; Gilmore and Head, 2018; Hanmer, 2020 and references therein; see Supplemental 1 for mapping references; Fig. 1a). The basic distributed extensional and shortening tectonic features that deform or comprise units i-iv and vi, and the purported crustal-scale strike-slip shear zones generally associated with either the margins of tessera terrains or with regional-scale "deformation belts" (ridge and fracture belts) that deform units iii-iv and vi, are the principal subject of this contribution.

Other, more complex features, also apparently unique to Venus, include (a) the ~2000 km diameter Artemis Corona structure (see Fig. 1a for location), variously interpreted by Spencer (2001) and Hansen and Olive (2010); (b) an equatorial, planetary-scale rift complex (e.g. Hansen, 2018; Hansen and López, 2018; Ivanov and Head, 2015) with associated novae, arachnoids and coronae of various geometries, generally interpreted as magmato-diapiric in origin (e.g Jurdy and Stoddard, 2007; Ivanov and Head, 2010; McGill et al., 2010; Gerya, 2014; Piskorz et al., 2014, and references in these papers. However, see Hamilton (2005, 2019) for an exogenic perspective; and (c) giant, commonly radiating, dyke swarms (Ernst et al., 1995, 2001, 2003, 2007; Studd et al., 2011), all of whose analysis is better undertaken from a tectonic rather than a structural geological perspective (e.g. Ivanov and Head, 2015; Hansen, 2018). These latter features are beyond the purview of the present contribution. Similarly, the Maxwell Mountains and associated structural features adjacent to Lakshmi Planum (see Fig. 1a for location), themselves a unique occurrence on Venus (e.g. Head, 1990; Vorder Bruegge et al., 1990; Solomon et al., 1991; Suppe and Connors, 1992; Keep and Hansen, 1994; Harris and Bédard, 2014a, 2014b), will not be considered here.

Ivanov and Head (2011, 2015) presented detailed observations to justify a time-relative stratigraphic context, calibrated in terms of fractions of the mean surface model age (T) as opposed to absolute years (Fig. 1b), that placed the deformation of tectonized units i-iv in a Global Tectonic Regime during the Fortunian and early Guineverian periods (however, see DeShon et al., 2000 for a dissenting, *"non-directional"* view). Within their global stratigraphy (Ivanov and Head, 2015, their figs. 1 and 19; Fig. 1b), complex deformation of the tessera terrains during the Fortunian Period broadly preceded the formation and extensional deformation of the lineated plains. Together these events broadly preceded a pulse of ridge belt formation (shortening), that

[4] https://www.nasa.gov/mission_pages/messenger/main/index.html
[5] https://www.nasa.gov/mission_pages/MRO/main/index.html
[6] https://www.nasa.gov/mission_pages/LRO/main/index.html

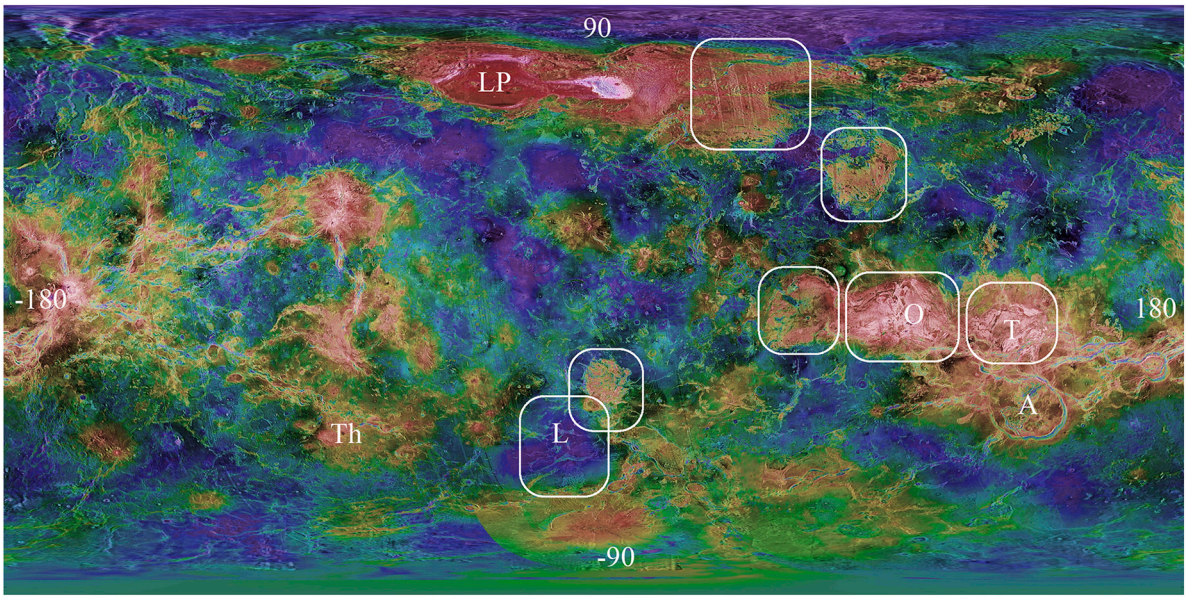

A

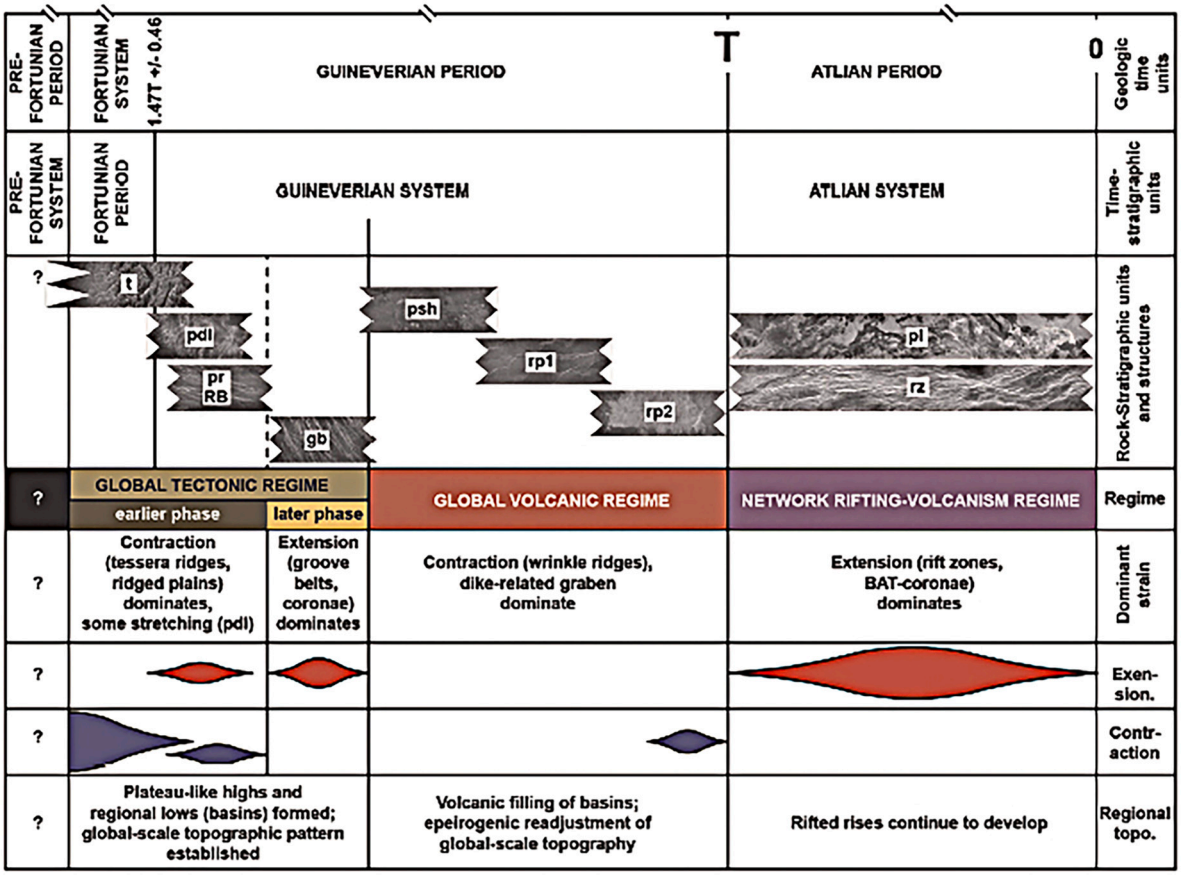

B

Fig. 1. Space and relative time on Venus. (A) Key locations on Venus cited in the text, plotted on a base provided by https://astrogeology.usgs.gov/search/map/Venus/Magellan/RadarProperties/Colorized/ Venus_Magellan_C3-MDIR_ClrTopo_Global_Mosaic_6600m (Magellan Team: Ford et al. (1993). A: Artemis Corona; LP: Lakshmi Planum; O: Ovda Regio; T: Thetis Regio; Th: Themis Regio. Maxwell Mountains are the white patch just east of Lakshmi Planum. White boxes indicate principal tessera terrains and Lavinia Planitia (L). (B) Global correlation chart for Venus. T is the mean model age of the surface and separates the Guineverian and Atlian periods. Fig. 19 in Ivanov and Head (2015). With permission from Planetary and Space Science.

preceded the formation of fracture belts (extension). The sequence tessera through fracture belts generally pre-dates the major episodes of volcanic plains formation (unit vi) that occurred during a Global Volcanic Regime of the late Guineverian Period. The volcanic plains were then deformed by dyke-related graben (extension), wrinkle ridges (shortening) and purported crustal-scale strike-slip shearing, as well as planetary-scale rift zones and magmato-diapiric features (Ivanov and Head, 2015, their fig. 19). Note that wrinkle ridges are found ubiquitously on Venus and in most post-tessera regional volcanic plains units (e.g. McGill, 1993; McGill et al., 2010). According to Ivanov and Head

(2015) *"The majority of tectonized terrains … are the products of tectonic resurfacing and are embayed by the vast volcanic plains and, thus, are older … These tectonized terrains … define a tectonically dominated regime of resurfacing that occurred at a global-scale near the beginning of the observable geological history of Venus"*. In other words, the venusian surface was modified by both structural and volcanic processes, with the former dominant during an early Global Tectonic Regime and the latter dominant during a later Global Volcanic Regime.

3. Distributed extensional tectonic features on Venus

On Venus, distributed extensional deformation has been extensively reported from tessera terrains and lineated plains, occurring as individual graben, plus generic linear features, commonly interpreted as extension fractures or normal faults (see Supplemental 1). They rarely occur in isolation. Rather, they tend to form regional-scale patterns covering large swaths of the planetary surface. Elsewhere on the vast venusian volcanic plains, the geometry of these patterns ranges from linear, to radial, to circumferential. Radial and circumferential patterns have been extensively studied on Venus, as well as on Mars and Earth, where they are attributed to large-scale tectonics associated with mantle plumes and lithospheric rifting (e.g. Ernst et al., 1995, 2001, 2003, 2007; Studd et al., 2011; Graff et al., 2018; Buchan and Ernst, 2019, and references in these papers). However, spatially extensive, penetrative, *linear* patterns of extensional features on Venus, sometimes referred to as *"ribbons"* or *"ribbon fabrics"*, are not well-understood (Hanmer, 2020 and references therein). They have been mapped as distributed patterns developed on the order of 1000 km or more, both along and across strike. In addition, they are penetrative down to the resolution of the remote imaging, without regional-scale strain localisation (Hanmer, 2020; see also Supplemental 1).

Individual graben were identified based observation of symmetrical, inward-facing, uniformly spaced pairs of inward dipping, planar slopes, assumed to be normal faults (e.g. Solomon et al., 1991, their figs. 13 and 24c; Solomon et al., 1992, their figs. 13, 14, 23 and 24; Squyres et al., 1992, their fig. 6; see also Stofan et al., 1993). However, other authors have empirically inferred extension across generic lineaments, interpreted as simple fractures on the basis of their morphology (e.g. Bindschadler et al., 1992; Banerdt and Sammis, 1992, their figs. 1, 2, 3 and 5; Banerdt et al., 1997, their fig. 8). As an example, for DeShon et al. (2000) a *"Lack of shear displacement along the fractures and consistent straight (i.e. non-undulating) fracture boundaries indicate*[s] *that the fractures are likely extension fractures"*. On off-world bodies across the inner Solar System, studies generally present such graben as the product of far-field tectonic extension by tensile fracture or, more commonly, normal faulting, in a single plate planetary context. In the case of individual graben this is may be a reasonable, first-order interpretation. However, graben and normal faulting on Venus have commonly been reported as comprising regional- and planetary-scale patterns (or fabrics) of distributed features (see Supplemental 1). In what follows I briefly review these areally extensive patterns in tessera terrains and volcanic plains.

3.1. Tessera terrains

Extensive, distributed, penetratively developed linear features (*"ribbons"* or *"ribbon fabrics"*) in tessera terrains on Venus have been consistently interpreted as graben (e.g. Ivanov and Head, 2015, their figs. 5 and 7; Hanmer, 2020 and references therein). According to Bindschadler et al. (1992), *"Most of the scarps are paired, forming grabens, but single, NW striking scarps, interpreted to be normal faults, also occur … The graben-like morphology of these features is a strong indication that they are extensional"*. Ribbons have beendescribed in detail by Hansen and Willis, 1996, 1998; Ghent and Hansen, 1999; Hansen et al., 2000) as periodic, uniformly close-spaced (2–6 km), pervasive, shallow (<1 km), narrow troughs, up to several kilometres wide by hundreds of kilometres long, with aspect ratios of 50–100+, bounded by symmetrical, opposite-facing, steeply dipping walls. They proposed that these features resulted from either dilated tensile fracturing (joint model), or from pairs of extensional normal faults (graben model). Because they considered that the normal faults in the graben model dipped at 75–90°, Hansen and Willis (1996) concluded that *"Dips of 75–90° are not consistent with classic fault theory … which predicts normal faults of ~60°, although steeper fault angles may result under near-surface transitional-tensile failure conditions or due to pre-existing weaknesses"*.

While Hansen and Willis (1996, 1998) locally favoured the joint model, they recognised a fundamental weakness in the argument: *"Pervasive formation of narrow ribbons across large areas, with extremely long aspect ratios and consistent width of individual ribbons, is most easily explained in a flat homogeneous layer - stress, and strain heterogeneities … would almost certainly preclude the formation of parallel ribbon structure over large areas"*. Although Hansen and Willis (1996) were specifically referring to the issue of the relative timing of associated folding, Hansen and Willis (1998) were well aware that this statement applies to any jointing scenario: *"… the crust must be virtually intact with few, if any, pre-existing fractures"*. Moreover, they stated that *"… it seems highly unlikely that tensile fractures could form over areas of hundreds of thousands of square kilometers on Venus, and yet they seem to have done just that"*. Seeking a solution to this apparent paradox, Hansen and Willis (1998) asked *"What if a region of Venus was somehow mechanically annealed of all, or essentially all, preexisting fractures prior to ribbon terrain formation?"*, as well as any form of mechanical layering (anisotropy) within the tessera crust. Although their wording was ambiguous (see Gilmore et al., 1998), Hansen and Willis (1998) clearly intended that such annealing would have been a thermal process (see also Hansen et al., 2000), which eventually led to formulation of a bolide-driven lava pond hypothesis for the "resetting" of the mechanical properties of tessera terrain crust (Hansen, 2006), that they also proposed applied to early Earth (Hansen, 2006, 2007, 2018; see Hanmer, 2020 for a detailed critical review).

The tensile fracture (joint) and paired normal fault (graben) models formulated for tessera terrains have both been used to place limits on the thickness (~1 km or less) of the contemporary rigid planetary crust in which they had formed, by invoking the classical boudinage model (e.g. Hansen and Willis, 1998; Ghent and Hansen, 1999; see critical review in Hanmer, 2020). Others took a different approach to the same question: *"To estimate the geometry of the troughs in this study, we assume an idealized graben, where both faults meet at a common depth … we assume that this depth is a mechanical discontinuity"* (Gilmore et al., 1998). Based on these assumptions, these authors derived depth to a very shallow brittle-ductile transition and estimated the upper lithospheric thermal structure of the planet at the time of graben formation.

3.2. Lineated and regional volcanic plains

Extensive volcanic plains on Venus are decorated by linear fabrics that present as distributed, periodically-spaced, penetratively developed, parallel lineaments. Ivanov and Head (2015, their figs. 1b, and 18 c, d) estimated that *"Densely lineated plains usually occur as small (tens to a few hundreds of kilometers across) outcrops, the surface of which is above the surrounding volcanic plains …* [and] *sometimes occur in groups where orientation of the lineaments is approximately the same. The groups of the densely lineated plains occurrences are a few thousands of kilometers across"*. According to these authors, *"The tectonic structures of densely lineated plains almost completely erase the original morphologic characteristics of the underlying* materials" (see also Ivanov and Head, 2011, their figs. 2b and 6). However, Ivanov and Head (2011, 2015) did not advance a generally applicable explanation for their proposed tectonic erasure. The distributed lineament patterns have been interpreted as uniform, parallel, penetrative graben, penecontemporaneous with regional volcanism in the early Guineverian lineated and Late Guineverian regional volcanic plains, over areas on the scale of 10,000 km^2 (Solomon et al., 1991, 1992). The distributed lineaments were described by

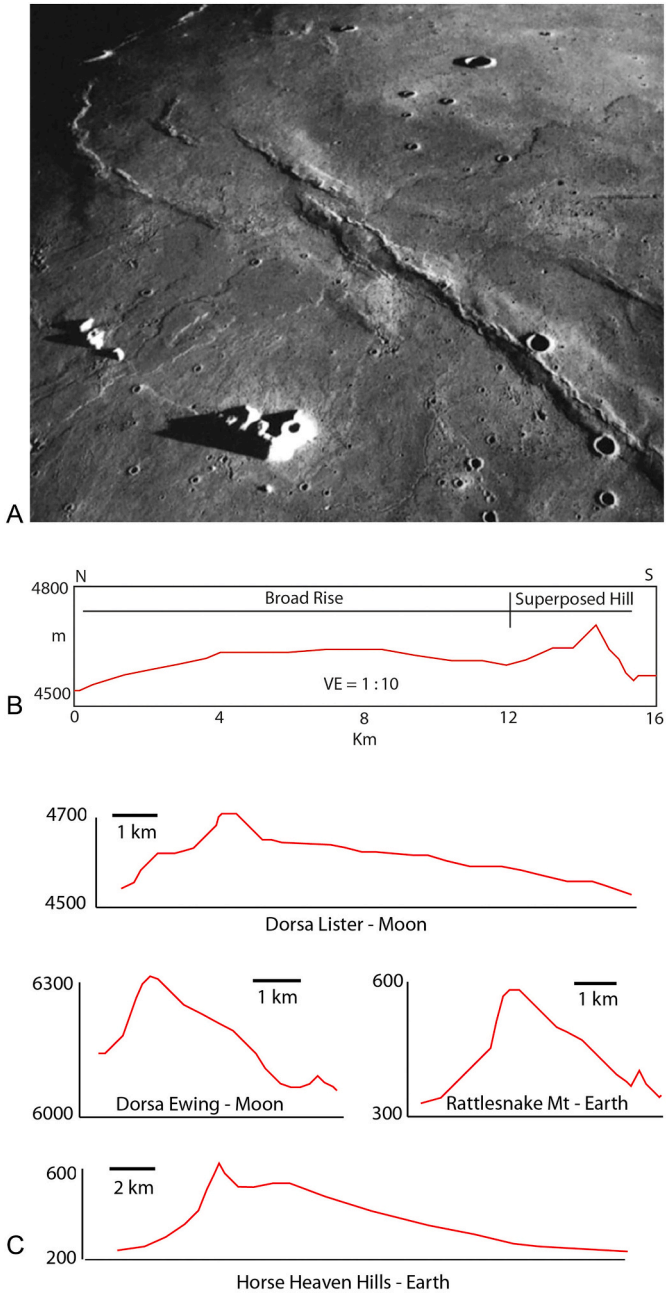

Fig. 2. Wrinkle ridges. (A) Wrinkle ridges in the southwestern part of Mare Imbrium on the Moon. Note that the ridges deform pre-existing flows, implying a structural origin. Field of view is ~400 km across; north is at the top of the figure. Fig. 1 in Plescia and Golombek (1986). With permission from the Geological Society of America. (B) Surface elevation profile across wrinkle ridge Dorsa Lister on the Moon highlighting the broad rise and superposed ridge (hill). Redrawn from fig. 1b in Golombek et al. (1991). (C) Topographic profiles across wrinkle ridges with arches on the Moon and analogous structures on the Columbia Plateau. Vertical scales are in meters. Redrawn from fig. 3 in Watters (1988). Discussed in the text.

Solomon et al. (1991, 1992) as straight, 100–500+ km long, <75 m wide, and periodic with a 1–2.5 km spacing, and were interpreted as representing widespread, modest extensional strain (Solomon et al., 1991, 1992; Squyres et al., 1992; Banerdt and Sammis, 1992; Banerdt et al., 1997, their fig. 8). Isolated, purportedly extensional lineaments were referred to as "grooves" (Squyres et al., 1992, their fig. 6).

Extensive sets of penetratively developed straight lineaments on Venus were described as tensile fractures (Banerdt et al., 1997), i.e. joints (e.g. Passchier et al., 2021 and references therein). However, interpretation of such fractures was problematic from the outset. According to Banerdt et al. (1997), *"The very close spacing of these features is perplexing"*. Solomon et al. (1991) suggested that *"The regular spacing of ... lineations may result from deformation of a surface layer whose thickness is nearly uniform"*. In addition, Solomon et al. (1992), applied a similar model to that used on tessera terrain by Gilmore et al. (1998; Section 3.1) to graben on the regional volcanic plains, and explicitly highlighted another major mechanical problem: *"The narrowness of the graben implies a shallow depth of deformation (only a few hundred meters if they are true graben and their bounding normal faults dip inward at 60°. The enigma of these and similar shallow structures is that their trends persist over large distances, implying the existence of structurally coherent sheets that are both very thin and areally extensive"*. Subsequently, Banerdt and Sammis (1992), pointed out that, given the observed widespread development of such lineaments with regular periodicity, this would require a geologically unrealistic, globally uniform thickness for the crustal layer involved in the jointing (however, see the detailed theoretical analysis of joint spacing / layer thickness relations by Chemenda et al., 2021; Chemenda, 2022). Moreover, Banerdt et al. (1997) went further: *"An implicit requirement of this model is that the layer have a relatively large tensile strength (implying only a small amount of pre-existing fracturing)"*. This is similar reasoning to that of Hansen and Willis (1998) and Hansen et al. (2000 and references therein; see Section 3.1).

3.3. Regional patterns of distributed extension on Venus are problematic

The identification of widespread, distributed, quasi-penetrative to penetrative, extensional features in the tessera terrains and volcanic plains raises a fundamental structural geological question: how does low-magnitude, periodic, extensional deformation occur over regional- and planetary-scale distances without resulting in strain localisation? (see Hanmer, 2020). The question can be restated as: how is strain localisation avoided in spatially widespread extensional deformation of natural materials?

By the axiomatic principle of least work done, strain localisation in natural materials is an unavoidable fact of basic structural geology. Where the deforming medium remains macroscopically coherent and continuous (plastic), natural deformation can involve a range of modes of strain softening with progressive deformation These may include dynamic grain size reduction (cataclasis and/or dynamic recrystallisation), anisotropic fabric development, and the rotation of planar elements regardless of nature or scale. However, such forms of strain localisation have generally been considered in the context of shortening and shearing (e.g. Poirier, 1980; Hobbs et al., 2015). In extension, the emphasis has been more on accounting for the periodic spacing of fractures, principally joints (e.g. Pollard and Segall, 1987; Pollard and Aydin, 1988; Wu and Pollard, 1991, 1992). For example, Wu and Pollard (1991, 1992) examined the propagation and spacing of tensile joints in layered materials in uniaxial, layer-parallel extension using a thin brittle layer of lacquer applied to a plexiglass sheet subjected to various strain magnitudes and strain rates. Crack number and length increased exponentially with strain, while crack spacing decreased linearly. With increasing strain rate, the crack number and average length rapidly stabilised, while the crack spacing reached saturation. Similar effects were observed when strain was applied in cycles.

Similarly, for the surface of Venus, Banerdt and Sammis (1992) applied a highly prescriptive shear lag modification of the foregoing analogue model, under-pinned by a very shallow-seated horizontal sliding interface beneath laterally extensive swaths of very narrow, close-spaced (<2.5 km) straight, parallel lineaments that they treated as tensile joints. In their analysis, the layer containing the periodic joints was stretched by the extension of its substrate to which it is coupled, but not rigidly bonded: *"... the elastic "rebound" of the plate is resisted by the substrate through a coupling traction on the base of the plate* [the shear lag], *and the tensile stress in the plate is diminished in a zone around the fracture.*

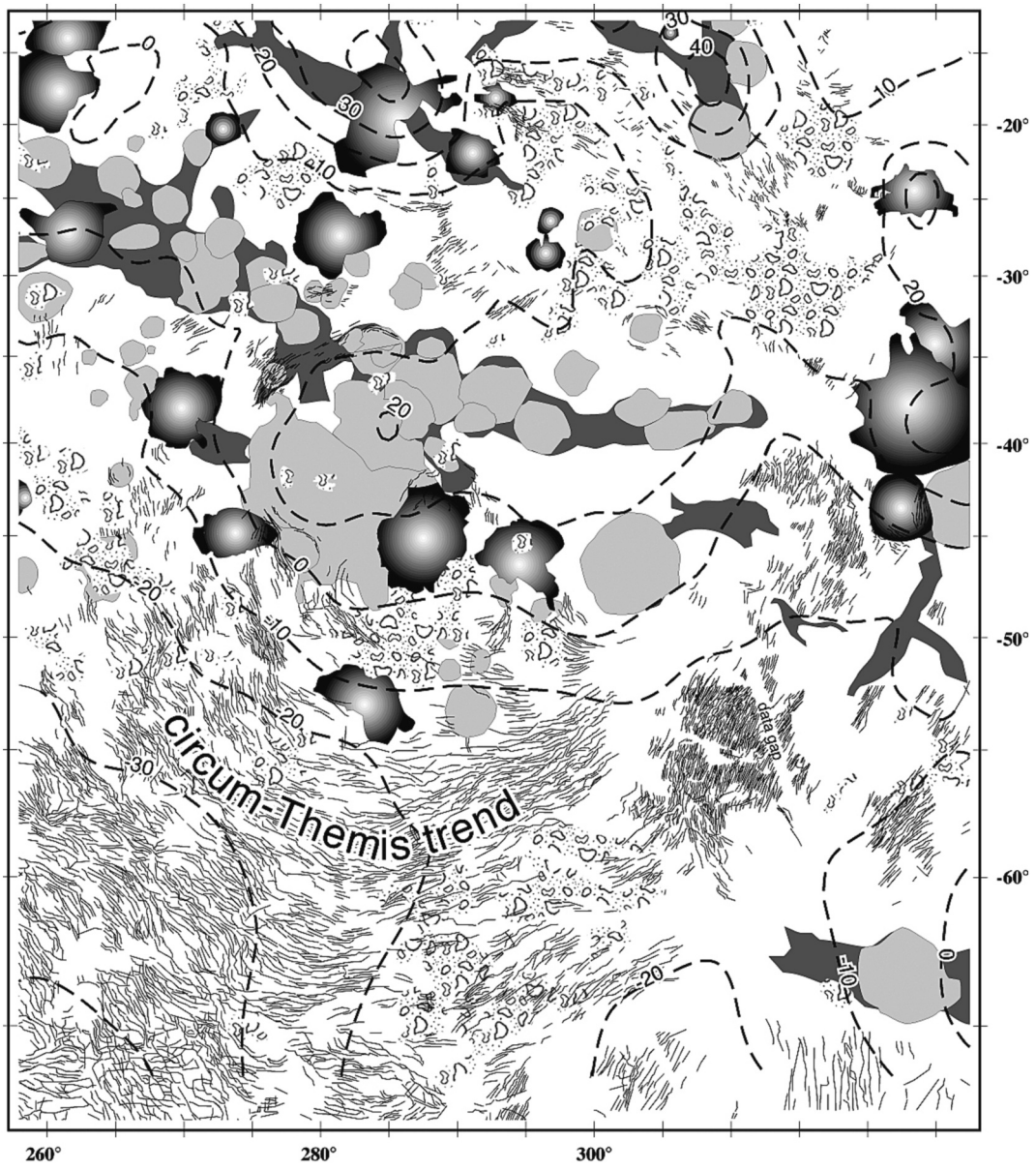

Fig. 3. Portion of the global wrinkle ridge map near Themis Regio, Venus. Black lines are individual wrinkle ridges. The shaded areas are coronae, large volcanoes and shield fields (light grey), and rift zones (dark grey). Dashed lines are contours of geoid height in meters. Fig. 9 in Bilotti and Suppe (1999). With permission from Elsevier.

The fracture stress … is exceeded at [a] *critical distance"*: hence the spacing of fractures.

Although the end results of the foregoing deformation experiments and theoretical calculations were indeed distributed, periodically-spaced, extensional fractures, Wu and Pollard (1992) explicitly noted that strain localisation was intentionally inhibited in their experiments, and they were cautious about direct application of their results to the natural case. In any event, Wu and Pollard (1991, 1992) analogue experiments dealt with tensile joints, as opposed to the normal faults of a graben model, and the tensile character of the venusian lineaments was an unsupported assumption on the part of Banerdt and Sammis (1992).

As noted above, other workers sought to explain the periodicity of distributed, close-spaced, extensional tectonic features in venusian tessera terrain by invoking a classical boudinage model (e.g. Hansen and Willis, 1998). However, the proposed model involves a relatively stiff surface layer, as opposed to a layer sandwiched between two less viscous layers (see Hanmer, 2020 for discussion). Others have appealed to numerical and analogue simulations of lithospheric-scale extension (e.g. Ruiz, 2007). However, in the examples invoked, the distributed normal faults that developed in the top surfaces of analogue models are short and discontinuous, and systematically present as families of similar facing faults, rather than opposite facing pairs (e.g. Corti, 2005). Moreover, numerical modelling indicates that extension will tend to localise in more efficient faults (e.g Montesi and Zuber, 2003), especially in non-newtonian materials such as rocks (e.g. Corti, 2005).

Alternatively, in a detailed review of penetrative, distributed ribbon fabrics in tessera terrains on Venus, Hanmer (2020) suggested that the published models are complex, internally contradictory, and inconsistent with well-established structural geological principles. Drawing on the theoretical work on shallow-seated mafic dyke emplacement driven by magmatic pressure (e.g. Pollard et al., 1983; Schultz et al., 2010), Hanmer hypothesised that interpreting penetrative graben fabrics as coupled to the emplacement of linear dyke swarms relatively late in the structural evolution of tessera terrains might provide a resolution for the apparent inconsistencies in the literature. I tentatively suggest here that a similar model may apply to extensive, penetrative, periodically-spaced

lineaments in the lineated and regional volcanic plains elsewhere on Venus. Note that the theoretical basis for the general model of magma-driven dyke emplacement was recently summarised and challenged by Kolzenberg et al. (2022). However, these authors were referring to dykes that breached the surface and were genetically associated with strike-slip deformation.

4. Shortening tectonic features: distributed wrinkle ridges vs lobate scarps

In contrast to the foregoing (Section 3), the regional volcanic plains on Venus are extensively decorated by vast swarms of distributed, regularly spaced, linear ridges.Referred to as *"wrinkle ridges"*, they are more widespread on Venus than on any other terrestrial planet (e.g. McGill, 1993; Banerdt et al., 1997; see Supplemental 1). Moreover, they have been considered to be the most common and least understood shortening tectonic features of telluric (rocky) off-world bodies throughout the inner Solar System (e.g. McGill, 1993; Schultz, 2000; Watters, 2004; Fig. 2a). Distributed wrinkle ridges, and potentially kinematically related, localised lobate scarps, have been identified as an assemblage of associated shortening tectonic features common to all the terrestrial planets (Watters, 1988). They are universally interpreted to represent low values of bulk strain (e.g. Sharpton and Head, 1988; Golombek et al., 1991; Solomon et al., 1992; Watters, 1992, 1993; Sandwell et al., 1997; Watters and Robinson, 1999; Bilotti and Suppe, 1999; Watters et al., 2009; Banks et al., 2012; Williams et al., 2013; Mueller et al., 2014; however, see Appendix). Notwithstanding, consideration of wrinkle ridges and lobate scarps across the inner Solar System begs the question of their definitions, and whether those definitions apply ubiquitously. In short, what exactly are wrinkle ridges and lobate scarps; how do they form; and do answers to these questions apply consistently on different planetary bodies, especially Venus?

Wrinkle ridges are universally interpreted on off-world bodies across the inner Solar System as shortening tectonic features according to various geometrical, kinematic, mechanical and dynamic models.The models involve reverse faults or thrusts and associated folds, and are derived on the basis of satellite-borne remote observation of ridge surface morphology. The models are supported by purported analogues on the other rocky planets and the Moon, as well as debatable terrestrial analogues (see Section 7).

On Venus, regional-scale patterns of periodically-spaced, generic ridges and wrinkle ridges were mapped as homogeneously distributed on the order of 1000 km or more, both along and across strike, without apparent regional strain localisation (Bilotti and Suppe, 1999, their figs. 2 and 9 to 13; Supplemental 1). At the regional- and planetary-scales, the distribution of wrinkle ridges appears to be quasi-circumferential about present-day topographical and geoid highs (see Fig. 3), leading Sandwell et al. (1997; Bilotti and Suppe, 1999) to propose a *"swell-push"* model whereby an elastic planetary crust underwent "flow" from the highs toward the topographical and geoid lows (plains) resulting in shortening. However, neither Sandwell et al. (1997), nor Bilotti and Suppe (1999), explicitly described or analysed the structural geology of individual wrinkle ridges, other than by empirical analogy with the surface morphology of features on other planets, including Earth. However, topographical surface morphological asymmetry constitutes the prima facie evidence for the vergence of proposed causative blind thrusts and associated folds in models of the formation of off-world shortening tectonic features across the inner Solar System (see below). It is therefore unfortunate that while the published 1:5,000,000 scale geological maps of Venus (Supplemental 1) graphically indicate the axial traces of positive relief features interpreted as wrinkle ridges, none report observations of the purportedly diagnostic asymmetry, not even in their marginal notes. Accordingly, in order to evaluate the state of knowledge of wrinkle ridges on Venus, it is necessary to include a review of the purportedly analogous shortening tectonic features invoked from across the inner Solar System.

In the context of the telluric bodies of the inner Solar System, the term *"wrinkle ridge"*, derived from *"mare ridge"* (Strom, 1972), is equivocal and seemingly difficult to define (e.g. Golombek, 1985; Sharpton and Head, 1988; Andrews-Hanna, 2020). On the surfaces of Mercury, Venus, Mars and the Moon it is applied to topographical features of very different morphologies and scale, even on a given planetary body (Watters, 1988; see also Watters, 1993; McGill, 1993; Watters and Johnson, 2010; Ruiz et al., 2012; Andrews-Hanna, 2020). The term *"wrinkle ridge"* was initially differentiated, arbitrarily, from the term *"lobate scarp"* according to occurrence. On any given body, wrinkle ridge was generally applied to periodically-spaced, ridge-like features that occur in volcanic plains, whereas lobate scarp was applied to episodic ridge-like features that occur in highland terrains (*highland scarps*; e.g. Watters, 1988).

Outside of the Soviet Union, early descriptions of wrinkle ridges were based on images taken from orbit by the Ranger, Apollo and Lunar Orbiter programs.[7] Strom (1972) described lunar mare ridges as low profile, elongate topographic arches topped by contorted secondary ridges. Howard and Muehlburger (1973) reported lunar mare ridges as asymmetrical (see also Maxwell and Phillips, 1978; Sharpton and Head, 1982, 1988; Golombek, 1985). Plescia and Golombek (1986; see also Watters, 1988, 1989) defined wrinkle ridges on the Moon and Mars as linear to sinuous, asymmetrical topographic highs with considerable surface morphological complexity.This included asymmetrical anti-formal shapes with tension cracks and graben along fold hinges (e.g. Mueller and Golombek, 2004, their fig. 8), plus overlapping en-echelon[8] lobes and symmetry reversals along strike. Axiomatic wrinkle ridges were divided into three surface topographical morphological parts: (i) a broad, linear rise; (ii) a superposed linear arch (the *"ridge"*); and (iii) a surmounting, commonly segmented, crenulated ridge (the *"wrinkle"*; e.g. Watters, 1988, 1989; Mueller and Golombek, 2004; Fig. 2b and c). The rise is up to 500 m high and 25 km wide, with gentle slopes (~1–6°). The arch is up to 200 m high and 6 km wide. The crenulated ridge is up to 100 m high and up to ~3000 m wide. *"Wrinkle-ridges on all planets exhibit this characteristic morphology. In fact, it is by this morphology alone that they are identified. Understanding this morphology, then, is necessary to understanding the ridges themselves"* (Aubele, 1989, my emphasis; see also Watters, 1988). However, many wrinkle ridges only present one or two of these morphological components, e.g. arches without sinuous ridges, or sinuous ridges without arches (e.g. Strom, 1972; Maxwell et al., 1975; Sharpton and Head, 1988; Zuber and Aist, 1990, their fig. 1; McGill, 1993; Banerdt et al., 1997; Schultz, 2000; Golombek et al., 2001; Mueller and Golombek, 2004; Andrews-Hanna, 2020). On Venus, this turns out to be the rule: e.g. *"wrinkle ridges on Venus generally consist of sinuous ridges without associated arches"* (McGill, 1993). Similarly, Lu et al. (2019) described lunar wrinkle ridges as low rises with no superimposed narrow wrinkles, no steep scarp faces, and uniformly symmetrical. Taken together, these multiple and diverse exceptions would seem to detract from the robustness of the axiomatic definition of wrinkle ridges presented above.

Lobate scarps (Fig. 4) have been reported from Mercury, Mars and the Moon. First identified as isolated, curved, asymmetrical ridges on Mercury (Strom et al., 1975), their surface topographical expression is usually presented as simpler, straighter and larger (>500 km long by >10 km wide) than that of wrinkle ridges. However, across the inner Solar System, the morphological definition of lobate scarps is equivocal. Much smaller (by at least an order of magnitude), commonly rectilinear features on the Moon were, and continue to be, defined as lobate scarps

[7] https://www2.jpl.nasa.gov/missions/past/ranger.html; https://www.nasa.gov/mission_pages/apollo/index.html; https://nssdc.gsfc.nasa.gov/planetary/lunar/lunarorb.html

[8] I prefer the term "en-relais" (Hanmer et al., 1997; Fig. 52) to distinguish this low-angle off-set configuration from classical high angle en-echelon arrays (e.g. Ramsay, 1967, pp. 447–8). However, I appear to be in a singular minority.

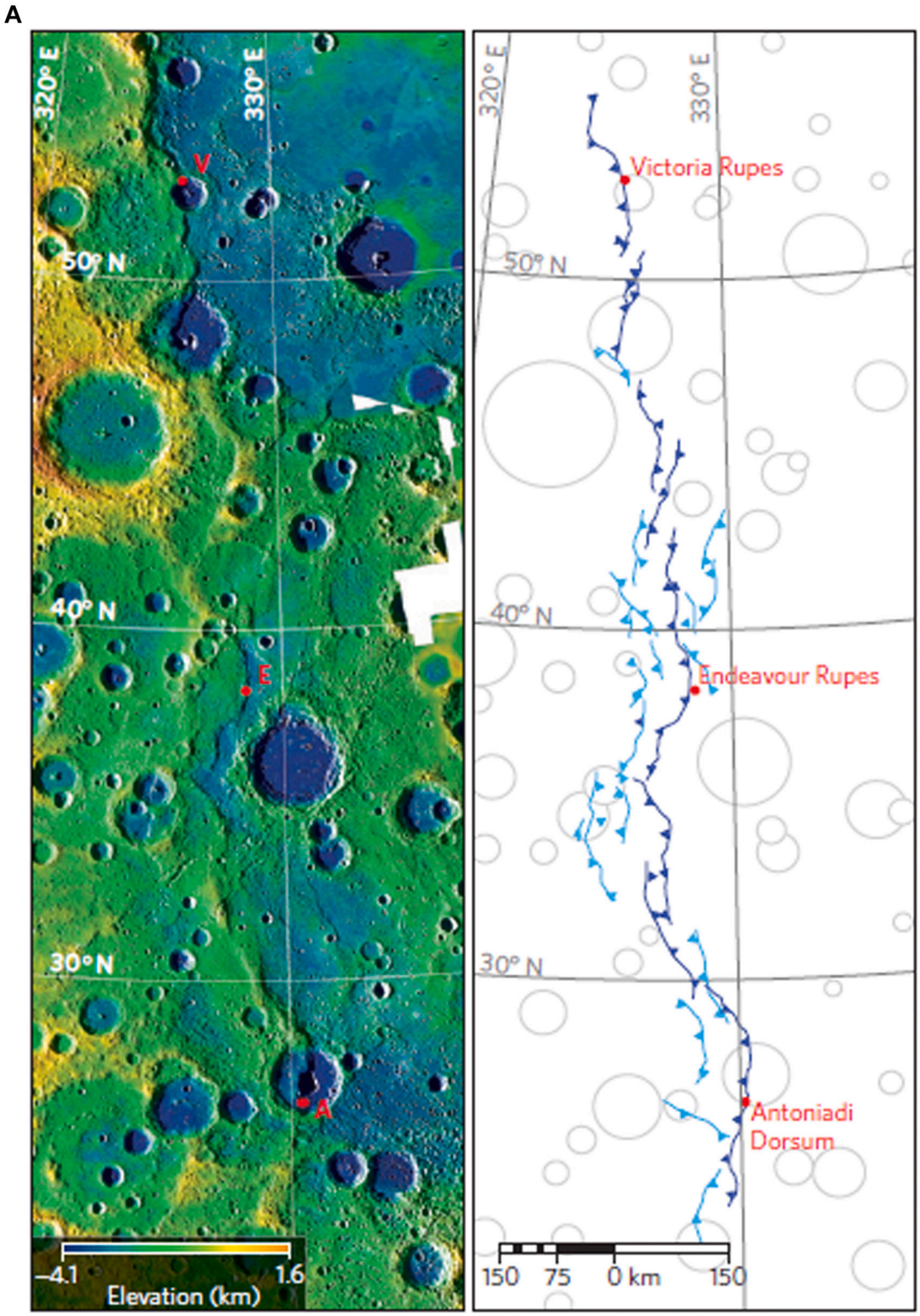

Fig. 4. Lobate scarps. (A) Fig. 3 in Byrne et al. (2014). With permission from Springer Nature. According to these authors the 1700 km long Victoria- Endeavour-Antoniadi system (VEA: see Fig. 5b for location) is one of the most prominent fold-and-thrust belts documented on Mercury, and consists of an assemblage of lobate scarps and high-relief ridges. Left panel: stereo digital terrain model overlaid on the global basemap. Right panel: surface traces of structures (arrows indicate down-dip direction), with pronounced craters outlined in grey. (B) Crater transected by a lobate scarp on Mars. Fig. 6 in Ruj et al. (2018). With permission from Elsevier. (C) LROC images of lunar lobate scarps. (b) Joy; (c): Barrow A; (d): Wilsing Z; (e): Romer P (northern section); and (f): Plummer C. North is up. Part of fig. 1 in Clark et al. (2017). With permission from Elsevier.

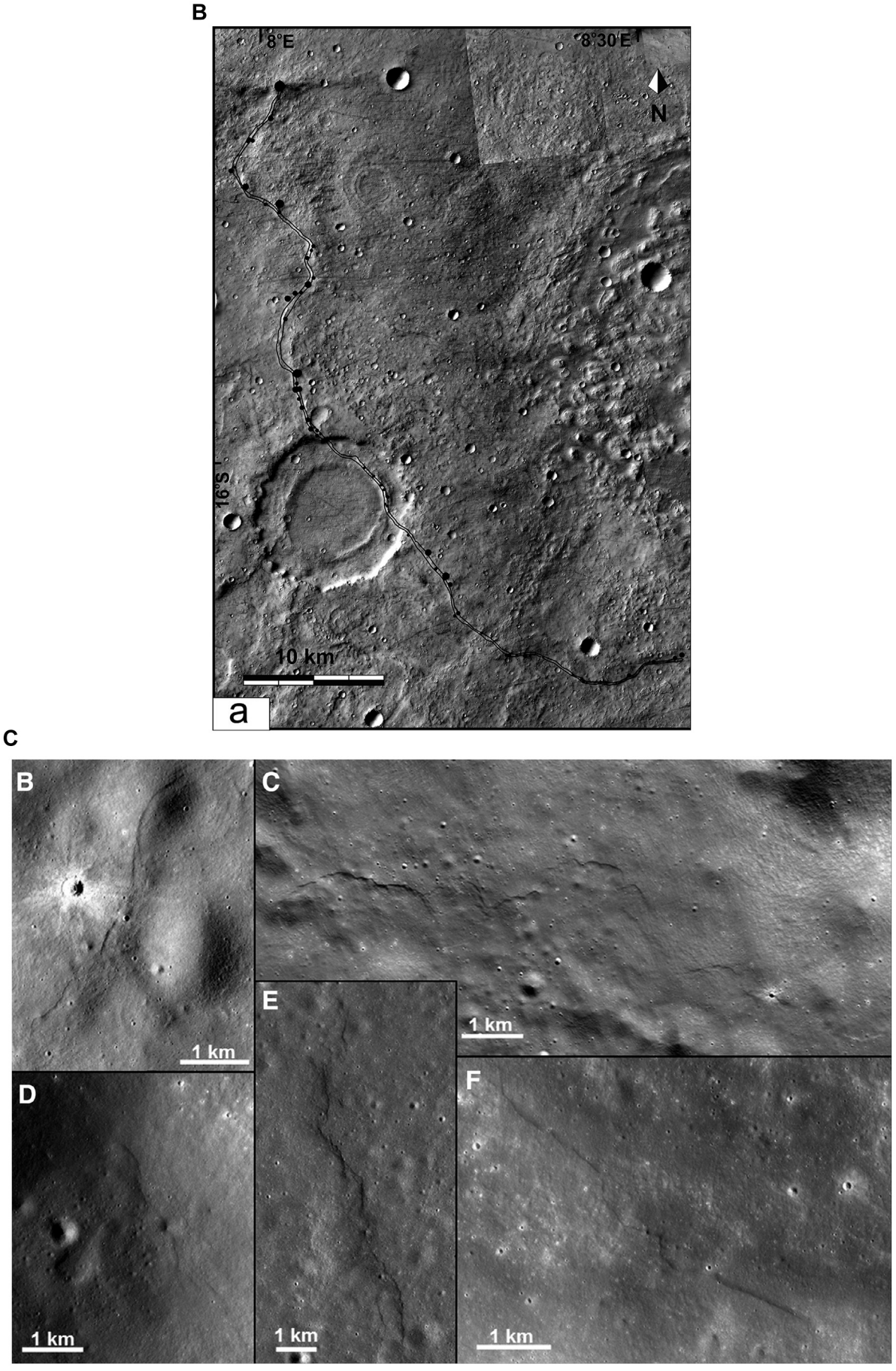

Fig. 4. (*continued*).

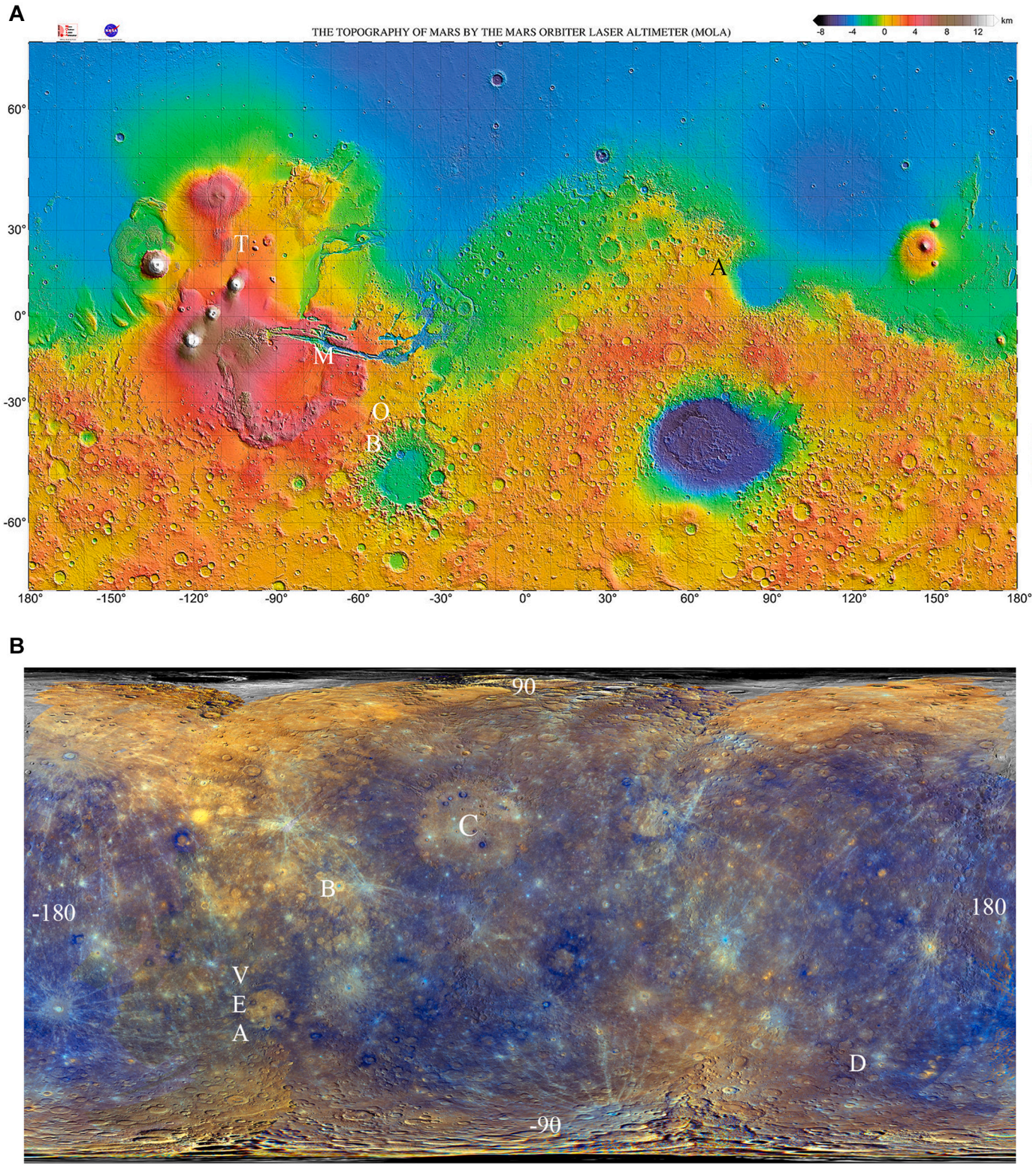

Fig. 5. (A) Key locations on Mars cited in the text, plotted on a base provided by https://attic.gsfc.nasa.gov/mola/images/mercat_med.jpg. A: Amenthes Rupes; B: Bosporos Rupes; M: Melas Chasma; O: Ogygis Rupes; T: Tharsis uplift. (B) Key locations on Mercury cited in the text, plotted on a base provided by https://solarsystem.nasa.gov/resources/531/enhanced-color-mercury-map/. B: Beagle Rupes; D: Discovery Rupes; VEA: Victoria-Enterprise-Antoniadi rupes. C is the Caloris Basin, for general reference.

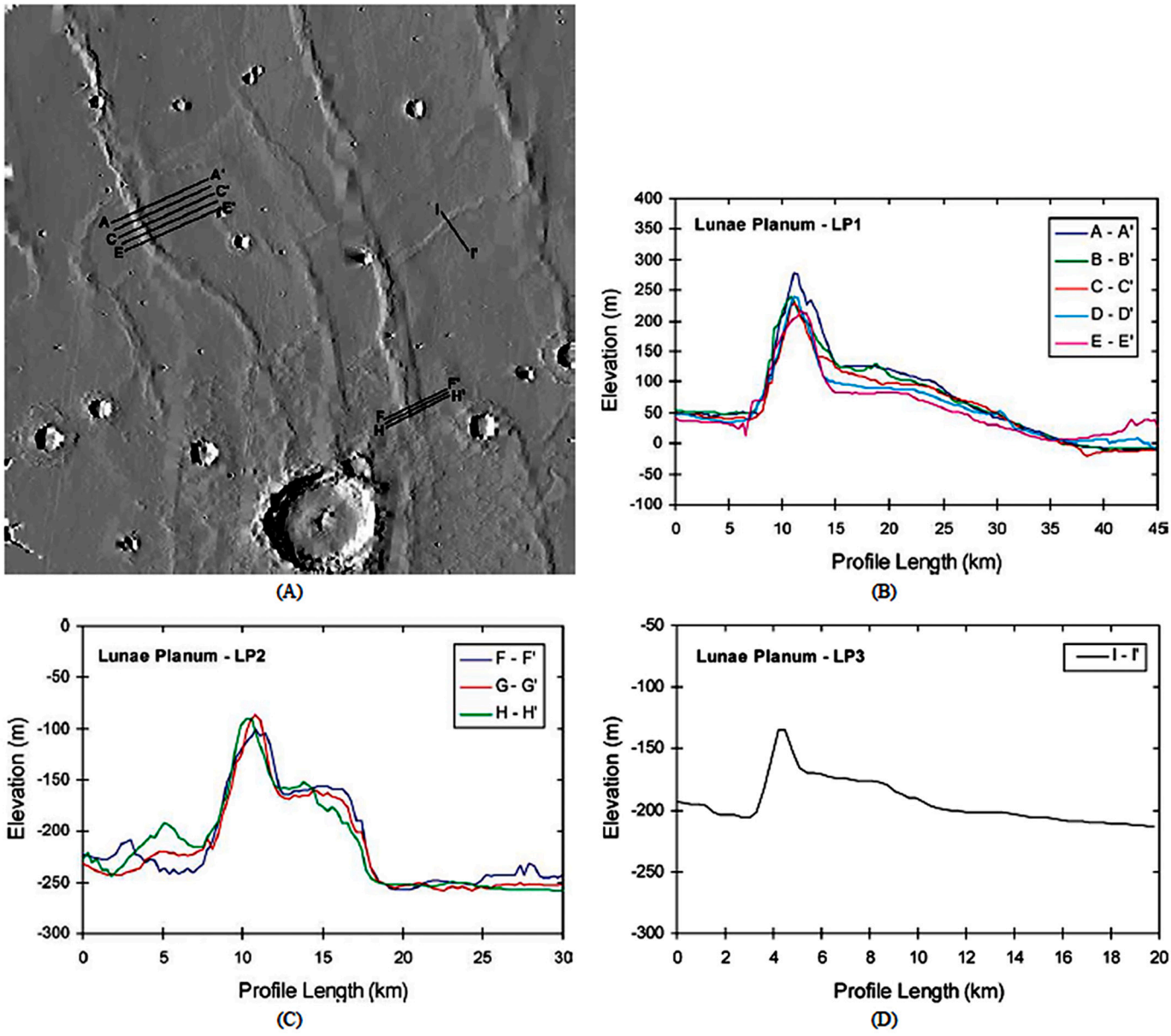

Fig. 6. (A) Shaded relief image of volcanic plains on Mars. (B) Profiles across a prominent wrinkle ridge (vertical exaggeration is ~ 60: 1). (C) Profiles across a moderate relief wrinkle ridge segment (vertical exaggeration is ~ 60: 1). (D) Profile across a small-scale wrinkle ridge cutting across the inter-ridge plains between two regularly spaced ridges (vertical exaggeration is ~ 50: 1). The locations of the profiles are shown in (A). Fig. 2 in Watters et al. (2004). With permission from Elsevier.

by their occurrence within the lunar highlands, as opposed to wrinkle ridges located in the lunar maria (Fig. 4c; e.g. Watters, 1988; Watters et al., 2010, 2012, 2015b; Banks et al., 2012; Li et al., 2018; Williams et al., 2013, 2019; Roggon et al., 2017; Clark et al., 2017; van der Bogert et al., 2018; however see Matsuyama et al., 2021). On Mars (Fig. 4b), lobate scarps were defined by (i) their size (locally comparable with Mercury); (ii) their isolated (localised) nature; and (iii) the proposed presence of surface-breaking (daylighting) reverse or thrust faults at the base of the scarp that cut pre-existing features in the planetary surface (e.g. Amenthes Rupes, see Fig. 5a for location; Watters, 1993; Watters and Robinson, 1999; Watters et al., 2000; Schultz and Watters, 2001; Mueller et al., 2014; Ruj et al., 2018). However, note the emphasis on folding by Schultz and Tanaka (1994). Despite this variety of morphologies, all are defined as lobate scarps to this day (e.g. Williams et al., 2013).

Although the surface scarp slopes of wrinkle ridges and lobate scarps are commonly reported as "steep", simple trigonometry applied to published profiles suggests a more complex picture. Most illustrated scarp slopes are in the range ~ 1–5° (e.g. Plescia et al., 1980; Plescia and Golombek, 1986; Zuber et al., 2010; Mueller et al., 2014; Ruj et al., 2018; Li et al., 2018; Peterson et al., 2020), with outlier values at 3–9° (Watters and Robinson, 1999), ~17° (Williams et al., 2019) and 5–30° (Banks et al., 2012). In addition, most published profiles across surface topographical morphologies distort the visual presentation of the landforms by using vertical exaggerations ranging from ~5:1 to ~30:1 (e.g. Watters, 1988, 1989; Golombek et al., 1990, 1991; Schultz and Tanaka, 1994; Watters and Robinson, 1997, 1999; Watters et al., 1998; Watters, 2003; Mueller et al., 2014), with outlier values of ~50:1 to ~140:1 (e.g. Watters, 2004; see Fig. 6). While this may be understandable for the purposes of detailed analysis, true-scaled versions of the topographical profiles are rarely presented for visual evaluation of their shape, and specifically their sense of asymmetry; the latter being essential to their

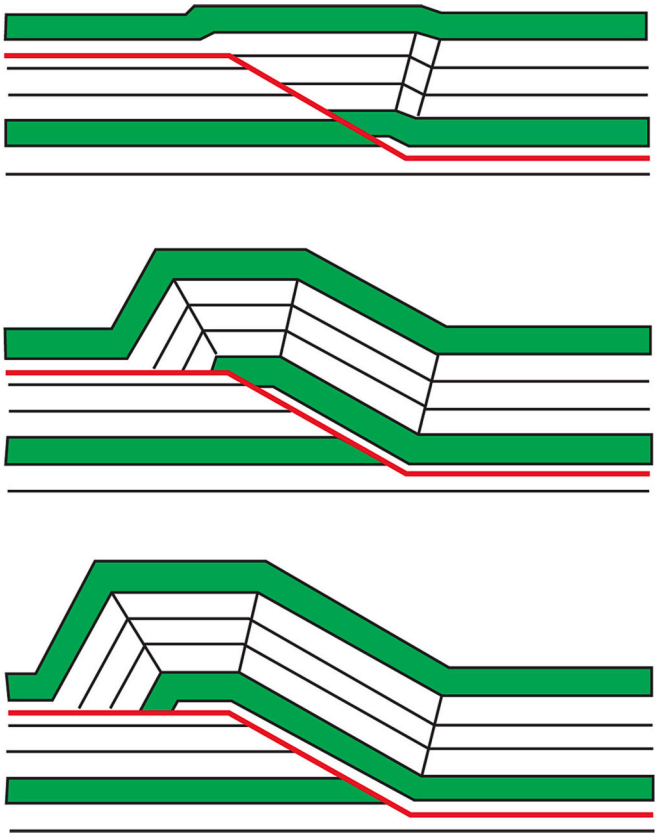

Fig. 7. Progressive kinematic development of fault-bend folds in response to a simple step in a decollement. Redrawn from fig. 3 in Suppe (1983).

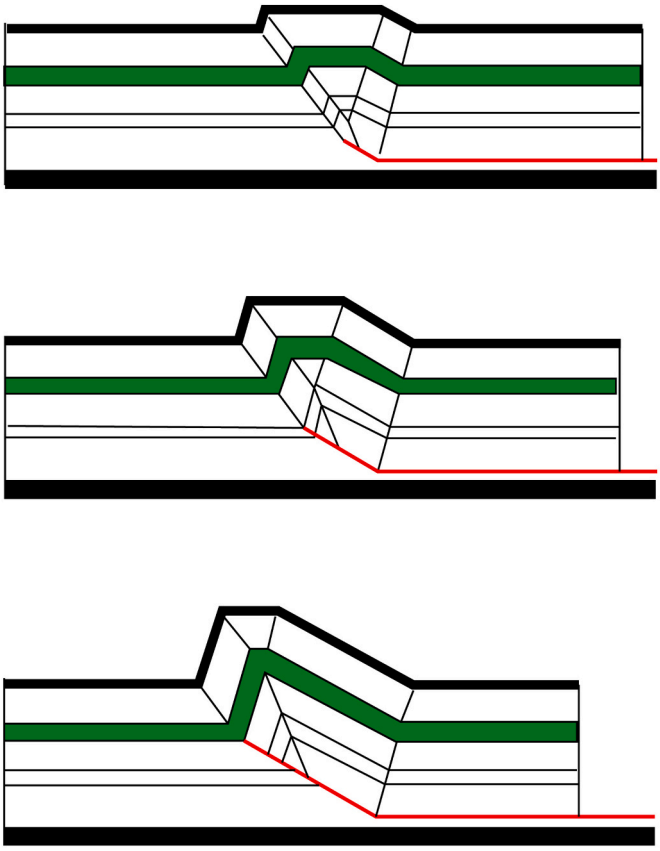

Fig. 8. Retrodeformable model of the progressive development of a simple-step fault-propagation fold. Redrawn from fig. 6 in Suppe and Medwedeff (1990). In contrast to fault-bend folds, hinges of fault-propagation folds shorten as the structure matures, oversteepening the front limb and lengthening the back limb as the fault propagates surfaceward.

kinematic and mechanical interpretation.

4.1. Formal definitions and interpretations

Topographical landforms defined as wrinkle ridges or lobate scarps were identified in remotely-sensed elevation data, or on the basis of surface imagery of Mars, Mercury and the Moon. However, these features are internally "closed" to remote satellite-based observation. Hence, their internal structural geology has been interpreted using empirical hypothetical models derived from morphological asymmetries observed in topographical profiles constructed normal to ridge/scarp trends. Based on the asymmetrical morphology of ridges on Mercury and Mars, and placing great emphasis on purported terrestrial analogues (see Section 7), Plescia and Golombek (1986; see also Watters, 1988) concluded that topographical "*similarities*" strongly suggest that planetary wrinkle ridges result from deformation associated with shallow-seated thrust faults (see also Howard and Muehlburger, 1973; Maxwell et al., 1975; Lucchitta, 1976), according to either a fault-bend folding (Fig. 7; Suppe, 1983; Connors et al., 2021) or a fault-propagation fold model (Fig. 8; see Suppe and Medwedeff, 1990; Suppe and Connors, 1992 for model details). However, in a rare study of the global distribution of wrinkle ridges on Venus, Bilotti and Suppe (1999) opted not to examine or analyse individual wrinkle ridges. They were interested in spatial variations of wrinkle ridge density, for which they only needed to map lineaments per se (see Fig. 3). Recall that, with a single local exception (Bethell et al., 2022), the symmetry characteristics of wrinkle ridges on Venus remain undefined (Supplemental 1).

It has long been known that the trace of the Discovery Scarp, the largest lobate scarp on Mercury, cuts diametrically across impact craters up to ~60 km wide (Strom et al., 1975; Fig. 9; however, see Appendix). Watters (1988) noted that lobate scarps on Mercury, are similar in morphology to lunar highland scarps, commonly cross a number of different geologic units. In contrast, wrinkle ridge structures do not, thereby providing the first structural geological criterion for discriminating between wrinkle ridges and lobate scarps. The former were associated with blind thrusts and folding, and the latter were associated with simple, daylighting thrusts. Note that the definitions of wrinkle ridge and lobate scarp were no longer morphological or geographical: they had now become model-driven, and thereby hypothetical.

Further consideration of the kinematics and/or mechanics of wrinkle ridges by Watters (1988; see also Aubele, 1989; Watters, 1989) was principally based on comparison with what was to become the most commonly cited terrestrial analogue (the Yakima Fold Belt, Columbia Plateau, Washington; Plescia and Golombek, 1986), subsequently critically re-evaluated and found to be incomplete by Crane (2020a; see Section 7). Combining these considerations, Watters (1988) proposed two potential kinematic models for the formation of individual wrinkle ridges: fault-bend folding (his *"flexure*-fracture"; Fig. 7) and fault-propagation folding (his *"fracture-flexure"*; Fig. 8).

Watters and Robinson (1997) made a number of telling observations regarding the morphology and kinematics of wrinkle ridges: *"Their complex nature is reflected in the variety of kinematic models that have been proposed for their origin ... the relative role of folding and thrust faulting is unresolved"*. Moreover, they stated that *" ... there is no unambiguous surface expression of thrust faulting associated with martian or other planetary wrinkle ridges"*. Furthermore *"Absence of clear surface expression of thrust faulting ... does not support models involving deeply rooted faults"*. They also stated that *"Although no clear surface expression of thrust faults have* [sic] *been found, thrust faulting likely plays an important role in the formation of wrinkle ridges. This assumption is based on comparisons with terrestrial analogues (Plescia and Golombek, 1986), particularly those in*

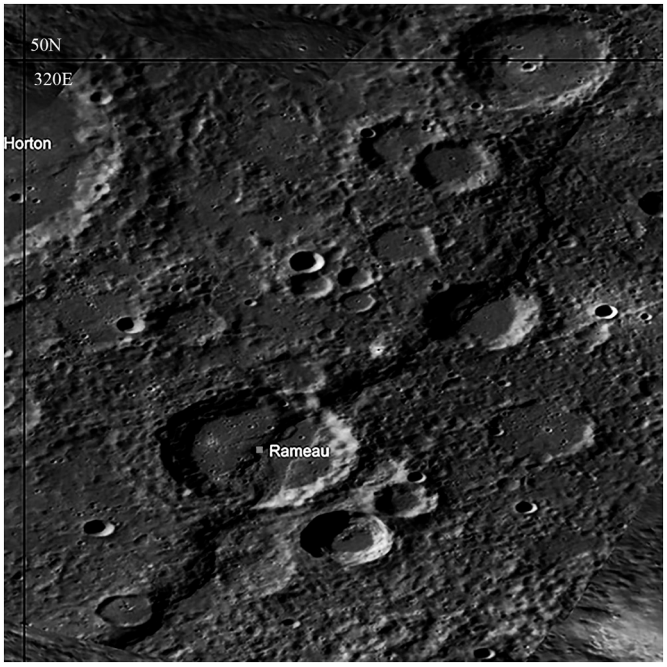

Fig. 9. Discovery Rupes, largest known lobate scarp on Mercury, ~550 km long, appears to transect 60-km-diameter Rameau crater (R), and smaller 40-km-diameter crater to northeast. This image was sourced from JMARS (**J***ava* **M***ission-planning and* **A***nalysis for* **R***emote* **S***ensing*) at https://jmars.mars.asu.edu/.

*the continental flood basalts of the Columbia Plateau (*Watters, *1988)"* (my emphasis). Still on the question of wrinkle ridges, Mueller and Golombek (2004) put it succinctly: *"The pronounced asymmetry of these ridges has been noted for its similarity to fault-related folds on Earth and forms a foundation for their interpretation based on terrestrial structural analogues"*.

4.2. *Buckling and the periodic-spacing of reverse/thrust faulting*

Wrinkle ridges and lobate scarps were identified as an assemblage of associated topographical features and regional patterns that vary in morphology and regional-scale distribution, both between rocky planetary bodies and across a given body (e.g. Watters, 1988, 1989; McGill, 1993). Regarding wrinkle ridges, some workers emphasised the role of reverse or thrust faulting to explain the topographical asymmetry, and of buckle folding to account for the periodic spacing (e.g Watters, 1988, 1989; Zuber and Aist, 1990). From this model horizontal shortening could be empirically derived, assuming that *"... all of the significant horizontal shortening is manifest in the topographic expression of the structure"*, and that the folds are chevron or box-style anticlines separated by broad, largely undeformed synclines (Watters, 1988). Thus unit shortenings (~0.01–0.2) and displacements (~20-800 m) across wrinkle ridges were derived on the Moon and Mercury. In a quantitative analysis of periodically spaced anticlinal ridges in a purported terrestrial analogue, the Yakima Fold Belt (see Section 7), deformed basalt flows were treated as a multilayer of elastic plates separated by frictionless, free-slipping interfaces, overlying a very weak substrate that buckled at a critical (dominant) wavelength in kink-fold style anticlines (Watters, 1989).This despite the presence of pervasive columnar jointing (Fig. 10). Similarly, on Mars, taking the Yakima Fold Belt as the best terrestrial analogue, basalt flows on the Tharsis Plateau (see Fig. 5a for location) deformed by periodically-spaced wrinkle ridges, were modelled both as a single member and as a multilayer, with a very weak substrate equated with impact-generated megaregolith, potentially water- or ice-rich at the time of deformation (Watters, 1991; see also Zuber and Aist, 1990). However, the analogy was strictly morphological: *"The morphology of the features in the Martian wrinkle ridge assemblages is virtually identical to their lunar analogs ... morphologically and dimensionally similar to the anticlinal ridges of the Columbia Plateau"* (Watters, 1991). Moreover, the analysis also explicitly included two fundamental assumptions: (i) that the megaregolith is granular and mechanically homogeneous, with a depth-dependent mechanical strength; and (ii) that the boundaries between a basalt multilayer, the megaregolith, and the underlying basement, are

Fig. 10. Columnar jointing in Columbia River basalts, Washington, a major component of the Yakima Fold Belt, seen here at Grand Coulee (image by the author).

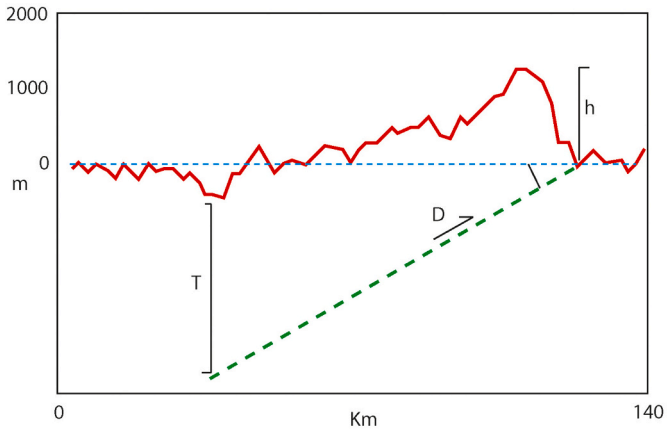

Fig. 11. Topographic profile across Discovery Rupes, Mercury (see Fig. 5b for location), and the geometrical parameters for 2D boundary element elastic dislocation forward modelling software package COULOMB, showing an underlying thrust fault of vertical depth T, fault-plane dip angle, and maximum displacement D. The best model fits are for $T = 35–40$ km, dip = 30–35, and D = 2.2 km. The depth of faulting is not to scale. Vertical exaggeration of topography is 1:18. Redrawn from fig. 2 in Watters et al. (2002b).

all discrete, flat and horizontal (Watters, 1991, his fig. 5). As Watters acknowledged, such boundary conditions may not apply in a kilometric-scale mega-impactite. I would go further: material and geometrical heterogeneity in such a medium is not conducive to periodic buckling.

With respect to lobate scarps, Watters (1993) re-affirmed the morphological comparison of martian examples with similar lobate scarps on the Moon and Mercury, and thereby empirically attributed the origin of the martian examples to a similar mechanism: i.e. slip on reverse or thrust faults (see also Watters, 1988). In contrast to wrinkle ridges, the presence of fault-related folding was not a requirement. However, the fundamental factor in their identification was still their location in the highland terrains, whatever their size. On Mars, wrinkle ridge to lobate scarp transitions were reported: *"... where structures extend* [from the volcanic plains] *into the highlands, the morphology of the wrinkle ridge changes to that of a lobate* scarp", potentially reflecting anisotropic layering in the volcanic plains favouring folding vs rheologically isotropic highland materials where folding was impeded (Watters, 1993; see also Williams et al., 2019).

4.3. Predominantly thrusting?

Taking a different approach to that of Watters (see Section 4.2), other workers described wrinkle ridges on the Moon and Mars (Fig. 2b) that appeared to show surface elevation offsets (mean ~ 55 m) derived from photoclinometry across gently sloping ridges (Golombek et al. (1990, 1991), however, see Watters and Robinson (1997) for detailed dissenting discussion). Golombek et al. (1991) proposed that the associated crustal shortening could be analysed as two components: (i) dominant slip on shallow faults dipping at ~25° beneath the wrinkle ridges, wherein the amount of slip could be estimated from the elevation offset; and (ii) subordinate, shallow-seated folding in response to fault slip, that accounted for the surface elevation morphology. Their empirical model, again based on comparisons with purported terrestrial analogues (see Section 7), implied that such faults must daylight in order to accommodate displacements of the order of ~100 m or more (see also Mueller and Golombek, 2004). Note that this model effectively negated the geometrical, kinematical and mechanical distinction between wrinkle ridges and lobate scarps proposed thereto (e.g. Watters, 1988).

Golombek et al. (1990) favoured crustal shortening by predominant slip on planar main faults, since neither folds, nor faults that flatten at depth, could explain the laterally extensive surface topographical elevation offsets across wrinkle ridges that they reported. Furthermore, they proposed that the gross structure of wrinkle ridges was different from typical fault-bend and fault-propagation folds (Figs. 6 and 7). According to these authors, abrupt dip changes at step-up ramps would result in abrupt surface elevation changes, which were not observed, and such fault-fold systems require more slip than was apparent. Most importantly, they proposed that, since wrinkle ridge spacing is ~50 km, the elevation offsets must be supported by equally long fault dips, extending to beneath the next ridge kinematically upstream. Such faults would cut through a significant mechanical lithospheric thickness, and therefore correspond to a thick-skinned (see Pfiffner, 2017 for definition) deformation model (see Watters and Robinson, 1997 for a dissenting view). However, the majority of workers favoured a thin-skinned deformation model (see Pfiffner, 2017 for definition) for wrinkle ridges. For example, Mangold et al. (1998, their fig. 2) proposed that martian wrinkle ridges showing irregular, curved, circular and en-echelon planform geometries had been influenced by pre-existing, shallow-seated structures and buried craters via their effects on shallow decollements (;see also Watters, 1993; McGill, 1993; Watters and Robinson, 1997; Byrne et al., 2014; Fegan et al., 2017). From the observation that impact craters associated with fluidised ejecta are preferentially spatially associated with volcanic plains affected by wrinkle ridges, Mangold et al. (1998) further proposed that there was a causal correlation between ground ice located in 1–10 km thick mega-regolith and wrinkle ridge formation. However, this involved an empirical assumption because Mangold et al. (1998) did not demonstrate that ground ice was actually present at the time of wrinkle ridge formation. In addition, many non-cryogenic planar weaknesses (e.g. shale interbeds, lava tops, weathered horizons) could equally serve to localise fault slip.

4.4. Elastic dislocation modelling

The mid-1990s saw a significant shift in the nature of research on wrinkle ridges and lobate scarps, with a greater emphasis placed on empirical numerical modelling (kinematic, mechanical, dynamic) of faulting and/or folding in elastic media. However, such modelling has systematically tended to under-estimate the contribution of the folding component in the case of wrinkle ridges (Crane, 2020a, 2020b). Watters et al. (1998) used a simple, empirical, kinematic model to calculate ~3.2 km horizontal shortening on a thrust fault assumed to be dipping at 25° beneath the large lobate Discovery Scarp on Mercury (see Fig. 5b for location), in accordance with the wrinkle ridge / lobate scarp distinction of Watters (1988). Similarly calculated horizontal shortening for other, smaller hermian lobate scarps was in the range 0.26–1.8 km for the same assumed fault dip. However, an important assumption in the Watters et al. (1998) model, apparently widely supported by the general absence of significant offsets in transected crater rims throughout the inner Solar System (see Appendix A.2), is that the daylighting of thrust faults associated with lobate scarps is incipient.In other words, the hanging wall is not translated over the fault ramp and onto the flat (planetary) surface of the footwall. Because the model does not address potential mechanisms for arresting the slip on thrust faults at the point where they intersect the planetary surface, this represents an arbitrary and geologically unrealistic constraint (however, see *"pre-peak"* deformation of Aubele, 1989; see also Appendix A.2). The same applies to subsequent elastic dislocation modelling across the inner Solar System that assumed the same constraint (e.g. Watters and Robinson, 1999; Schultz and Watters, 2001; Watters and Schultz, 2002; Watters et al., 2002b).

The 2D boundary element elastic dislocation forward modelling software package COULOMB was introduced to planetary geology of the inner Solar System by Schultz (2000) and Schultz and Watters (2001; see also Watters and Schultz, 2002; Watters et al., 2002a; Watters, 2004; Fig. 11). Use of COULOMB has since become a standard practise in planetary science, despite reservations expressed by some regarding its use in the analysis of inelastic finite deformation. For example, Cole and Andrews-Hanna (2017) cautioned that *"On Earth, elastic dislocation*

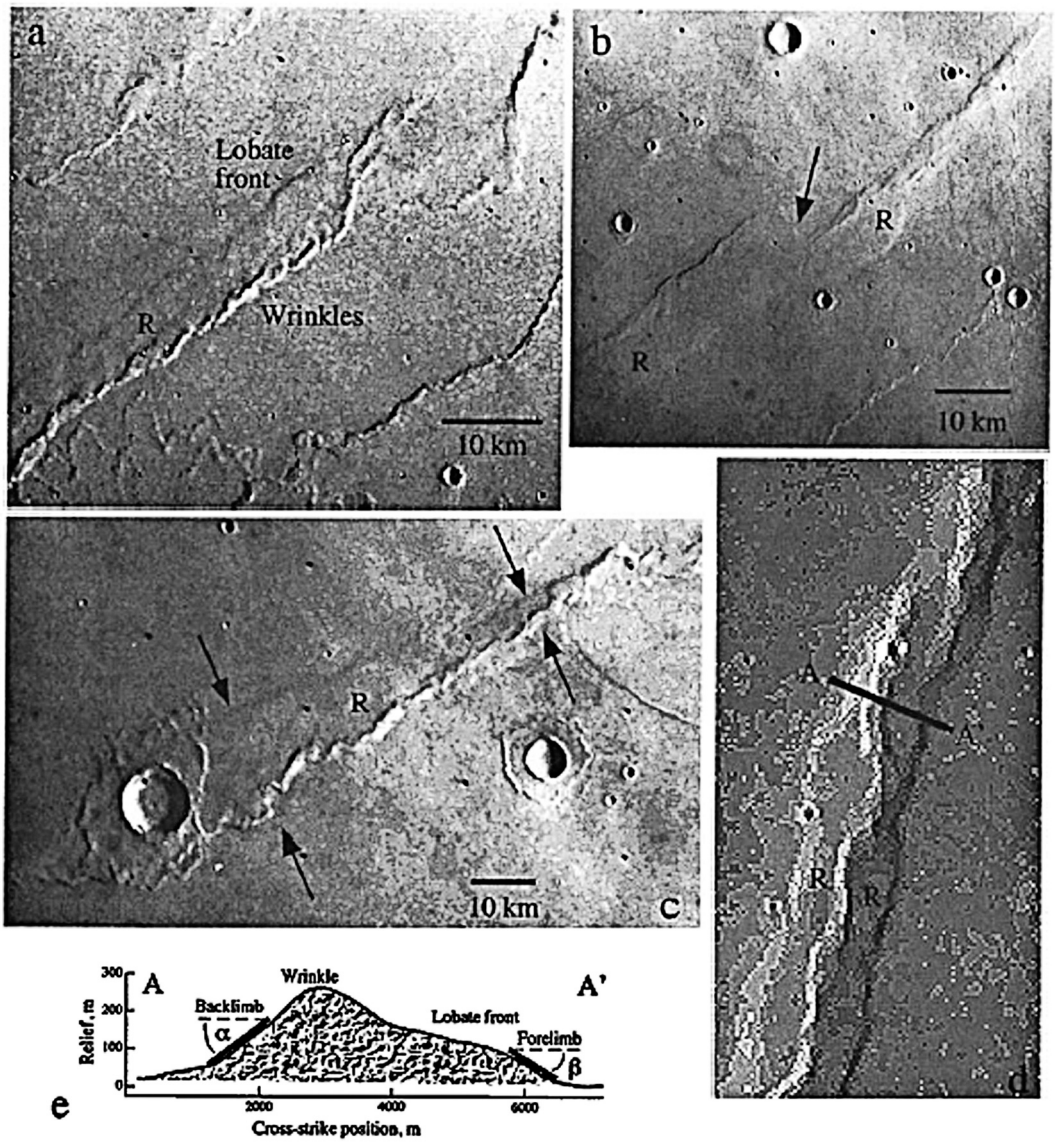

Fig. 12. Examples of wrinkle ridge structures from Mars. The main ridge antiform is indicated by "R"; North is toward upper right in A-C. (A) wrinkle ridge showing lobate ridge front and wrinkles (echelon backthrust faults); vergence is east to west. (B) echelon ridge showing lateral ramp (arrow) developed between wrinkles and ridges; vergence is west to east. (C) wrinkle ridge showing decrease in ridge width along strike (arrows) toward termination (upper right part of frame); vergence is east to west. (D) wrinkle ridge with echelon wrinkles located along centre of ridge showing location of topographical profile A-A' . (E) Measured topography of wrinkle ridge in D. Profile length is ~5 km, showing backlimb and forelimb angles. Fig. 1 in Schultz (2000).

models are generally applied to single earthquakes in which most deformation away from the fault plane is elastic … before the topography has been modified by the accumulated long-term viscous response at deeper levels". In addition, the technique is commonly applied as a single fault slip event (e.g. Peterson et al., 2020). However, Zuber et al. (2010) cautioned that *"To be consistent with strain rates predicted from thermal history models and the amount of shortening required to account for the underlying large-offset faults, ridges and scarps on Mercury likely developed over geologically substantial time spans"*). Remote application of such models to off-world structural geology requires justification. However, the foregoing cautions have not been directly addressed by studies that employ COULOMB. Note also that the modelling technique generally involves the empirical insertion of a mature fault into a homogeneous, isotropic, elastic medium prior to application of the deformation increment to be analysed. While mathematically effective, this introduces yet another geologically artificial step into the analytical process.

Notwithstanding these reservations, COULOMB was applied to the geometry, kinematics and dynamics of the Amenthes Rupes lobate scarp on Mars, and to the Discovery Scarp on Mercury (Schultz and Watters, 2001; Watters and Schultz, 2002; Watters et al., 2002b). Empirically determined best fit fault parameters to explain the lobate scarp surface topographical morphologies were planar thrust faults dipping beneath the lobate scarp at 25–35°, with the lower (trailing) fault tip located at 25-40 km depth (e.g. Fig. 11). In short, according to the modelling, thrusts associated with large lobate scarps cut the entire thickness of the planetary elastic lithosphere at the time they formed, thereby confirming the thick-skinned nature of deformation associated with lobate scarps (see also Watters et al., 2000; Watters, 2003), in contrast to thin-skinned wrinkle ridges.

Having applied the 2D elastic dislocation modelling COULOMB software to lobate scarps, Watters et al. (2004) applied it to wrinkle ridges on Mars (Fig. 6). He found that the complex surface topographical morphology of wrinkle ridges (arches and superposed ridges and wrinkles; see Section 4) was best fit by a thin-skinned model of a blind listric thrust fault, comprised of segments of different dip and slip to a maximum depth of <5 km, that may root into a decollement located at

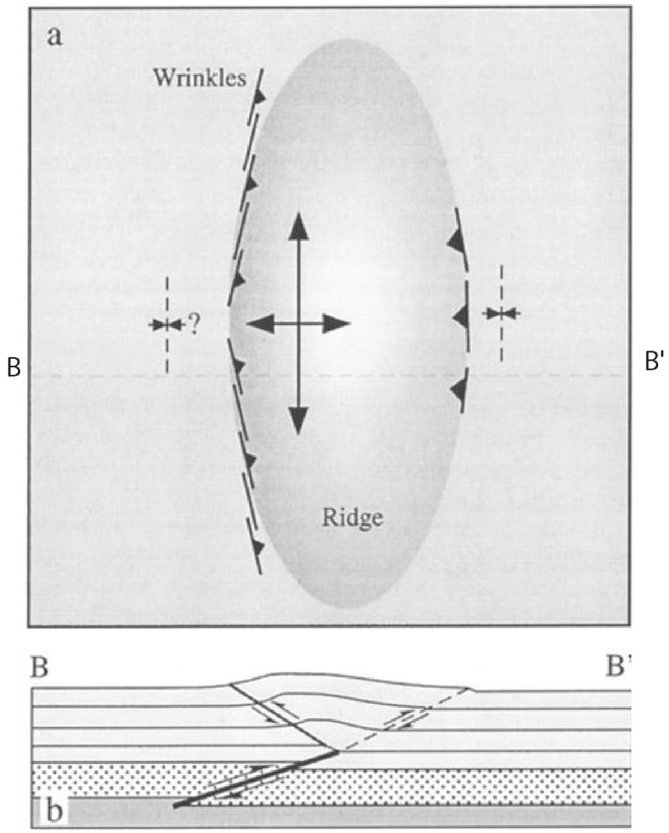

Fig. 13. Synoptic blind thrust model for wrinkle ridges; overall direction of thrusting is left to right. (Upper) Structural map showing major elements of wrinkle ridge morphology; along-strike length is greatly reduced, relative to ridge width, in the figure. Section line B-B′ shows position of cross section given in lower frame; surface breaks of thrust faults are shown with teeth on upper plate; anticlines and potential synclines are shown by converging and diverging arrows, respectively. Upper plate of wrinkle ridge-blind thrust fault system includes the ridge and extends to its left. (Lower) Cross section showing blind thrust fault (heavy line showing thrust displacement) beneath flexural slip anticline, backthrust fault(putative wrinkle), and up-dip prolongation of main fault surface (dashed). Fig. 4 in Schultz (2000).

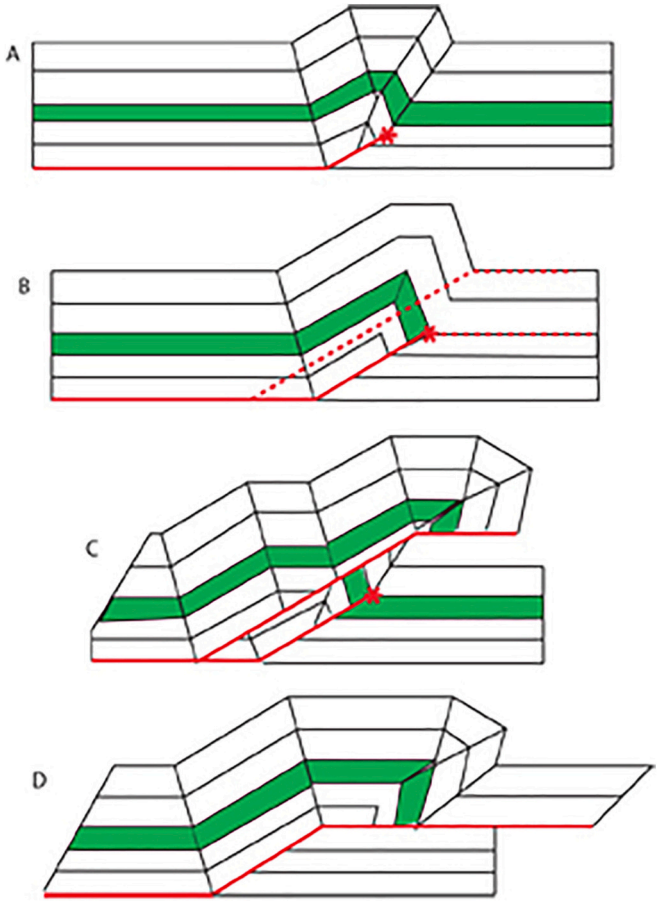

Fig. 14. Kinematic evolution of a thrust-truncated fault-propagation fold according to Wallace and Homza (2004). Green layer is a marker that has no mechanical significance; red lines are thrusts (solid) or potential thrusts (dashed). (a) and (b) Evolution of a fold formed by propagation of a ramp tip according to the model of Suppe and Medwedeff (1990). (c) and (d) Two different modifications of the fold in (b). (c) Breakthrough above and hindward of the ramp tip in (b); identical geometries in the upper part of the fold can be attained by breakthrough of either fault-propagation or detachment folds. (d) Breakthrough is from the ramp tip to an upper flat, thereby destroying the ramp tip. After fig. 2 in Wallace and Homza (2004). Discussed in the text. (For interpretation of the references to colour in this figure legend, the reader is referred to the web version of this article.)

the top of a potentially ubiquitous martian megabreccia. In this model, the primary thrust rooted into the decollement directly below the kinematically upstream edge of the arch. Watters et al. (2004) compared the results of this thin-skinned modelling with the thick-skinned model of Golombek et al. (1991, 1990) and re-affirmed that thick-skinned deformation applies to lobate scarps, not to wrinkle ridges (however, see Peterson et al., 2020 for a possible thick-skinned interpretation of wrinkle ridges on Mercury). According to Watters et al. (2004), both fault-bend and fault-propagation models (Figs. 7 and 8) can account for the development of arches.

4.4.1. *Reversed symmetry wrinkle ridges in COULOMB*

Schultz (2000) had a different perspective on wrinkle ridge morphology and kinematics, compared with other workers. He presented wrinkle ridge topographical asymmetry in terms of a shallow-sloping forelimb ahead of a *"lobate front"*, with the wrinkle sitting above a steep backlimb slope (Figs. 12 and 13). This is potentially confusing. In short, he presented scarp slopes as back slopes and vice versa, wherein back slopes are located on the leading edge of the wrinkle ridge model, thereby placing scarp slopes at the trailing edge. In addition, he considered both folding and periodic wrinkle ridge spacing as functions of slip on the blind thrust, in contrast to previous models that invoked critical wavelength fold periodicity to account for ridge spacing (e.g. Watters, 1988, 1989, 1991; see Section 4.2). Schultz (2000) was critical of prior work, finding that *"… previous qualitative fault-based scenarios contained in the literature … lack a firm physical basis or predictive capability for wrinkle ridge morphology …"* and *"… for relating the morphology and topography of wrinkle ridges to the postulated subsurface structure"*. He added that *"… secondary structures are sometimes drawn artistically in the near surface"* (my emphasis).

Schultz (2000) introduced an empirical mechanical model, inspired by the work of Cooke and Pollard (1997), Roering et al. (1997) and Nino et al. (1998). He proposed that wrinkle ridges are the *"surface expression of anticlines that grow above a blind thrust as a result of both flexural-slip folding of near-surface strata and the nucleation and growth of echelon arrays of backthrust faults"*.Model backthrusts result from slip on horizontal layering in the vicinity of the upper (leading) tip of the primary thrust or reverse fault. Furthermore he proposed that spatial distribution of slip impedance and slip enhancement on the main thrust, predicted by his COULOMB modelling, can determine ridge spacing without the requirement for buckling. In Schultz (2000) new, synoptic model for wrinkle ridge formation (Fig. 14), *"Wrinkle-ridge-like morphologies can be produced due to slip along blind thrust faults … if layers above the upper fault tip slip along bedding and fold … and if backthrust faults develop"*. The

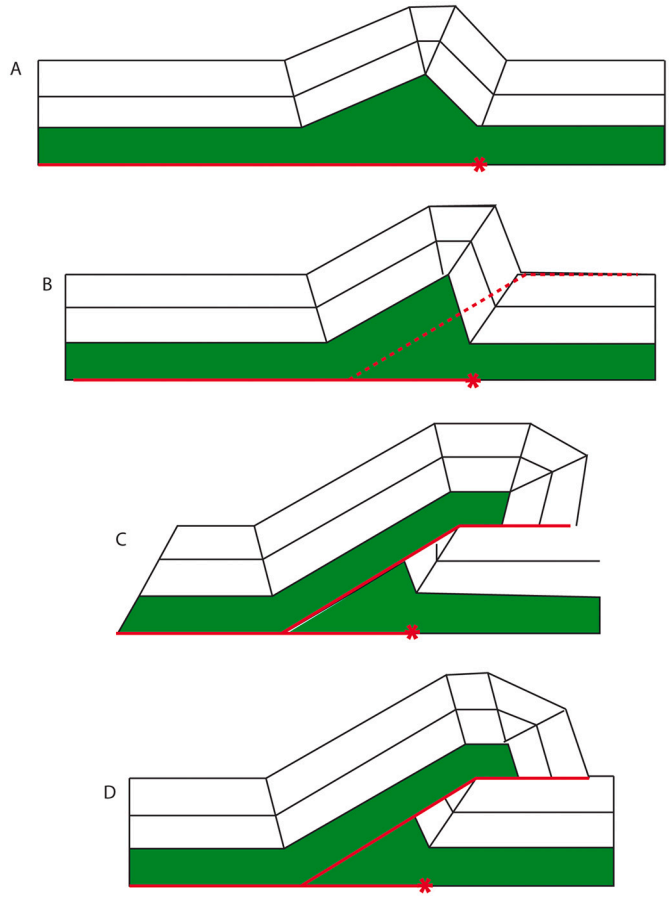

Fig. 15. Kinematic evolution of a thrust-truncated detachment fold according to Wallace and Homza (2004). Lower green layer is incompetent, upper layer is competent. (a) and (b): Evolution of a detachment fold with fixed hinges and rotating limbs. This figure emphasises that, although the geometry of the upper parts of the folds in Figs. 16 Ab and 16 Bb is identical, the depth to the decollement of a detachment fold is not uniquely determined by fold geometry, if detachment depth varies during fold growth by structural thinning or thickening of the incompetent layer. (c) and (d): Two different modifications of the fold in (b) by truncation and displacement along the trajectory shown by the dashed line. In (c), simple rotation of the hanging-wall ramp over the footwall ramp to-upper-flat transition results in the layer-parallel shear gradient shown. In (d), collapse and extension of part of the forelimb and flat crest of the fold allow rotation of the hanging-wall ramp without a layer-parallel shear gradient. After fig. 3 in Wallace and Homza (2004). Discussed in the text. (For interpretation of the references to colour in this figure legend, the reader is referred to the web version of this article.)

successful development of the backthrust is enhanced by near-surface flexural slip folding, which acts to reduce the stress magnitude at the upper (leading) tip of the main thrust, and *"determines mechanically whether a wrinkle ridge or a lobate scarp develops above the blind thrust"* (see also Watters, 2004; Andrews-Hanna, 2020). Okubo and Schultz (2004) were unequivocal: *"Back thrusts are not predicted (and do not occur) in mechanically homogeneous crust"*. However this assumption is contradicted by even simple analogue thrust experiments in isotropic sandbox systems with passive layering, as well as their numerical equivalents (e.g. Malavielle, 1984; Willett et al., 1993; Lin et al., 2005, their figs. 5–7; Saha et al., 2013, their fig. 6).

4.5. A paradigm shift?

To date, no axiomatic wrinkle ridge on an off-world telluric planetary body in the inner Solar System has been *demonstrated* to be the product of reverse or thrust faulting, with or without folding. Many hypotheses, models and interpretations have been proposed, but a robust "field" example is lacking (see above). Picking up on this, Cole and Andrews-Hanna (2017) examined an erosionally resistant ridge exposed in 3D in the wall of Melas Chasma, Mars (see Fig. 5a for location) as a test case for the geometry of faulting associated with wrinkle ridges. They concluded that (i) their results were incompatible with the notion of thick-skinned thrusting wherein faults descend to depths of 10s of kilometres because the faults would be too long to account for the observed ridge spacing on Mars; (ii) thin-skinned deformation begs the question of the accommodation of shortening at depth; and (iii) their results were incompatible with models of basement thrusting succeeded at shallower levels by layer-parallel shear within a layered cover sequence (cf. Schultz, 2000). Such conclusions provided little support for any of the previous models and hypotheses to explain wrinkle ridges.

Peterson et al. (2020) studied shortening tectonic features (*"… often suggested to be analogous to wrinkle ridges"*), in the volcanic smooth plains of Mercury. They estimated that the majority of the faults associated with their ~50 to >200 km long study features penetrate to greater than 15 km depth. Accordingly, they concluded that the thrusting is generally thick-skinned. However, they did not clarify whether the shortening tectonic features in the smooth plains are indeed wrinkle ridges, or not. This is important because, if they are, they would be thick-skinned, in contrast to most previous studies of wrinkle ridges throughout the inner Solar System. Alternatively, if they are lobate scarps occurring in plains materials, they would further blur the distinction between wrinkle ridges developed in anisotropic materials and lobate scarps developed in isotropic media.

In recent years some workers have become increasingly uncomfortable with the published, multifaceted, internally contradictory distinction of wrinkle ridges vs lobate scarps (e.g. Klimczak et al., 2019; however, see Karagoz et al., 2022). Byrne et al. (2014) departed from the original mechanical definition of lobate scarps formulated by Watters (1988) and Watters et al. (1998), stating that *"Lobate scarps are characterized by a steeply sloping scarp face and a gently sloping back limb, probably represent*[ing] *a monocline or asymmetric hanging-wall anticline atop a blind or surface breaking thrust fault, and are generally larger and presumably accommodated more shortening than wrinkle ridges"* (my emphasis; see also Mueller and Golombek, 2004; Giacomini et al., 2020). Byrne et al. (2014) preferred the term *"compressional tectonic features"* to describe what others had hitherto referred to as wrinkle ridges and lobate scarps (see also *"shortening tectonic features"* of Peterson et al., 2020; Byrne et al., 2015; Banks et al., 2015; Crane, 2020a). Klimczak et al. (2018) explicitly questioned and rejected the value of lobate scarp vs wrinkle ridge terminology based on surface topographical morphology: *"…* [this] *classification scheme breaks down in many cases due to the large variability of the shape of these landforms*". Their doubts were shared by Crane, 2020b: *"While asymmetric topography has been associated with landforms called lobate scarps and symmetric topography has been associated with so-called wrinkle ridges, many studies acknowledge that these titles represent endpoints on a broad spectrum of complex topographic patterns … a complexity that likely indicates variability in subsurface structures as well"*.

5. Is surface morphology structurally diagnostic of shortening mode?

For the better part of half a century, all of the foregoing reasoning has been based upon the premise that simple models of fold and thrust geometry, kinematics, mechanics, and even dynamics, can be constructed to replicate satellite-based remote observations of topographical morphologies of ridges on off-world planets of the inner Solar System. However, in a detailed study of fault propagation and detachment fold modelling, Wallace and Homza (2004) clearly showed that (i) a given asymmetrical surface morphology can be produced by different fold-thrust models; and (ii) a given fold-thrust model can produce different surface morphologies (Figs. 14, 15 and 16). Their kinematic modelling

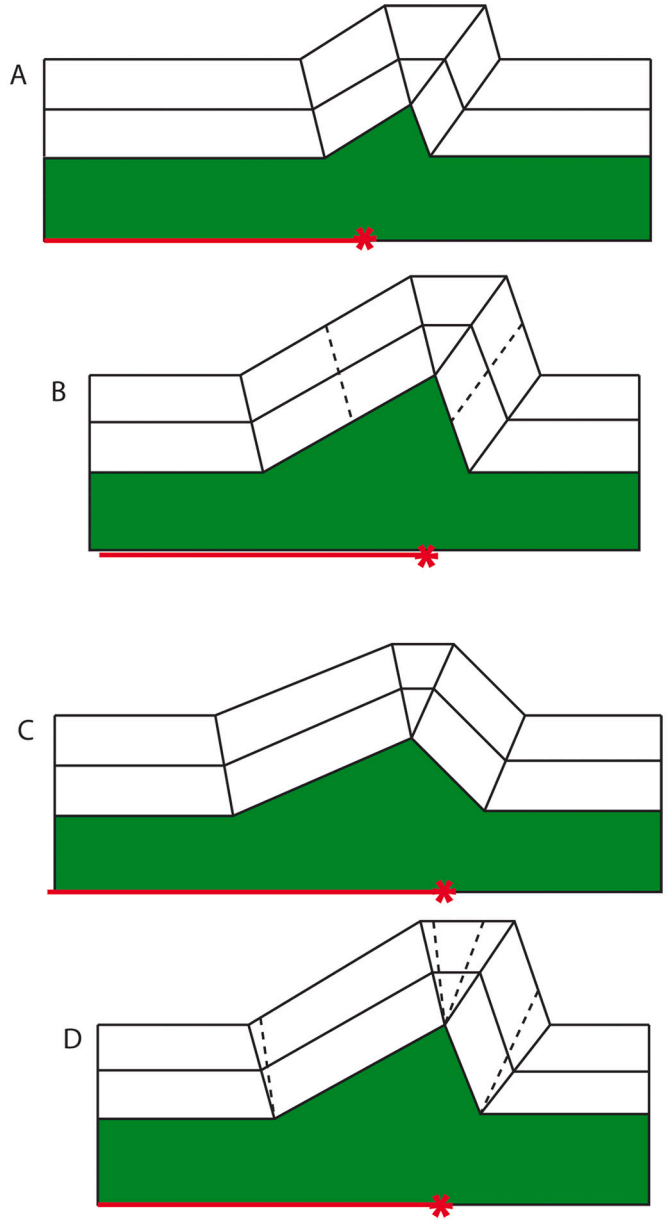

Fig. 16. Different kinematic models for detachment folds according to Wallace and Homza (2004). Lower, green layer is incompetent, upper layer is competent. (a and b): Kinematics of a migrating hinge, non-rotating limb detachment fold. Constant limb dip and constant detachment depth are maintained by outward migration of the synclinal hinges. Dashed lines in (b) indicate the position of the synclinal hinges in (a). The forward synclinal hinge migrates with a propagating decollement tip. (c and d) Kinematics of a fixed hinge, rotating-limb detachment fold. Fixed hinges require steepening of limbs and a change of structural thickness of the incompetent layer to accommodate change in the area of the fold core. Hinges are fixed to points at the incompetent-competent layer contact, but must rotate to allow parallel folding of the competent layer. Dashed lines in (d) indicate the position of the synclinal hinges in (c). The decollement tip does not propagate with fold growth. After fig. 5 in Wallace and Homza (2004). Discussed in the text. (For interpretation of the references to colour in this figure legend, the reader is referred to the web version of this article.)

unambiguously showed that fault propagation folds can be modified and truncated by flat-ramp-flat break-through thrusting, that may or may not daylight, without major change in the overall signature of the surface topographical morphology. The principal changes in surface morphology with progressive deformation are due to widening and/or rotation of segments of the folded anisotropy, and fold hinge migration (Fig. 14). These considerations were not included in the elastic dislocation modelling of off-world shortening tectonic features (wrinkle ridges and lobate scarps) reviewed in Section 4.4.

Similar results were obtained by Wallace and Homza (2004) for modification and truncation of a detachment fold (developed above a confined, layer-parallel, contractional fault) by a daylighting break-through thrust ramp (Fig. 15). Indeed, (i) a detachment fold with a migrating hinge and non-rotating limbs associated with a propagating detachment tip, and (ii) a fold with a fixed hinge and rotating limbs associated with a non-propagating detachment tip both produce identical surface morphologies (Fig. 16). Wallace and Homza (2004) were unequivocal: *"... the geometric conditions that are necessary for a fault-propagation fold and are diagnostic for a detachment fold can be documented only if the geometry of the core of the fold is well known"*, a requirement that is not met by remote observation of "closed" topographical features from orbit. Note that competency contrasts included in Wallace and Homza (2004) model fold profiles can be matched off-world by stiff layered basalts and less competent, weathered lava tops or regolith. In short, Wallace and Homza (2004) demonstrated that surface topographical morphology is not geometrically, kinematically or mechanically diagnostic in the manner in which it has been extensively used in off-world planetary structural geology of the inner Solar System. Note also that Plotek et al. (2021) showed that topologies and asymmetries predicted by fault bend folding, fault parallel flow and inclined-shear models can also be satisfied by a backlimb trishear model (Fig. 17). In any event, simplistic fold-thrust models, such as those used in elastic dislocation modelling of off-world shortening tectonic features are demonstrably geologically unrealistic (e.g. Cawood and Bond, 2020; Butler et al., 2020; Crane, 2020a, 2020b).

6. Regional patterns of distributed shortening are problematic

So far, I have reviewed the development of thought regarding distributed off-world shortening tectonic features at the level of individual structures. However, wrinkle ridges and lobate scarps have commonly been reported from Venus as penetratively developed map-scale patterns. Linear, sub-parallel, periodically-spaced, very high aspect ratio (100 s) features, are uniformly distributed over vast areas measuring hundreds to thousands of kilometres both along and across strike. They are also reported as occurring with intersecting, reticulate (net-like) geometries (see next Section). This raises at least two fundamental structural geological questions which have not been directly addressed to date: (i) how does uniform, distributed, low-magnitude shortening associated with periodic faulting occur over regional-scale distances (see Section 6.3); and (ii) how does it occur without resulting in regional-scale strain localisation (see Section 6.4).

6.1. *Intersecting wrinkle ridge patterns*

Numerous studies within the inner Solar System have reported local- to regional-scale patterns of at least two sets of ridges, including reticulate (Raitala, 1988) or polygonal configurations, mutually intersecting at medium to high angles. They were interpreted according to the thrust/fold wrinkle ridge models reviewed above (Chicarro et al., 1985, their fig. 2d; Watters and Chadwick, 1989, their fig. 1; Squyres et al., 1992, *"superposed"* wrinkle ridges; Watters, 1993, his fig. 6; McGill, 1993, his figs. 1, 4 and 5; Mangold et al., 1998, their fig. 2; 2000, their fig. 2; Bilotti and Suppe, 1999, their fig. 1b; DeShon et al., 2000, their fig. 4; Mueller and Golombek, 2004, their figs. 4, 5 and 6; Young and Hansen, 2005, their fig. 2; Ivanov and Head, 2011, their figs. 9c and d; Williams et al., 2019, their fig. 6; Fig. 18). In all cases, both sets of wrinkle ridges are periodically spaced, and interpreted as the polyphase product of fault-bend folding (see Fig. 7) in basaltic lava flow sequences, potentially associated with up to 90° rotation of the principal compressive stress in the horizontal plane (e.g. Watters, 1989, 1991).

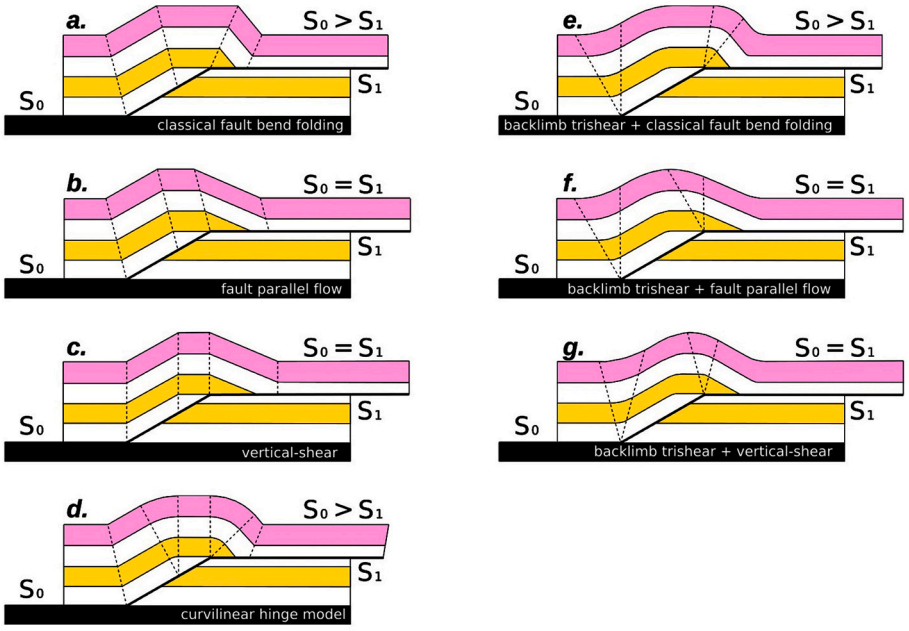

Fig. 17. Different geometric-kinematic models for a single step fault bend fold according to Plotek et al. (2021). A: classical fault bend model. B: Fault parallel flow model. C: Incline-shear model. D: Curvilinear hinge model. E, F and G show backlimb trishear with asymmetries that satisfy those of A, B and C, respectively. S0 is applied slip; S1 is transmitted slip. Fig. 1 in Plotek et al. (2021). With permission from Elsevier.

Exceptionally, on Mars, Watters (1993) interpreted reticulate patterns in terms of local subsidence, that *"... may have been facilitated by magma-ice interactions within the* [underlying?] *highland* [material]" (Fig. 18b). However, this ad hoc hypothesis would not be generally applicable to reticulate wrinkle ridge patterns identified on Venus or Mercury. On Venus, McGill (1993) observed that *"In most places there are two or more sets of wrinkle ridges ... and commonly one of these persists over a very large area ... Intersection relationships indicate that these domains differ in age"*. However, DeShon et al. (2000) proposed that some sets were coeval. Moreover, McGill (1993) suggested that regionally extensive wrinkle ridge patterns tend to be overprinted by more local patterns. Global- and regional-scale mapping on Venus indicated that the local patterns tend to be concentric about, and perhaps related to, local magmatic or volcanic features (Basilevsky, 1994; Bilotti and Suppe, 1999, their fig. 10; Supplemental 1). Note that this is a potentially different setting from the reticulate patterns of intersecting wrinkle ridge sets.

At least two major problems are presented by intersecting, regional-scale wrinkle ridge sets. First, regardless of the relative timing of the ridge sets, buckling of layering by a set of folds tends to pin the layers and impede slip with respect to a second set of folds imposed at a high angle. Second, applying a wrinkle ridge model that includes periodically-spaced reverse or thrust faulting would lead to a dilational, chaotic pattern of fracturing, rather than a systematic, non-dilational, bimodal reticulate pattern. This isespecially the case in a near-surface brittle environment where the dampening effect of confining pressure would be minimised (e.g. Hanmer, 1989). Note that, regarding Mars, Watters et al. (2004) acknowledged that *"Bifurcating, crisscrossing, and cross-cutting wrinkle ridges indicate a complex pattern of deformation and evolution of stresses that are a challenge to both thick- and thin-skinned models"* (see also Watters and Chadwick, 1989). On Venus, Sandwell et al. (1997) explicitly opted to avoid intersecting wrinkle ridge patterns. Again regarding Venus, McGill (1993) sought a possible solution by analogy with multiple joint sets: "... *members of a younger set commonly terminate against older, through going joints because the older joints act as barriers to the propagation of the younger joints. Similar relationships are common where two sets of wrinkle ridges intersect on Venus"* . The unrecognised problem here is that joints and faults are not mechanically analogous. Axiomatically, joints do not involve slip, unlike reverse/thrust faults (e.g. Passchier et al., 2021 and references therein).

6.2. *Regional- to planet-scale linear patterns*

Planetary scientists commonly appeal to terrestrial analogues to justify kinematic, dynamic and mechanical interpretations of distributed shortening tectonic features on off-world bodies of the inner Solar System (see Section 7). However, off-world shortening tectonic features are also represented in regional- to global-scale map patterns. Regional-scale patterns of fold-and-thrust belts are well-documented and understood on Earth (e.g. Hubbert and Rubey, 1959; Dahlstrom, 1970; Elliott, 1976; Chapple, 1978; Coward and Kim, 1981; Price, 1981; Boyer and Elliott, 1982; Suppe, 1983; Boyer, 1986; Butler, 1986, 1992; Pfiffner, 2014; see Butler et al., 2018 and references therein). Nonetheless, as Butler et al. (2020) cautioned, *"Subsurface interpretation in frontier fold–thrust belts ... is an exercise in uncertainty management"*; all the more so when one is limited to remote observation of surface topography from orbit.

Terrestrial patterns of shortening tectonic features represent extensive, linear belts of folds and thrusts within which strain localises as regional-scale master faults that accommodate most of the imposed bulk shortening as deformation progresses. However, vast swarms of periodically-spaced, minimum displacement thrusts that incipiently daylight, uniformly developed over vast distances both along- and across-strike, are not characteristic features of terrestrial tectonics. Nor are well-behaved, multiple sets of thrusts that mutually intersect at high-angles.

By contrast, the extensive, distributed nature of regional and global-scale patterns of off-world wrinkle ridges (Fig. 19a, b and c) is inherently mechanically problematic on at least two counts: (i) volume-constant (isochoric) deformation is commonly assumed, rather than justified, on Mercury and Mars (see Section 6.3); and (ii) the common absence of regional-scale strain localisation (see Section 6.4), as revealed by the map-scale patterns on (a) Mercury (e.g. Melosh and McKinnon, 1988, their fig. 7); Byrne et al., 2014, their fig. 2; Klimczak et al., 2015, their fig. 2; Watters et al., 2015a, their fig. 3a; Peterson et al., 2020, their fig. 1; Giacomini et al., 2020, their figs. 1, 2, 4, 6, 8, and 10); (b) Venus (e.g. Squyres et al., 1992, their fig. 5a; Banerdt et al., 1997, their fig. 2;

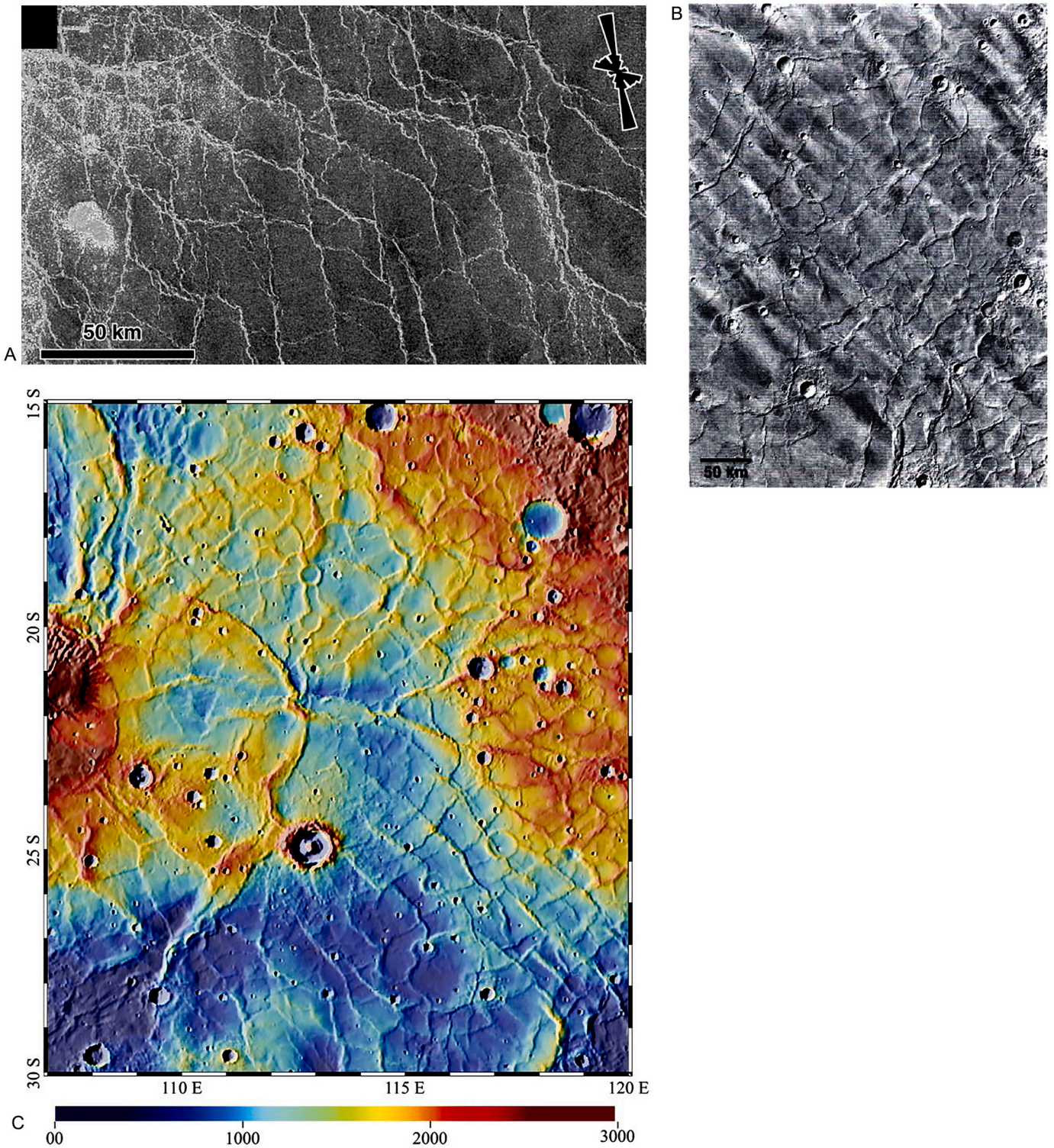

Fig. 18. (A) Wrinkle ridges on a volcanic plain onVenus. Note the bimodal orientations. The rose diagram at upper right is weighted by wrinkle ridge length. Part of fig. 1 in Bilotti and Suppe (1999). With permission from Elsevier. (B) Wrinkle ridges form an intricate, reticulate pattern on Mars. Fig. 6 in Watters (1993). According to that author, numerous circular wrinkle ridges indicate the influence of buried craters on the formation of these structures and the importance of subsidence. (C) Colour-shaded relief map from a MOLA digital elevation model, Mars. Fig. 5 in Mueller and Golombek (2004). According to these authors, ridges in this region are noted for their circular morphology, interpreted as being produced by shortening of buried craters. Scale of this image is approximately 60 km per degree latitude. Colour bar denotes surface elevation of surface in meters relative to the Mars geoid. Discussed in the text. (For interpretation of the references to colour in this figure legend, the reader is referred to the web version of this article.)

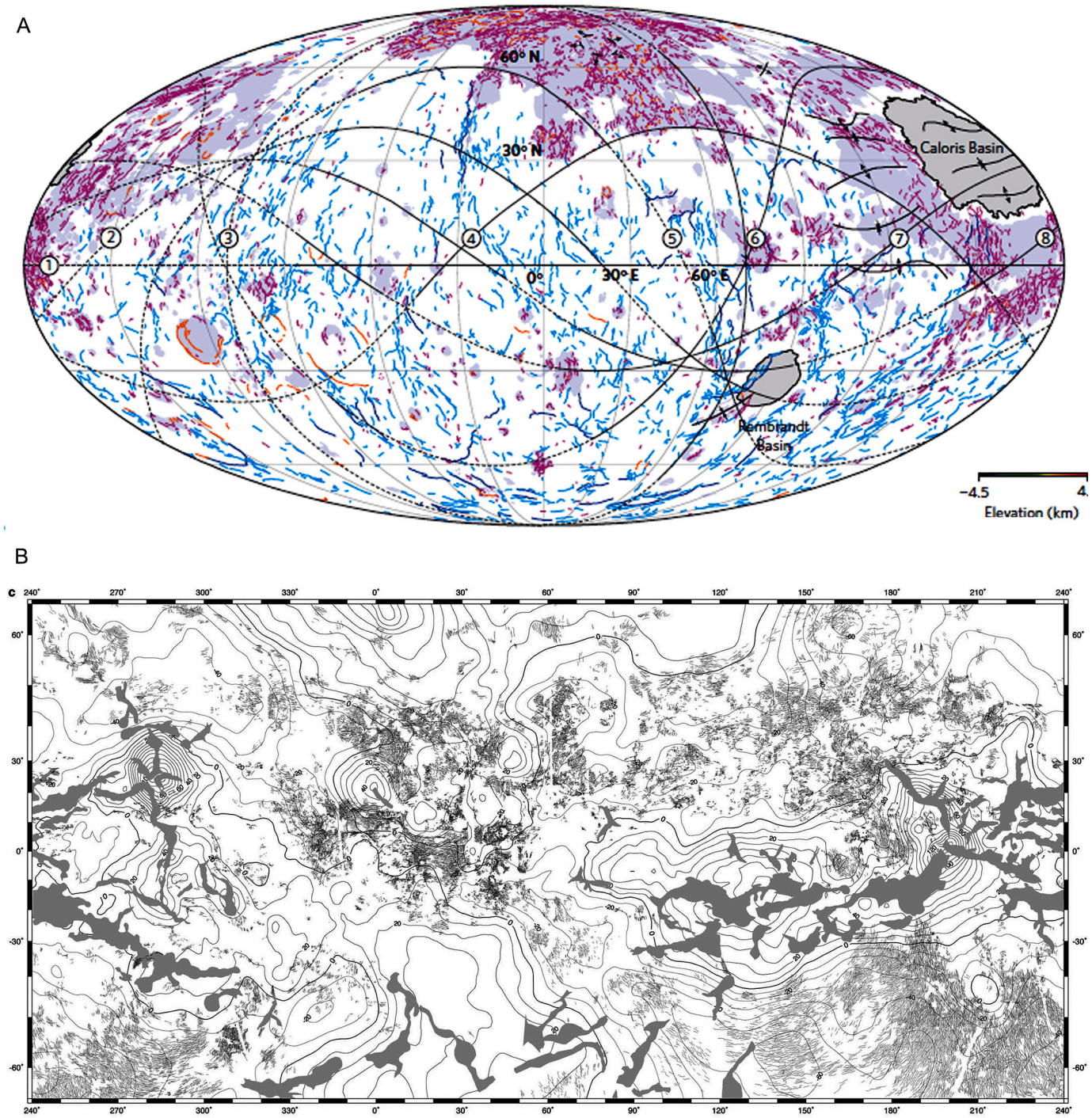

Fig. 19. Regional and global-scale maps of wrinkle ridge distribution patterns on Mercury, Venus and Mars. (A) ~6000 shortening structures on Mercury, classified as thrust-fault-related landforms on volcanic plains. Line colours (purple, blue and orange) correspond to different types of plains. Black lines mark the crests (opposing arrows) and troughs (facing arrows) of long-wavelength topographic undulations. Fig. 2 in Byrne et al. (2014). With permission from Springer Nature. (B) Global wrinkle ridge distribution on Venus is draped over contours of geoid height (units in meters); grey polygons are rift zones. Fig. 2 in Bilotti and Suppe (1999). With permission from Elsevier. (C) Hemisphere-scale distribution of ridges occurring in (a) the old terrains and (b) the smooth plains of Mars. A = Argyre; EL = Elysium. Fig. 4 in Chicarro et al. (1985). With permission from Elsevier. (For interpretation of the references to colour in this figure legend, the reader is referred to the web version of this article.)

Sandwell et al., 1997, their fig. 2; Bilotti and Suppe, 1999, their fig. 2; Young and Hansen, 2005, their fig. 2; Hansen and Olive, 2010, their fig. 1; Fernández et al., 2010, their figs. 2 to 6; Hansen, 2018, her figs. 1 and 2); and (c) Mars (e.g. Chicarro et al., 1985, their fig. 4; Watters, 1993, his plates 1 and 2; Schultz and Tanaka, 1994, their fig. 1; Mège and Masson, 1996a, 1996b, their fig. 1 in both). Locally, this also holds true for the Moon (Fig. 20a and b), at least for parallel wrinkle ridges (e.g. Yue et al., 2015, their fig. 4), as well as lobate scarps (e.g. Watters et al., 2015b, their fig. 2; Williams et al., 2019, their fig. 6). With respect to Venus, McGill (1993), addressing one aspect of the issue, put it succinctly: *"How*

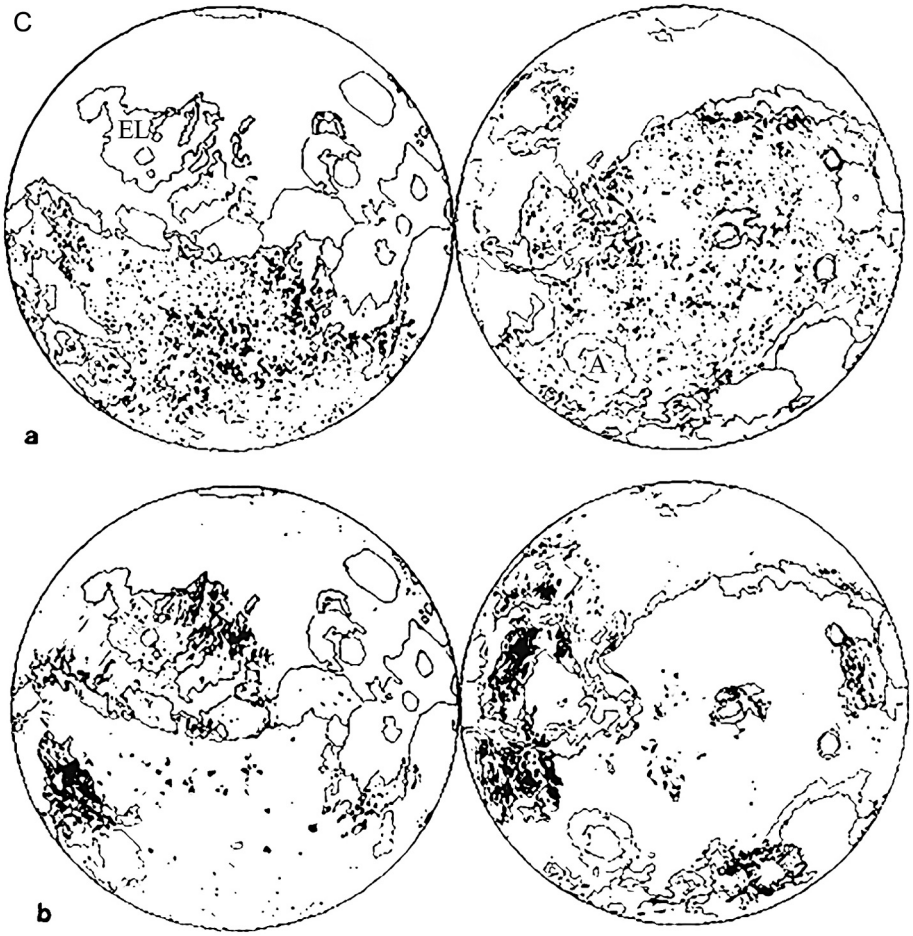

Fig. 19. (*continued*).

orientations of stress trajectories can maintain coherence over such great distances in a thin plate is one of the major problems of venusian structural geology".

6.3. Distributed low magnitude bulk strain

As noted above, most off-world distributed shortening tectonic features (a.k.a. wrinkle ridges) in the inner Solar System have been interpreted to represent low values of bulk strain. This raises the issue of generating widespread, distributed shortening associated with very low bulk strains by the transmission of far-field imposed compressive stress, especially if deformation is not isochoric (volume-constant). On the Moon, low values of shallow-seated shortening should be accommodated by compaction of the porous regolith, (e.g. Binder and Gunga, 1985; Watters et al., 2010; Clark et al., 2017), although thickness estimates appear to be highly variable (e.g. Zhu et al., 2021; Izquierdo et al., 2021). Such non-isochoric deformation would impede the transmission of far-field compressive stress over long distances. Binder and Gunga (1985) were well aware of this issue. Regarding their sandbox analogue experiments, they stated that *"... if the material is not reasonably well packed, no thrust faults form. The entire shortening ... is taken up by compaction"*. Megaregolith has also been identified as a mechanically important feature in the formation of extensive, distributed shortening tectonic features on Mars (e.g. Golombek, 1985; Watters, 1988, 1991; Zuber and Aist, 1990; Mangold et al., 1998), and significant regolith is reported (e.g. Langevin, 1997; Fegan et al., 2017) or inferred (e.g. Watters, 2021) on Mercury. Accordingly, one may ask how compressive stress can be extensively transmitted through porous natural media resulting in only very low values of bulk strain, other than via a body force, such as gravity sliding (e.g. McGill, 1993), and how that would apply on vast, flat volcanic plains? In addition, how applicable is elastic dislocation modelling (see Section 4.4) with respect to shallow-seated reverse and thrust faults in highly porous media, especially if the porous medium is rheologically heterogeneous? These questions have not been directly addressed in the planetary science literature.

6.4. Lack of localisation of distributed shortening strain

As noted above, strain localisation in natural materials is an unavoidable fact of structural geology. Classical terrestrial manifestations of strain localisation during shortening in the brittle field would include regional-scale master thrust faults, such as those that characterise the Canadian Rockies and Appalachians (e.g. Wheeler et al., 1996 and references therein), to name but two examples. However, the regional- and global-scale map patterns of shortening tectonic features mapped on Venus, as well as Mercury and Mars (Fig. 19a, b and c), while extending over distances well in excess of 1000 km across strike, do not show a marked tendency for deformation to be localised in regional-scale master reverse or thrust faults. Instead, as noted above, they are characteristically described as representing low values of distributed strain. The principal exceptions to this are the largest lobate scarps on Mars (e.g. Amenthes Rupes; see also Ogygis, Phrixi and Bosporos rupes; see Fig. 5a for locations) and Mercury (e.g. Discovery Rupes; Victoria and Endeavour rupes and Antoniadi Dorsum; see Figs. 4a, 5b and 21 for locations) that occur in splendid isolation (e.g. Watters et al., 2000), yet they have been compared to terrestrial fold-thrust belts (e.g. Byrne et al., 2014). However, large, off-world lobate scarps might be more readily compared, at least geometrically, with similarly isolated thrusting

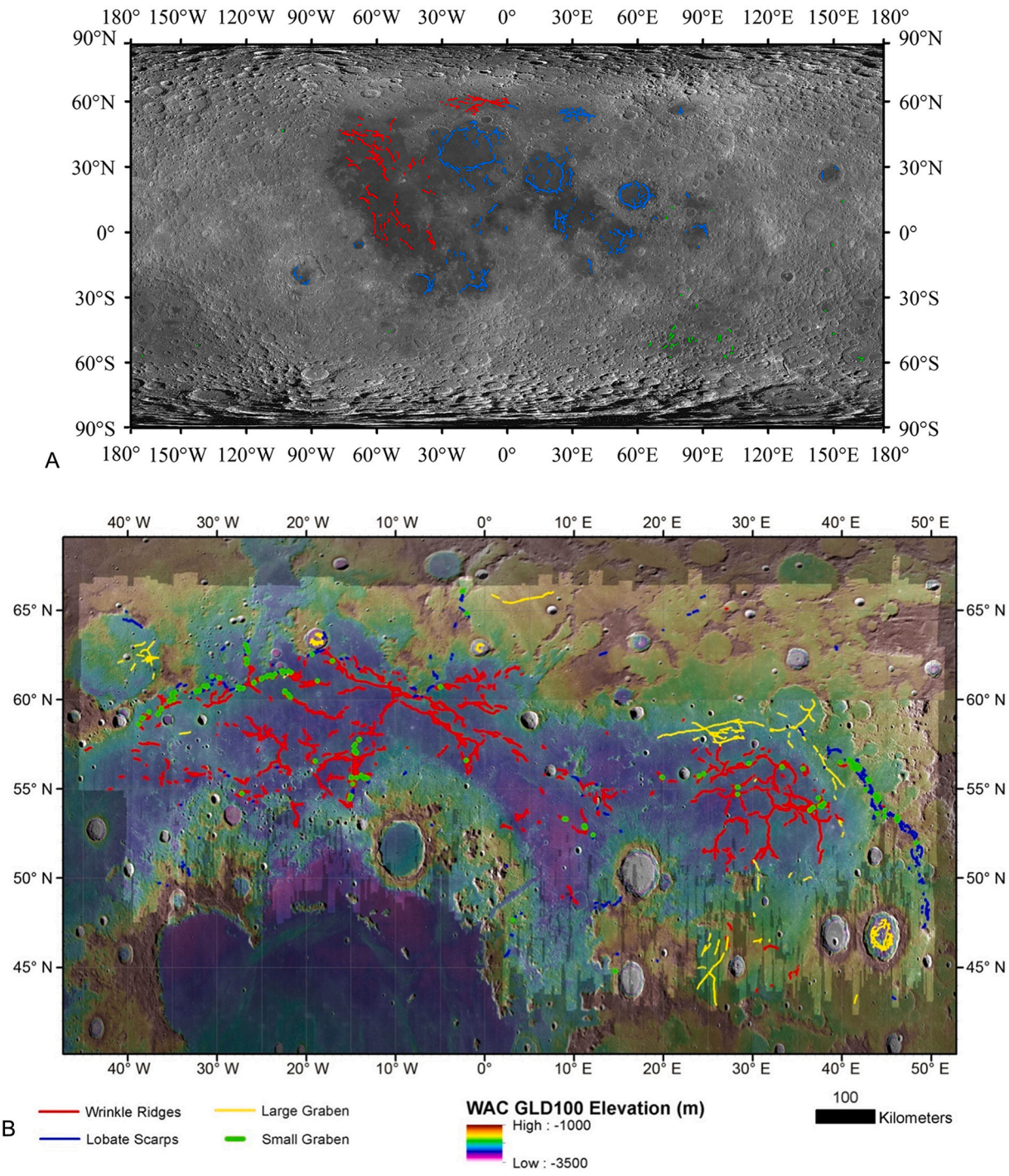

Fig. 20. Regional and global-scale maps of wrinkle ridge distribution patterns on the Moon. (A) Global distribution of lunar wrinkle ridges. Blue, red, and green lines represent segments of concentric, parallel, and isolated ridges, respectively. Screen capture of fig. 4 in Yue et al. (2015). (B) Tectonic map of Mare Frigoris, Moon, draped over colorized shaded relief. Wrinkle ridges (red), lobate scarps (blue), large and small graben (yellow and green, respectively) are shown. Fig. 6 in Williams et al. (2019). With permission from Elsevier. Discussed in the text. (For interpretation of the references to colour in this figure legend, the reader is referred to the web version of this article.)

reported from terrestrial Archean (e.g. Hanmer and Greene, 2002; Hanmer et al., 2006), Neoproterozoic (e.g. Hanmer, 1988b; Hanmer and McEachern, 1992; Nadeau and Hanmer, 1992) and Phanerozoic settings (e.g. Xue et al., 2021), albeit now exposed in the mid- to lower-crust. Specifically regarding Venus, Solomon et al. (1991) suggested that the lack of strain localisation *"… reflect*[s] *a crustal response to mantle dynamic processes … A strong coupling of mantle convection to the upper mantle portion of the lithosphere, probably because Venus lacks a mantle low-viscosity zone, leads to crustal stress fields that are coherent over large distances"*. However, this suggestion does not explain the non-localised nature of the local structural response to far-field boundary conditions, because localisation of deformation is a function of strain, strain rate, local material properties and strain softening, rather than stress fields (e.g. Poirier, 1980; Hobbs et al., 2015). The general absence of regional-scale strain localisation in distributed deformation patterns on off-world bodies of the inner Solar System in general, and Venus in

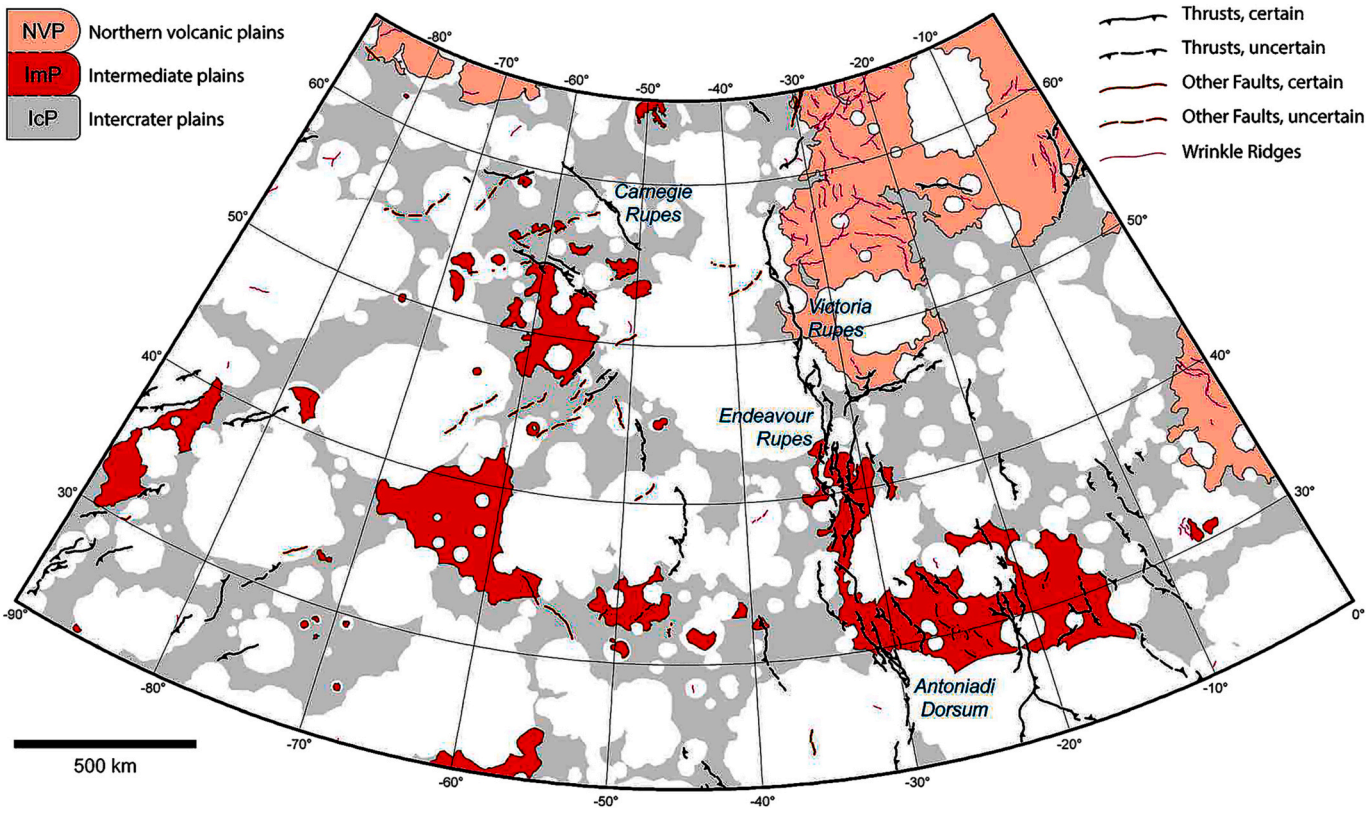

Fig. 21. Simplified version of the geological map of part of Mercury, including the Victoria-Enterprise-Antoniadi lobate scarp array (VEA; see Fig. 5b for location). Fig. 3 in Galluzzi et al. (2019). Discussed in the text.

particular, is indeed *"enigmatic"* (Solomon et al., 1992) and *"perplexing"* (Banerdt et al., 1997).

7. Terrestrial analogues of wrinkle ridges revisited

Given the difficulties inherent in remote geological mapping of off-world telluric bodies in the inner Solar System, it is not surprising that most basic structural geology studies of such bodies have turned to terrestrial analogues to support their interpretations. This, despite Ghail (2002) caution that *"The subjectivity of this process can limit the ability to constrain the range of geologically-plausible interpretations"*. Most terrestrial analogues have been cited in support of models of off-world distributed shortening, and will be reviewed here in that light. The principal exception to this was the invocation of graben in the Utah Canyonlands as an analogue for tessera terrain ribbons (Ivanov and Head, 1996; Hansen et al., 1999, 2000), to which Schultz et al. (2007) has provided a comprehensive dissenting view.

Since the mid-1980s, the spectrum of cited terrestrial analogues for distributed shortening on off-world telluric bodies in the inner Solar System has progressively contracted, now favouring only a select few. Plescia and Golombek (1986) is the single, most frequently cited paper regarding terrestrial analogues for wrinkle ridges. On the basis of previously published studies by others, Plescia and Golombek (1986) presented six terrestrial sites, ranging from the Yakima Fold Belt, Washington, via recent surface-breaking seismic faulting, to the asphalt of a deformed tennis court and the congealed crust of a Hawaiian volcanic crater. Of these examples, the Yakima Fold Belt is still the most extensively cited in subsequent studies: e.g. *"The Yakima folds … are the best wrinkle ridge analogues on Earth … and provide a unique opportunity to determine a wrinkle ridge structural model"* (Mege and Reidel, 2001).

Plescia and Golombek (1986) were well aware that they were comparing surface topographical morphologies. They described " … *examples of surface deformation on Earth that are morphologically similar to the wrinkle ridges observed on the Moon, Mars, and Mercury"*, and concluded that *"The similarity in morphology and structural setting of both groups of features suggest* [sic] *that they are the result of similar deformation mechanisms"*. Most tellingly, *"Because these* [terrestrial analogues] *are morphologically similar to planetary wrinkle ridges, we conclude that wrinkle ridges, are also the result of deformation of surface rocks over thrust faults*" (my emphasis). Essentially, this has remained the basis for invoking terrestrial analogues ever since. However, careful reading of the original papers cited by Plescia and Golombek (1986) calls their application as analogues for off-world structures into question.

7.1. Yakima Fold Belt

Plescia and Golombek (1986) presented the Yakima Fold Belt as a set of *E*-W trending, asymmetrical ridges, <150 km long by up to 6 km wide, commonly associated with anticlines. However, local field studies (e.g. Barrash et al., 1983) did not report the rise-ridge-wrinkle surface topographical morphology of axiomatic wrinkle ridges (see Section 4). Rather, Barrash et al. (1983) described a tectonic context of polyphase deformation with evolving, complex tectonic boundary conditions, including basement uplift: *"the* [Columbia] *plateau cannot be fully understood until it is placed into the larger picture of late-Cenozoic tectonism of the western United States"* (see also Reidel et al., 1994; Kelsey et al., 2017). Geophysical studies have also highlighted the crustal-scale complexity of the Columbia Plateau upon which the Yakima Fold Belt is located (e.g.; Blakely et al., 2011). Seismology has revealed that this complexity is due to superposed episodes of extension and shortening, and gravity gradients may indicate the presence of tilted fault blocks or half graben at depth (Catchings, 1994; Saltus, 1994). Indeed, the central Columbia Plateau may be underlain by a continental rift system (Catchings and Mooney, 1988). In addition, the Yakima Fold Belt sits in the back arc of the Cascadia convergent margin, very close to the pole of plate rotation for Oregon Coast Range domain relative to North America

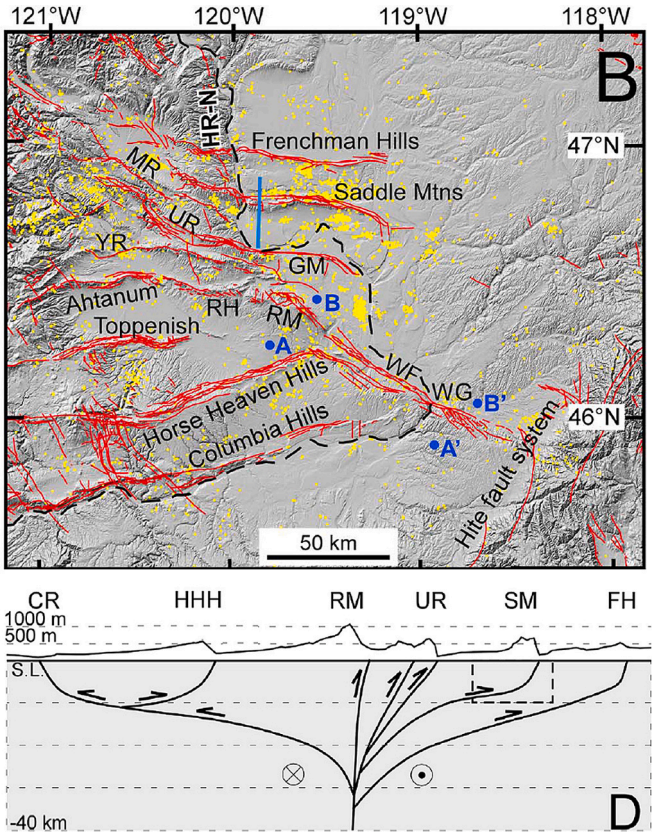

Fig. 22. Upper: Digital elevation model of the Yakima Fold Belt, Washington, and associated faults. Red lines are faults; yellow dots are earthquakes greater than magnitude 2 since 1970. Black dashed line is the Columbia River. MR = Manastash Ridge; UR = Umtanum Ridge; GM = Gable Mountain; YR = Yakima Ridge; RH = Rattlesnake Hills; RM = Rattlesnake Mountain; WG = Wallula Gap; HR-N = Hog Ranch-Naneum anticline. Part of fig. 2 in Pratt (2012). Lower: N-S topographic profile near the blue line in the top image, with a possible splay fault (flower structure) interpretation for the faults forming the Yakima Fold Belt (note different scales above and below sea level). The only control on fault depth is beneath the Saddle Mountains (SM; dashed rectangle); the remaining geometries are inferred from generalised studies of strike-slip splay faults. Part of fig. 4 in Pratt (2012). (For interpretation of the references to colour in this figure legend, the reader is referred to the web version of this article.)

(Blakely et al., 2011 and references therein). This structural complexity, directly related to a terrestrial plate tectonic setting, does not compare well with vast volcanic plains on off-world single plate planets of the inner Solar System.

Local field mapping studies of parts of the Yakima Fold Belt also highlight major differences with respect to models of axiomatic wrinkle ridges. For example, Hagood (1985) described and illustrated box-style folding associated with reverse faults and thrusts, supported by abundant cross-sections that include extensional accommodation faults that do not correspond to the geometrically simple elastic dislocation modelling of off-world wrinkle ridge models (see Section 4.4). He observed that thrust faults steepen with depth, and questioned the existence of an underlying decollement. In addition, the axiomatic rise-ridge-wrinkle surface topographical morphology of off-world wrinkle ridges is absent (see also Reidel et al., 2021, their figs. 5 and 10).

Modelling stress fields, Pratt (2012) evaluated the Yakima Fold Belt as a set of splay faults at the NW end of a controversial, possibly dextral strike slip, Olympic-Wallowa Lineament (OWL), potentially part of a set of megashear fault systems that bound the northern edge of the Basin and Range province located to the South (Fig. 22). According to this interpretation, folding developed after thrusting when the regional principal shortening direction rotated. He proposed that the Yakima Fold Belt corresponds to a thin-skinned flower structure (see Christie-Blick and Biddle, 1985 for model details; Fig. 22). However, the required fault dip flattening is not apparent in the seismic profile presented (his fig. 4), and only a single thrust is indicated as antithetic (his fig. 4d). In another seismic study, Kelsey et al. (2017) drew *"inferred"* thrust faults that flatten with depth, from which they derived balanced cross-sections. However, this is not apparent from their seismic sections (their fig. 11), and they admitted that fault plane orientations are difficult to see below ~500 m depth. Note that Reidel et al. (2021) challenged the existence of strike-slip motion on the OWL. In addition, their figs. 5 and 10 clearly show most frontal ridge slopes as subtended by reverse faults that steepen with depth. They also show that back-thrusting above the frontal ridge slopes (Schultz, 2000; see Section 4.4.1) is extremely rare.

Crane (2020a) was the first study to critically evaluate the Yakima Fold Belt as an analogue for off-world wrinkle ridges. She found that the analogy was incomplete:traditional elastic dislocation modelling (see Section 4.4) had hitherto focused on *"reproducing topography and not reproducing cross sectional geology"*. Moreover, it had underestimated the contribution of the fold component of shortening required to account for the topographical landforms by 60–90% (see also Crane and Klimczak, 2019). Nonetheless, Crane (2020a) found that fault-bend fold models (Fig. 7) were the most appropriate for constructing cross sections across Yakima Fold Belt ridges. She also determined that faults associated with the topographical ridges dip very shallowly (3–10°), then steepen and shallow again with depth (see also Hagood, 1985; Reidel et al., 2021), in contrast to the simple planar or listric faults simulated in elastic dislocation modelling. Crane (2020a) concluded that the *"lost shortening"* is a major gap in planet-scale interpretations based upon global contraction.

7.2. Other analogues

Plescia and Golombek (1986) also proposed less well-known terrestrial analogues for off-world wrinkle ridge formation, including then recent seismic slip along a ~ 37 km strike-parallel section of the Meckering fault, Australia, which broke the ground surface in sandy lateritic soil (Gordon and Lewis, 1980). Plescia and Golombek (1986) stated that *"In most places, an anticlinal or monoclinal ridge formed, although locally a clean fault break developed ... The anticlines are asymmetric in profile; thrust faults developed at the base of the steeper side. Splaying of the main thrust at the surface into smaller parallel and antithetic faults is common. Antithetic faulting results in ridges that are bounded on both sides by thrust faults ... These antithetic surface faults most likely merge into a single east-dipping fault at depth"*. However, this simple description does not correspond to the complex surface topographical morphology of axiomatic off-world wrinkle ridges (rise, ridge and wrinkle) associated with blind thrusts (see Section 4). In addition, images of the Meckering fault (their figs. 3 and 4) provided no direct evidence for the proposed antithetic back-thrusting. Importantly, neither the survey report by Gordon and Lewis (1980), nor a more recent summary of the Meckering fault (Johnston and White, 2018), report antithetic thrusting or fold asymmetry reversals. Instead, emphasis was placed on the role of strike-slip motion in determining the overall surface morphological patterns. In addition, Gordon and Lewis (1980, their figures 74 and 75) interpreted the Meckering fault as the rim and base of a concave-upward *"spherical cap"* located above, and driven by, an unseen strike-slip shear zone hidden at depth, associated with modern plate tectonic interaction of Western Australia and the Indian-Australian plate (their fig. 90). Moreover, the subsurface Meckering fault occurs in high grade metagranites and metasediments of the Yilgarn Craton, more akin to a lobate scarp environment than a layered wrinkle ridge setting (see Section 4). Once again, one might question the Meckering fault as an appropriate analogue for structural interpretation of the crust of a single plate planet.

Similarly, Plescia and Golombek (1986) described recent seismic slip

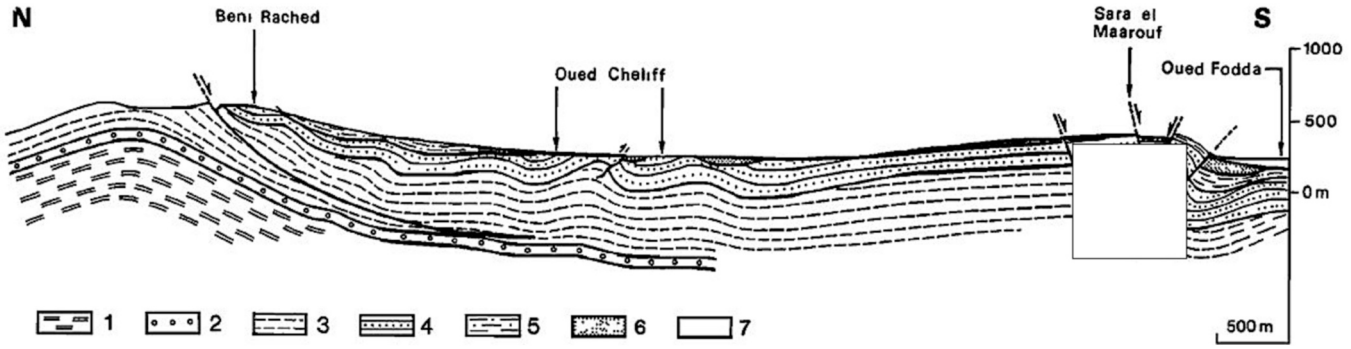

Fig. 23. N-S geological cross-section between Beni Rached and Oued Fodda, Maghreb Ranges, Algeria. Numbers 1–7 refer to various marls, sandstones and conglomerates. Fig. 29 in Philip and Meghraoui (1983). Discussed in the text. With permission of John Wiley and Sons.

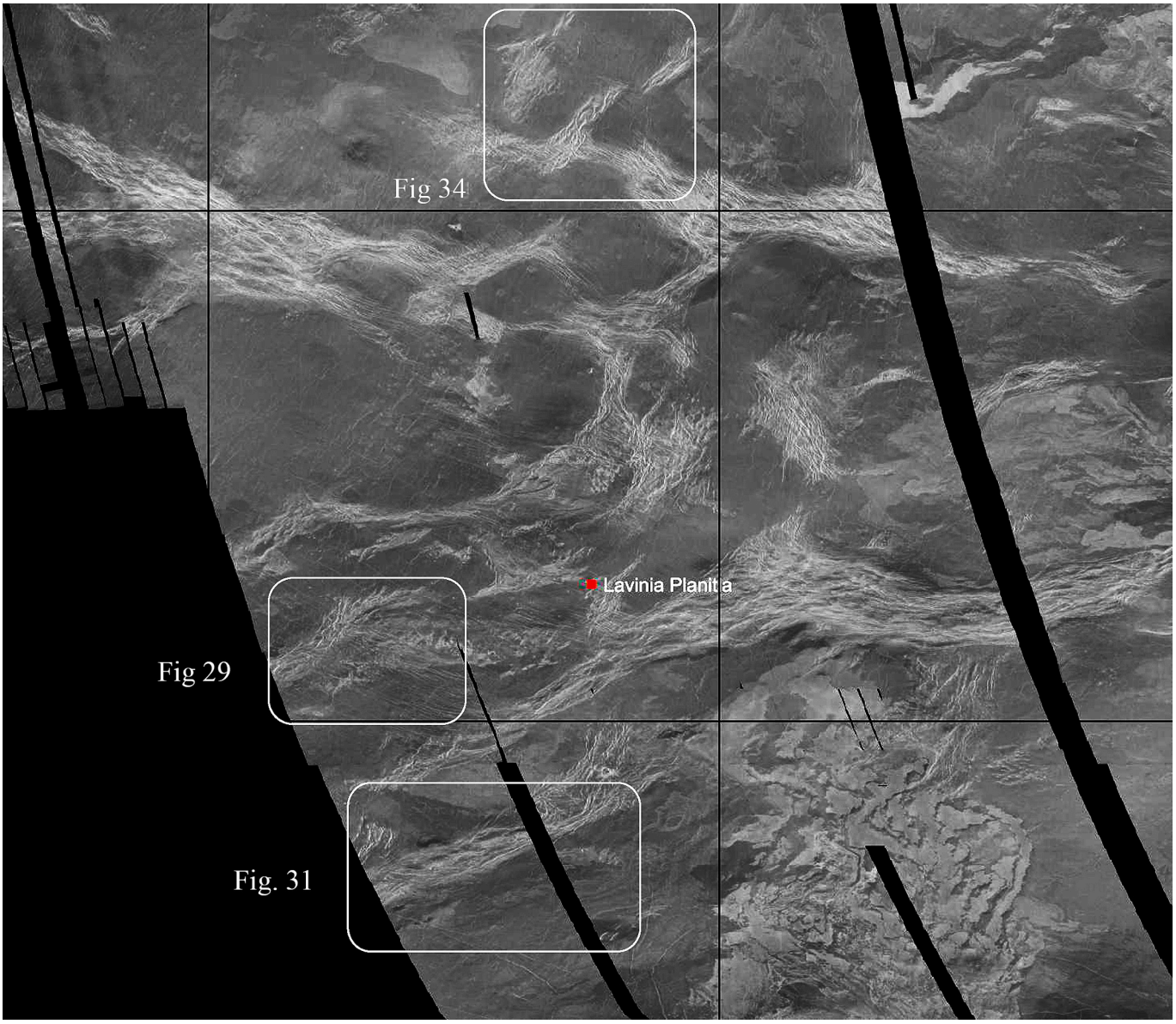

Fig. 24. Lavinia Planitia, Venus; see Fig. 1a for location. Deformation belts are radar light and rough. Volcanic plains are radar dark and smooth. Grid squares are ~750 km across. White boxes indicate locations of Figs. 29, 31. The base image was sourced from JMARS (**J***ava* **M***ission-planning and* **A***nalysis for* **R***emote* **S***ensing*) at https://jmars.mars.asu.edu/.

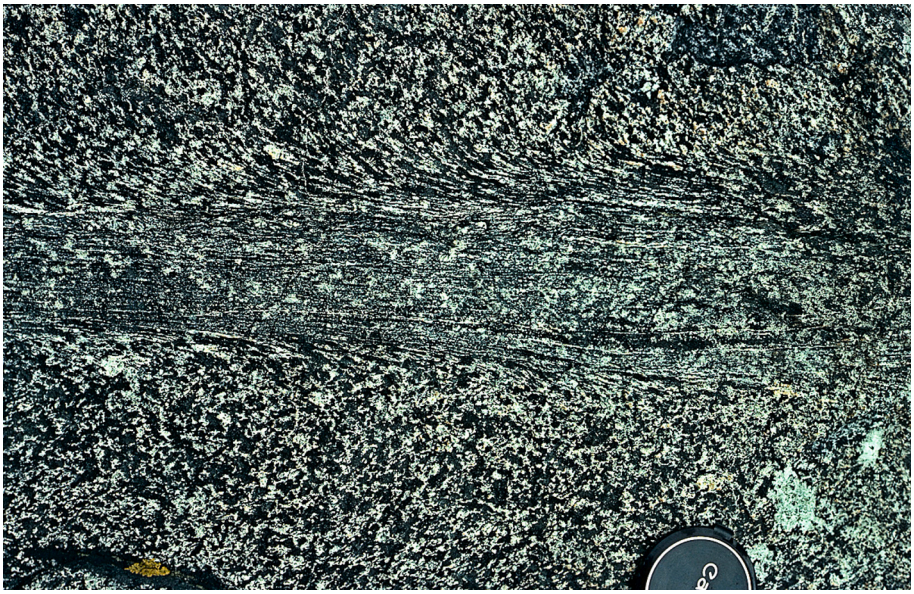

Fig. 25. Classical shear zone developed in isotropic gabbro illustrating strain localisation, strain gradients,strain softening, and the rotation of fabric elements with progressive deformation. See Ramsay and Graham (1970) for detailed discussion of this occurrence (image by the author).

along a ~ 40 km strike section of a NE-trending fault zone associated with the El Asnam earthquake, Algeria, stating that *"The presence of a low-angle thrust fault* [daylighting] *at the base of the anticline, dipping back beneath the structure, suggests that the anticlinal deformation developed in response to drag along the fault"*. However, the El Asnam earthquake was located in a plate tectonic context: *"... the* [E-W trending] *Maghreb Ranges where the African continent is in contact with the oceanic lithosphere of the Algerian-Provence basin ... display the characteristics of continent-continent collision tectonics"* (Philip and Meghraoui, 1983). Again, this is a very different setting from that of off-world wrinkle ridges on single plate telluric bodies. Indeed, Philip and Meghraoui (1983) compared their study area to the Jura region of the French Alps. In addition, at the regional scale, the Maghreb Ranges are predominantly a fold belt with minor thrusting (Philip and Meghraoui, 1983, their fig. 1). These authors were well aware of the tectonic complexity of their study area: *"... the tectonic event related to the E1Asnam earthquake was relatively complex ... The variety of observed structures and the complexity of deformations are in contrast with the descriptions of surface ruptures which accompany thrust fault earthquakes such as those of San Fernando, California"* (see also their figs. 24 and 25 of detailed cross-sections illustrating complex folding associated with thrusting). They also described a 15 km long segment of listric extensional faulting located due north of the thrust fault zone, and implied that *"the general pattern corresponds to a southward movement of all the* [intervening] *... plateau"* (see also their figs. 28 and 29; Fig. 23), a configuration not reported for off-world wrinkle ridges (Section 4). Most importantly, as in the case of the Meckering fault, these descriptions do not reflect the rise-ridge-wrinkle surface topographical morphology of off-world wrinkle ridges. In addition, *"... during the 1980 earthquake only a fraction of deformation has been involved in the faults* [sic] *activation"* (Philip and Meghraoui, 1983, their fig. 34), which does not correspond to the models of off-world wrinkle ridge formation (see Section 4).

Some authors who favoured a thick-skinned interpretation of large lobate scarps on off-world planets have invoked the Wind River mountains, part of the Laramide Province, Wyoming, as a terrestrial basement-uplift analogue (e.g. Golombek et al., 1990; Watters et al. (1998); Mueller et al., 2014; Klimczak et al., 2018). However, seismic imaging (e.g. Smithson et al., 1979) has shown that the Wind River mountains are underlain by a major thrust dipping at <50° that accommodated 14 km of vertical motion and 26 km of horizontal shortening, which developed after a major, overturned anticline locked up. Most importantly, the transition from Sevier thin-skinned thrusting to Laramide thick-skinned basement uplift tectonics was driven by a shallowing of an underlying plate tectonic subduction zone beneath western North America (e.g. Saylor et al., 2020; Orme, 2020). Again, it is unclear how this would apply to off-world single-plate planets of the inner Solar System.

8. Strike-slip crustal-scale shear zones on Venus?

A number of studies have reported crustal-scale shear zones and/or broad zones of purportedly non-coaxial strain associated with deformation belts on Venus (e.g. Vorder Bruegge et al., 1990; Hansen and Willis, 1996; Koenig and Aydin, 1998; Kumar, 2005; Romeo et al., 2005; Fernández et al., 2010; Harris and Bédard, 2014a; Galluzzi et al., 2019). Moreover, some have suggested that such features may be indicative of some form of ancient mobile lid tectonics (e.g. Vorder-Bruegge and Head, 1990; Romeo et al., 2005; Harris and Bédard, 2014a, 2014b; Byrne et al., 2021). Crustal-scale strike-slip shear zones have been reported from two principal structural associations on Venus: the margins of tessera terrains, and regional-scale, localised *"deformation belts"*. Having reviewed the basic structural geology of tessera terrains in detail elsewhere (Hanmer, 2020), I will briefly recap published descriptions of deformation belts here before discussing the reported evidence for the presence of strike-slip shearing.

8.1. Deformation belts

Deformation belts affected extensive volcanic plains during the Early Guineverian Period, i.e. younger than the tessera terrains and lineated plains (Ivanov and Head, 2015; Fig. 1b), and appear to be unique to Venus within the inner Solar System (see Fig. 24). They are commonly divided into extensional fracture belts (Solomon et al., 1991; Fernández et al., 2010; Ivanov and Head, 2011, 2015; Guseva and Ivanov, 2019), and ridge belts interpreted as primarily the products of shortening (Zuber, 1987; Frank and Head, 1990; Kryuchkov, 1990; Solomon et al., 1991, 1992; Squyres et al., 1992; Ivanov and Head, 1996, 2011, 2015; Banerdt et al., 1997; Koenig and Aydin, 1998; Young and Hansen, 2005; Fernández et al., 2010; cf. ridge belt as applied as a geographical location on Mars by Schultz and Tanaka, 1994; Mège and Masson, 1996a, 1996b; Mège and Ernst, 2001). However, some deformation belts may be hybrid features, comprising both shortening and extensional structures parallel to the deformation belt axis, and potentially associated

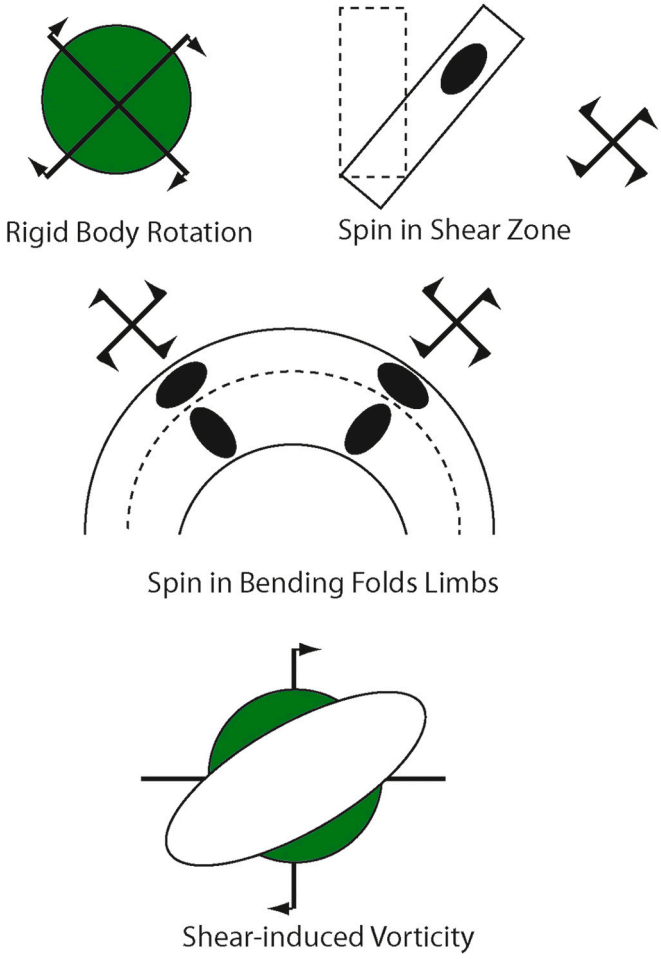

Fig. 26. The rotational component of the flow is the average angular velocity of material lines with respect to an external reference frame. This can be accommodated in a number of ways. Spin is the rotation of the instantaneous stretching axes with respect to the external reference frame, whereas shear-induced vorticity is the rotation of material lines with respect to the instantaneous stretching axes. Redrafted from fig. 13 in Hanmer and Passchier (1991).

with strike-parallel shearing (e.g. Frank and Head, 1990; Banerdt et al., 1997; Rosenberg and McGill, 2001; McGill et al., 2010). Hence, identifying a deformation belt as ridge-type or fracture-type is commonly equivocal.

Fracture belts (Solomon et al., 1991, 1992; Squyres et al., 1992, their fig. 10; Banerdt et al., 1997, their fig. 6; Fernández et al., 2010) are also referred to as groove belts (e.g. Solomon et al., 1991; Ivanov and Head, 2011, their figs. 9a and 10; Ivanov and Head, 2015, their figs. 1d, 12, 15 and 18 g, h; Guseva and Ivanov, 2019). They are 50–200 km wide by over 1000 km long (Ivanov and Head, 2011), and developed on extensive Early Guineverian volcanic plains during a Global Tectonic Regime (Ivanov and Head, 2015; Fig. 1b). Within the limitations of the available Magellan altimetry data, Squyres et al. (1992) estimated their positive relief as <1 km above the adjacent volcanic plains. Fracture belts have been described as globally distributed, complex patterns of linear to arcuate faults and fractures oriented parallel to the axis of the belt, with graben up to 2 km wide by several tens of kilometres long, all formed in broad-scale *"tensional environments"* (Ivanov and Head, 2015). Similarly, *"Fracture belts … have a morphology suggestive of at least near-surface stretching … One possibility is that fracture belts are dominantly extensional structures, perhaps localised into belts by patterns of lithospheric heating or igneous intrusion"* (Solomon et al., 1992). Faults were reported to be periodic and close-spaced (several 100 m), forming bands several 100

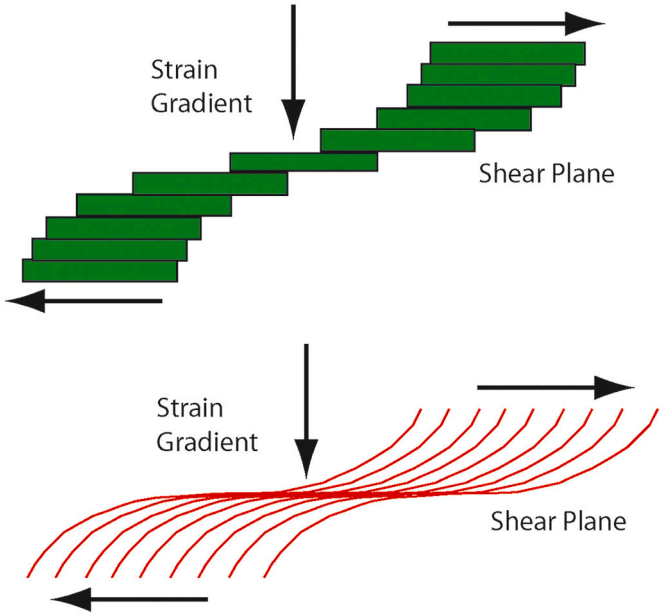

Fig. 27. Discontinuous (upper) and continuous (lower) strain gradients associated with shear zones. Redrawn from fig. 19 in Hanmer and Passchier (1991).

km wide, regularly distributed at 20–30 km intervals within fracture belts(e.g. Solomon et al., 1992, their fig. 30). Despite these extensive geometrical descriptions (see also Supplemental 1), Banerdt et al. (1997) concluded that *"Concentrated deformation occurs in deformation belts, the nature and origin of which are problematic … It is not evident how fracture belts formed, with both extensional features and elevated topography; the process by which deformation is concentrated into belts is also unclear"* (my emphasis). However, the extensive literature on low-angle terrestrial detachment (normal) faults, well-known from the mountain ranges of the southwestern U.S.A., clearly shows that *"extensional features"* can indeed be associated with significant positive relief (e.g. Wernicke, 1981, 1985; Davis and Lister, 1988; Lister and Davis, 1989, and references therein).

Ridge belts form sinuous patterns of elevated terrain, ~500 m high, 30–400 km wide, and 200–2000 km long, located on the volcanic plains of Venus, commonly spatially associated with, and mutually parallel to, wrinkle ridges that occur extensively between the ridge belts (e.g. Squyres et al., 1992; Fernández et al., 2010; Young and Hansen, 2005; see also Supplemental 1). Internally, they comprise close-spaced longitudinal ridges, 5–20 km wide (2–3 km wide according to Solomon et al., 1992), that may be broad, discontinuous, paired, parallel, or anastomosing (e.g. Frank and Head, 1990). The ridges were interpreted individually as folds spaced at 5–10 km intervals (e.g. Squyres et al., 1992), or collectively as fold and thrust belts (e.g. Mueller and Golombek, 2004). According to Solomon et al. (1991), ridge belts were *"… generally interpreted to be compressional features"*. However, their justification was inherently model-driven: " … *the primary argument for a compressional origin for the belt is simply its elevated topography … The generally positive relief of the belts supports the hypothesis that they are the products of lithospheric shortening and crustal thickening"*. However, that relief is modest and, as noted above, extensional terrestrial detachments faults are also associated with positive relief. Frank and Head (1990) further observed that ridge belts form a geometrical continuum from simple broad arches to asymmetrical belts, and concluded that complex deformation histories could not be excluded, potentially involving, transverse shortening and extension with longitudinal shearing. Furthermore, although Fernández et al. (2010) estimated that ridge belts represent very modest shortening magnitudes (<0.1%). Notwithstanding, Ivanov and Head (2015) compared ridge belts with fold and thrust belts on Earth.

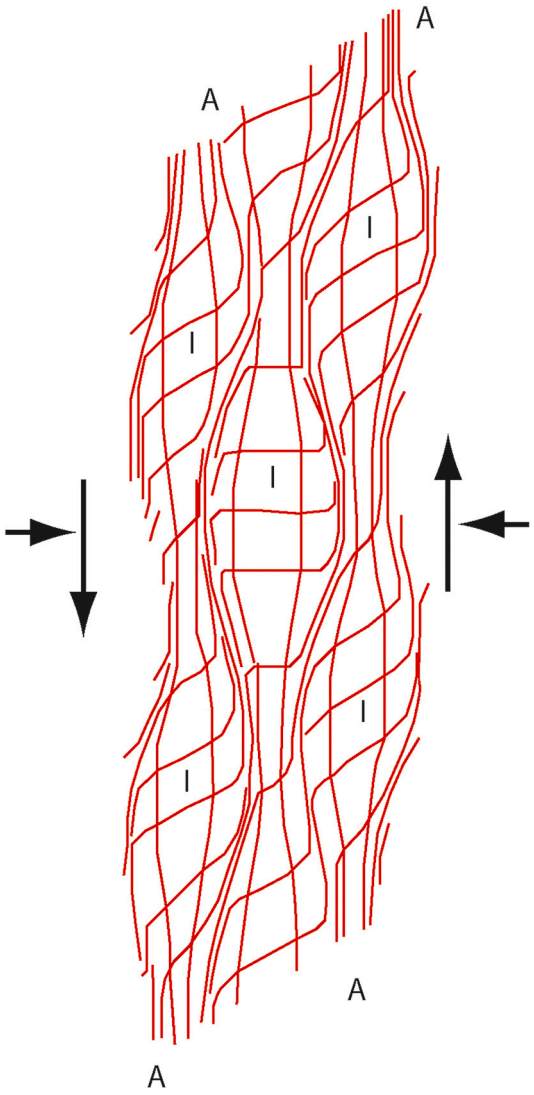

Fig. 28. In bulk general noncoaxial flow, relatively low resistance to slip on locally developed anisotropy (A) enhances the ability of those segments to accommodate the simple shear component of the flow (large arrows), as opposed to the pure shear component (small arrows). Less anisotropic parts of the deforming medium (I) are less efficient in accommodating the simple shear component. Hence the components of the general noncoaxial flow are spatially partitioned. Modified after Bell (1985).

8.2. Determinants of shear zone development

According to Fernández et al. (2010), *"There seems to be a resistance in planetary geology to recognising strike-slip faults"*. However, identifying crustal-scale shear zones is not a simple undertaking. Even on Earth, prior to 1980, crustal-scale terrestrial shear zones were commonly mistakenly identified as stratigraphic volcano-sedimentary sequences, or plutonic corridors (e.g. Davidson, 1984; Hanmer, 1988a, 1988b; Hanmer, 1989, 1991; Hanmer and McEachern, 1992; Nadeau and Hanmer, 1992; Hanmer et al., 1992, Hanmer et al., 1995). Moreover, some purported crustal-scale shear zones have since been shown not to be as extensive or significant as previously thought (compare Bak et al., 1975 with Hanmer et al., 1997). Accordingly, a brief recap of the structural geological determinants of shear zone development and their constraints is appropriate here.

The modern criteria for identifying natural shear zones, both theoretically and in the field, were established by Ramsay and Graham (1970; see also Ramsay, 1980; Berthe et al., 1979a; Bell, 1981, 1985; Simpson and Schmidt, 1983; Bell and Hammond, 1984; Hanmer, 1988a, 1988b; Hanmer and Passchier, 1991; Hanmer and McEachern, 1992; Nadeau and Hanmer, 1992; Fossen and Cavalcante, 2017). Briefly, a shear zone is a 3D planar or curviplanar volume of localised strain and strain softening (Fig. 25; e.g. Poirier, 1980; Hobbs et al., 2015) associated with non-coaxial flow (vorticity and/or spin; Fig. 26; see Means et al., 1980; Lister and Williams, 1983, for model details), potentially with a concomitant component of bulk coaxial flow (e.g. transpression). The localisation of strain within the shear zone requires the presence of a strain (or volume loss) gradient (Fig. 27), which may be continuous (e.g. Ramsay and Graham, 1970) or discontinuous (e.g. Berthe et al., 1979a). The rotational component of the deformation (vorticity and/or spin) may be homogeneously or heterogeneously partitioned within the shear zone (e.g. Bell, 1981, 1985; Bell and Hammond, 1984; Fig. 28).

Identification of the rotational component of the deformation in a postulated shear zone involves more than observation of the static geometry of the finite strain state (e.g. Hanmer and Passchier, 1991; Simpson and De Paor, 1993). It requires observation-based dynamic reasoning whereby viable progressive deformation mechanisms / processes can be justifiably proposed to have transformed an initial state or configuration, via at least one observed, defensible, intermediate step, into the final state (e.g. Hanmer, 1986; Hanmer, 1990; Fig. 25). In most cases, this is equivalent to tracking the rotation of the principal axes of finite strain with progressive deformation. Most importantly, the width of shear zones is determined by a combination of thermal and structural softening. At the crustal scale, the thermal activation and strain rate sensitivities of silicate rheologies (e.g. White, 1976; White et al., 1980) impose a maximum width of ~25 km attainable by an individual localised strike-slip shear zone (e.g. Hanmer, 1988a; Hanmer et al., 1992), even at slow geological strain rates (e.g. Pfiffner and Ramsay, 1982; Fagereng and Biggs, 2019), before wholesale melting disrupts the crustal structure. Note that, although Fossen and Cavalcante (2017, their fig. 18; see also Fossen et al., 2022) claim that shear zone width scales with displacement, they do not address the competing roles of thermal and structural softening in determining shear zone thickness (see Hanmer, 1988a). As will be shownbelow, these structural geological determinants and constraints outlined in this section are commonly not addressed in studies that report crustal-scale strike-slip shear zones on Venus.

8.3. Non-coaxial flow in deformation belts?

Solomon et al. (1992) were well aware of the mechanical and dynamic issues regarding strike-slip motions in the absence of a mobile crust (see also Fernández et al., 2010). Nonetheless, Solomon et al. (1992, their fig. 8) reported apparently deflected lineaments across a ~ 40–50 km wide ridge belt in Lavinia Planitia (Fig. 24) that they interpreted as indicative of belt-parallel sinistral shearing: *"... an old set of plains grooves exhibits an S-shaped bend consistent with distributed left-lateral shear as it crosses the ridge belt"*. However, Solomon et al. (1991, their fig. 8) drew the same grooves as non-sigmoid, straight lines (Fig. 29). They also considered, but did not demonstrate that, absent a strain gradient, the blocks between the lineaments might have rotated, "book-shelf" style (e.g. Mandl, 1987; Fig. 30), in response to shortening normal to the ridge-belt. In any event, both they and Solomon et al. (1992) preferred a shearing model: *"These relations support the hypothesis that shear often accompanies shortening in ridge belt deformation"*. Solomon et al. (1991, 1992) did not appear to recognise that ~40–50 km is a very extreme width for any shear zone, let alone one developed at a planetary surface. Nor did they consider the possibility that the reported deflections might be a function of abrupt strain refraction across a rheologically weak corridor (e.g. Treagus, 1983, Treagus, 1988 for model details). Note that, Squyres et al. (1992, their fig. 14) did illustrate one very small example of potential evidence for sinistral shear along a ridge belt margin, also located in Lavinia Planitia, supported by an observed strain gradient and rotation of surface features with progressive strain.

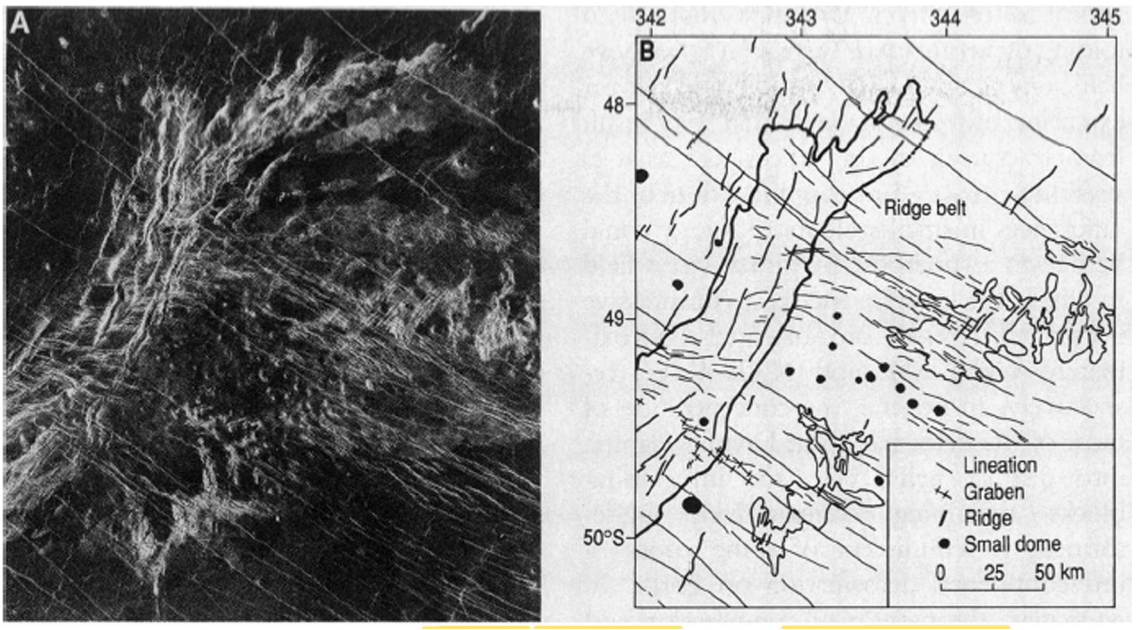

Fig. 29. Ridge belt in Lavinia Planitia, Venus (see Fig. 24 for location). Fig. 8 in Solomon et al. (1991), visually enhanced in Photoshop. According to these authors, the belt, rises to 200 m above the surrounding plains and consists of NE-trending ridges 1 to 5 km wide, spaced 5 to 15 km apart. It is transected by tectonic lineations, some of which are graben, trending primarily E-W to NW. Some of these lineations curve as they approach, and appear to be offset horizontally across, the ridge belt. The combination of positive relief and horizontal offset suggests that this ridge belt was formed by a combination of compression and left-lateral shear. Discussed in the text.

Fig. 30. "Book-shelf" style rotation of blocks of banded mylonite in the dextral Great Slave Lake shear zone, Northwest Territories, Canada (Hanmer, 1988a; Hanmer et al., 1992). Note that the sense of rotation of fracture delimited "dominoes" in the upper part of the dark band (top and left of centre) is opposite to that in the light band (bottom), a reflection of the general non-coaxial nature of flow in the shear zone. Book-shelf style rotated dominoes are not an indicator of shear sense (see Hanmer and Passchier, 1991, their fig. 66; image by the author).

However, such observations are exceedingly rare in the venusian literature.

Koenig and Aydin (1998) suggested that, in a ~ 75 km wide section of a ridge belt in Lavinia Planitia, *"the spatial and temporal relationships between the Molpadia Linea deformation belt and an associated fracture system indicate that the fractures were formed as the result of strike-slip faulting localized along the belt"* (Fig. 31). They interpreted ridges and fractures, located in the wall rocks on one side of the ridge belt, as

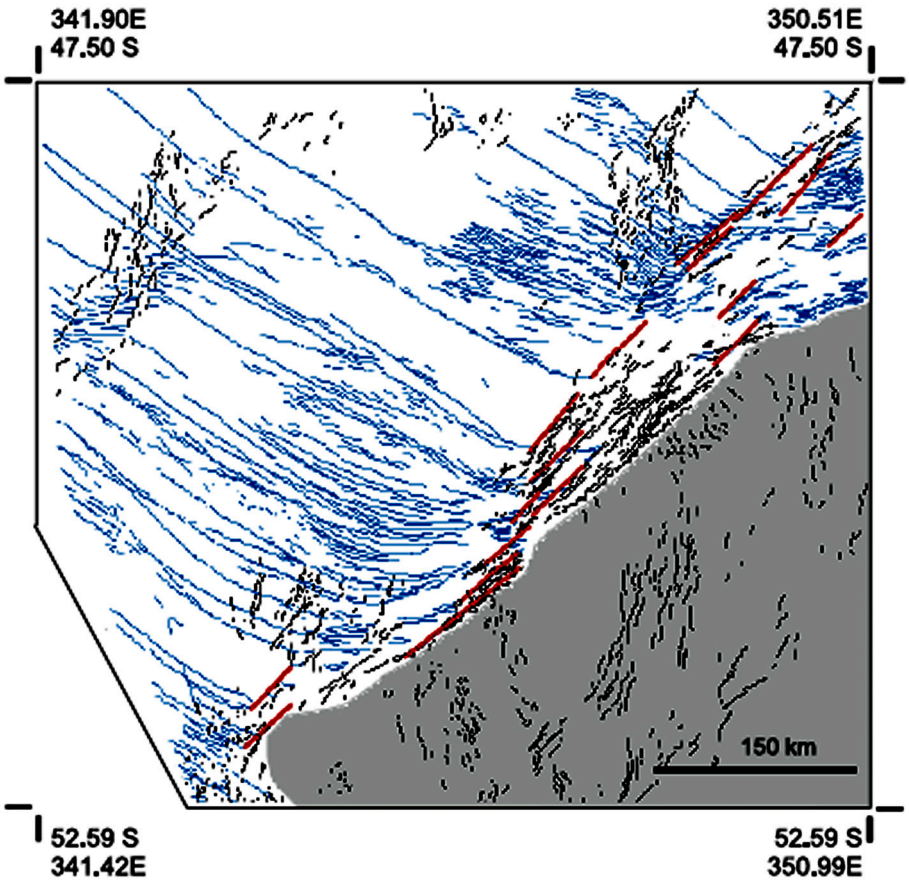

Fig. 31. Ridge (fold) and fracture map of a ridge belt in Lavinia Planitia (see Fig. 24 for location). Fig. 3 in Koenig and Aydin, 1998. According to the authors, black lines are ridges, blue lines are fractures, and red lines represent strike-slip faulting planes along ridges. Northwest-trending fractures appear younger than the northeast-trending ridges within the ridge belt. Grey shading indicates young lava flows that embay deformation belt, and may cover secondary structures south of the ridge belt, or may be moderately deformed by strike-slip motion. Discussed in the text. With permission of the Geological Society of America. (For interpretation of the references to colour in this figure legend, the reader is referred to the web version of this article.)

having formed in the terminal compressional and extensional quadrants of the belt, respectively (see Chinnery, 1966; Coward, 1976; Ramsay, 1980 for model details; Fig. 32). However, the studied section represents a 675 km long segment (i.e. ~50%) of the ~1200 km long by <200 km wide belt (Fernández et al., 2010). It is unclear how this fits with a terminal quadrant model. Koenig and Aydin (1998) did not recognise this discrepancy; nor did they attribute the purportedly terminal quadrants to individual strike-slip faults within the overall belt. Instead, they proposed that *"The strike-slip motion along Molpadia Linea is probably a consequence of a slight rotation of the maximum compressive stress away from belt normal, resolving a component of lateral shear across the belt"*. However, this ignores the well-known stress refraction effect due to material anisotropy that would effectively dampen any such *"slight rotation"* of the principal stresses (e.g. Donath, 1968; Cobbold et al., 1971).

Other studies (e.g. Solomon et al., 1992; Fernández et al., 2010) have reported sigmoid ridges internal to ~100 km wide ridge belts, interpreted by the authors as fold structures according to the classical wrench fault model (see Wilcox et al., 1973; Sylvester, 1988 for model details; Fig. 33). However, Fernández et al. (2010, their figs. 2, 5, and 9) drew the internal ridges either at ~45° or parallel to ridge belt boundaries, without intermediate orientations (Fig. 34). Other rectilinear features, assumed to be extensional fractures, contiguous with and parallel to similar features external to the ridge belts, were drawn at an angle of ~45° to the belts, but of opposite angular sign to the internal ridges. From these observations, despite the general absence of strain gradients, of rotation of material lines with progressive strain, or of strain localisation, all at the scale of the deformation belts in question, Fernández et al. (2010) erroneously identified both the presence of strike-slip motion along the belts, and a purported sense of displacement. Most importantly, the predominance of ~40–45° angles with respect to ridge belts reported by Fernández et al. (2010), interpreted by them in terms of non-coaxial flow, would imply that shearing along the deformation belts was universally incipient simple shear (e.g. Ramsay and Graham, 1970). This is geologically unrealistic, given the size of the purported shear zones.

Similarly, inspired by Squyres et al. (1992), Fernández et al. (2010) attempted to kinematically interpret 50 to >100 km wide fracture belts in terms of transtensional lateral shear on the basis of the geometry of periodic, close-spaced lineaments mapped as graben and extensional fractures within the belts, but without providing supporting evidence (see their figs. 2, 3 and 5). They stated: *"En-echelon bands of sigmoid grabens are often bounded by … straight fractures … Their orientation, geometrical association with extensional structures and straight traces enables us to suggest that* [the straight fractures] *are predominantly transcurrent structures or oblique faults trending parallel to the strike-slip component at* [sic] *a zone of oblique rifting"*.

Fernández et al. (2010, their fig. 10) interpreted the fracture belts in question as crustal-scale transtensional shear zones, citing the laboratory modelling of McClay et al. (2002) as an analogue. However, the model transtensional features developed by McClay et al. (2002) are rift zones whose internal faulting comprised families of uniformly facing rotating and slipping dominoes, as opposed to the classical graben structures proposed by Fernández et al. (2010). In addition, the *"straight fractures"* identified by Fernández et al. (2010) as *" oblique faults trending parallel to the strike-slip component"* were clearly identified by McClay et al. (2002, their fig. 6) as the result *syn*-propagation refraction of the normal faults within the rift belts of their experiments: "… [with] *increased extension, the tips of some of these intrarift faults propagated such that they curved parallel to the rift* axis", as opposed to rotation of the finite strain axes with progressive deformation. Indeed, the sense of curvature of the intrarift faults is opposite to that expected from the transtension proposed by Fernández et al. (2010). Furthermore, as in the case of ridge belts, the lineaments presented by Fernández et al. (2010, their figs. 2

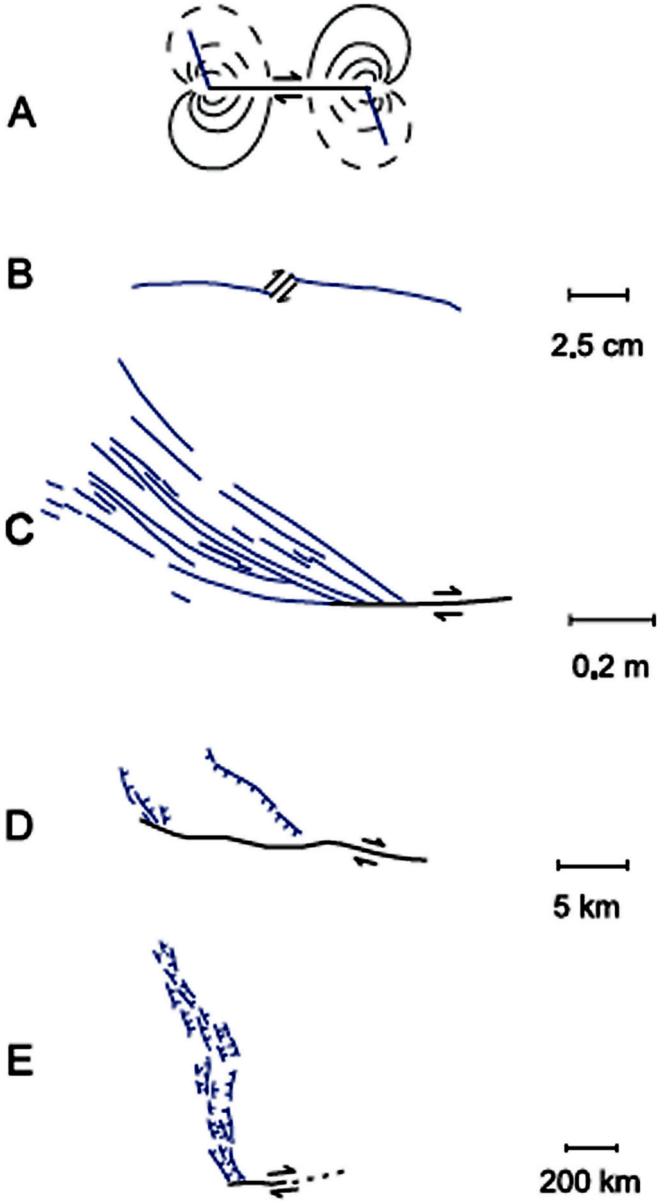

Fig. 32. Terrestrial examples of secondary fractures related to strike-slip motion. Fig. 4 in Koenig and Aydin (1998). According to these authors, these examples illustrate various geometrical characteristics of extensional structures related to strike-slip faults observed in Lavinia Planitia. (A) Theoretical antisymmetric distribution of tensile (dashed) and compressive (solid) stresses around right-lateral fault. Blue lines indicate secondary fractures at fault tips oriented at 70° to fault plane. (B) Experimental model of secondary fracture growth showing great extent of fractures relative to fault plane. (C) Secondary fractures localised at end of strike-slip fault in granite highlighting multiple nature and curving geometry of extensional features. (D) Termination of the Imperial fault, California, and transition from master strike-slip fault to normal faults. (E) Large-scale normal faults and graben of Baikal rift, Siberia, related to strike-slip faulting. B, C, and E are reversed to show right-lateral sense of motion. With permission of the Geological Society of America. (For interpretation of the references to colour in this figure legend, the reader is referred to the web version of this article.)

and 10a) are generally straight, and lie at ~40–45° to the fracture belt boundaries. They were arbitrarily interpreted as lying in the shortening quadrants of the instantaneous strain ellipsoid of shear zones, from which shear-sense was again erroneously derived.

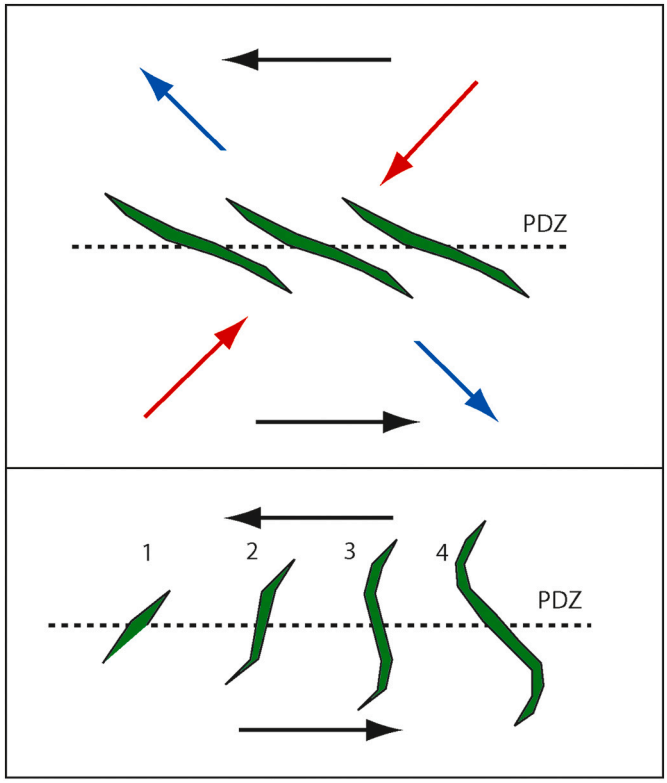

Fig. 33. Upper: Incipient sigmoid geometry of en-echelon folds in left simple shear. Principal axes of instantaneous shortening (red arrows) and extension (blue arrows) and the shear couple (black arrows) are indicated. PDZ is principal displacement zone. Adapted from fig. 16 in Sylvester (1988). Lower: Rotation and progressive propagation (1–4) of fractures in a left shear couple. Adapted from fig. 30 in Sylvester (1988). (For interpretation of the references to colour in this figure legend, the reader is referred to the web version of this article.)

8.4. Non-coaxial flow and tesserae margins - Ovda and Thetis regiones?

The most intensely studied candidate strike-slip structure on Venus is the Thetis boundary shear zone in eastern Aphrodite Terra (Davis and Ghail, 1999; Tuckwell and Ghail, 2003; Kumar, 2005). According to these authors, an ENE-trending corridor of localised, heterogeneous strain separates two craton-like tesserae (Ovda and Thetis regiones; see Fig. 1a for locations). The corridor was described by these authors as either ~1200 or ~ 2500 km long, by 50–200 km wide, with sinuous boundaries such that the narrowest part of the corridor wraps around a local promontory on Ovda Regio (Davis and Ghail, 1999, their figs. 3 and 4; Tuckwell and Ghail, 2003, their fig. 1). However, continuity of the proposed deformation corridor is not obvious in the images presented (Fig. 35). Davis and Ghail (1999) and Tuckwell and Ghail (2003, their fig. 3) reported sets of discrete lineaments, interpreted as fault scarps, oriented at either low or high average angles to the corridor boundaries. On the basis of lineament geometry, they interpreted these features as Riedel R, R' and P faults (see Tchalenko, 1970; Wilcox et al., 1973; Sylvester, 1988 for kinematic model details; Fig. 36), indicative of a *"sinistral strike-slip fault network"* (Fig. 37). From a series of empirical assumptions (*"An upper estimate of extension is obtained if it is assumed that each radar bright line represents a fault that accommodates 500 m of extension. A minimum estimate is provided by the assumption that each lineament is a 500-m-wide graben with a 200-m-deep flat floor bounded by normal faults dipping at 60°"*), Tuckwell and Ghail (2003) estimated overall fault slip of the order of a few tens of kilometres. However, they described the Riedel R faults as en-echelon and systematically right stepping, which could be also be consistent with *dextral* rather than

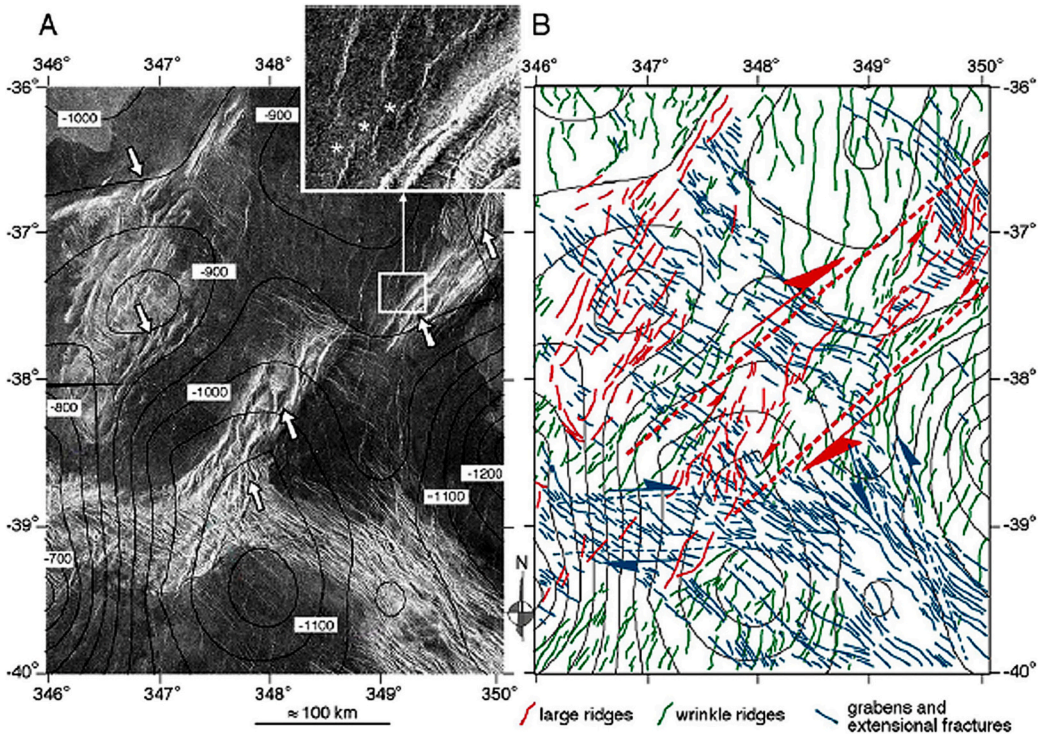

Fig. 34. Structural analysis of deformation belts in Lavinia Planitia, Venus (see Fig. 24 for location). Part of fig. 2 in Fernández et al. (2010). According to these authors, the enlarged area on the left (inset) shows a right-stepped pattern of sigmoid wrinkle ridges near a ridge belt. White arrows point to examples of right-stepped individual ridges within the main ridge belt. Structural map (right) with interpretation of the horizontal displacement sense for transpressional (red arrows) and transtensional (blue arrows) structures. Red, green and blue lines are large ridges, wrinkle ridges and graben or extensional fractures, respectively. Discussed in the text. With permission from Elsevier. (For interpretation of the references to colour in this figure legend, the reader is referred to the web version of this article.)

sinistral shear (e.g. Hanmer et al., 1997 and references therein; Fig. 38; see also Escher et al., 1976, their fig. 82). In any event, the angular relations reported by Tuckwell and Ghail (2003; Fig. 37) again imply overall incipient shearing deformation, which is difficult to reconcile with the development of a strike-slip deformation zone more than a thousand kilometres in strike length.

Kumar (2005) studied the NE portion of the feature described by Davis and Ghail (1999) and Tuckwell and Ghail, 2003), which he called the Thetis boundary shear zone (TBSZ). He described the TBSZ as *"1000-km-long, 50- to 200-km wide, curvilinear, strike-slip shear zone … defined by a system of arcuate anastomosing shear zones appearing as multiple sets of gentle to strongly curved lineaments … which closely resemble the continental-scale brittle-ductile to ductile shear zones on Earth*", specifically referring to the Great Slave Lake shear zone (see Hanmer, 1988a; Hanmer, 1991; Hanmer et al., 1992). The western part of the TBSZ includes the narrow segment in front of the local promontory on Ovda Regio (Fig. 39), previously described by Tuckwell and Ghail (2003). Kumar described similar features to those reported by Davis and Ghail (1999) and Tuckwell and Ghail (2003). However, he interpreted them as mega-scale equivalents of C/S and C′ *"-like"* fabrics (Fig. 40; see Berthe et al., 1979a, 1979b for model details), although he was well aware that *"… it is difficult to define the deformation bands* [C planes] *robustly with the available resolution of SAR images"*. However, according to his model, some of his *"C bands"* correspond to ~25 km wide zones developed at the surface of the planet (see his fig. 4e). He described the S fabric as comprising close-packed topographical ridges that he interpreted as folds, and the C planes as parallel to the TBSZ boundaries. He explicitly equated the C planes with the R faults of Davis and Ghail (1999) and Tuckwell and Ghail (2003), and the S fabric elements with their extensional graben. In addition, he reported the S fabric as sigmoid, and curving into the bounding C planes. However, this is not supported by the evidence presented (Figs. 39 and 40). In his fig. 6, the S fabric comprises straight, undeflected ridges between discrete discontinuities (potentially faults of undefined kinematic significance and relative timing?). Moreover, he presented no evidence for strain gradients at any scale. Furthermore, Kumar (2005) described S fabric ridges as wrinkle ridges, including *"paired"* wrinkle ridges, which contradicts well-established buckling theory (see Biot, 1961; Ramberg, 1962, 1963, 1964). Given the concept of wrinkle ridges as the product of folding and thrusting of initially horizontal layering (see Section 4), and the nature of strike-slip structures as steeply dipping, this description is very difficult to follow, let alone justify. Most importantly, the C/S model is based on microfabric development in isotropic granite, wherein the fine-grained S foliation wraps asymmetrically around larger, stiffer plagioclase grains, tangential to which the C planes develop as discrete, narrow bands of grain size reduction and strain softening (Berthe et al., 1979a; Fig. 41). Most importantly, the model depends on the pene-contemporaneous formation of the S and C planes, most readily demonstrable in an initially isotropic granite. Without such a demonstration, purported C planes are simply a crenulation fabric of unknown age and kinematic significance (Hanmer and Passchier, 1991, p.32). In the context of his proposed strike-slip model, it would appear that Kumar (2005) was confounding the Wilcox et al. (1973) model, which can account for upright folding of an initially horizontal layering, with the geometry of the Berthe et al. (1979a, 1979b) model of vertical fabric development in isotropic media.

Finally, Kumar (2005) compared the TBSZ with shear zones in Brazil where *"Granulite-facies rocks, migmatitic gneisses, granites and some supracrustal belts comprising the metamorphosed volcanic and sedimentary rocks are the major rock types exposed in this shear zone belt"*. However, the Brazilian shear zones are deeply eroded, whereas erosion is not an established characteristic of the currently visible Venusian surface (e.g. Arvidson et al., 1992; Way and Del Genio, 2020; however, see Khawja et al., 2020; Byrne et al., 2020); an issue that Kumar (2005) did not address. In addition, Kumar (2005) stated that *"… the tightly spaced, sigmoidal folds defining the S bands in the western segment, and those sigmoidal folds parallel to the imbricate shear zones in the eastern segment would suggest weak near-surface layers favoring ductile deformation close to the surface"*. However, terrestrial structural geology of strike-slip crustal-scale shear zones would suggest the opposite: i.e. it is the deformation that leads to strain softening and to the localisation of deformation (e.g. Poirier, 1980; Hobbs et al., 2015).

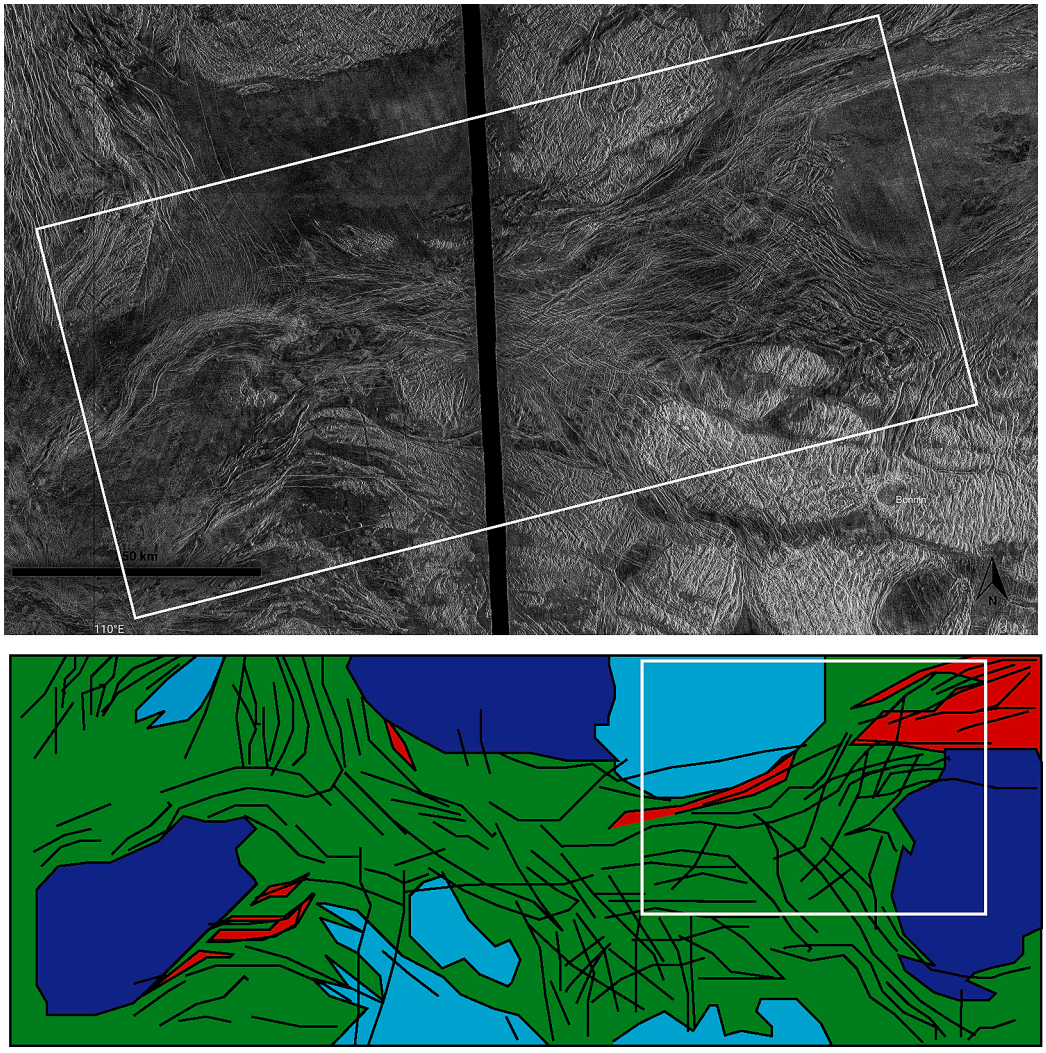

Fig. 35. Top: Image of the area centred on 3 N and 114E between the margins of Ovda Regio (upper field) and Thetis Regio (lower field), Venus (see Fig. 1a for location), sourced from JMARS (**J***ava* **M***ission-planning and* **A***nalysis for* **R***emote* **S***ensing*) at https://jmars.mars.asu.edu/. Scale bar = 250 km. North is up. The black band indicates no data. The oblique white rectangle shows the location of fig. 3 of Davis and Ghail (1999), as well as their fig. 4. Bottom: Lineament map sketched from figure 4 of Davis and Ghail (1999). Black lines represent lineaments associated with strike-slip and extension deformation. Regional volcanic plains are green, tesserae light blue, transtensional basins are purple, and transpression ridges in red.The small white box is the location of Fig. 37. According to Davis and Ghail (1999), a crustal-scale strike-slip zone is located between Ovda and Thetis regiones. . Discussed in the text. (For interpretation of the references to colour in this figure legend, the reader is referred to the web version of this article.)

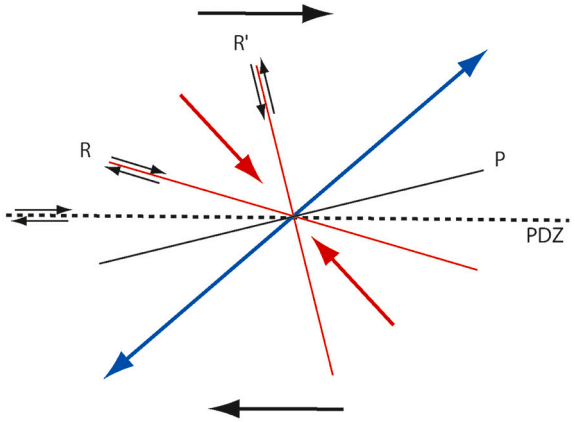

Fig. 36. Reidel model of dextral simple shear. Synthetic R and antithetic R' shear (red lines), and P fractures, are indicated, as well as the principal displacement zone (PDZ, dashed). Red arrows indicate the principal axis of shortening; blue arrows indicate axis of extension. Adapted from fig. 6 in Sylvester (1988). (For interpretation of the references to colour in this figure legend, the reader is referred to the web version of this article.)

8.5. *Non-coaxial flow and tesserae margins - south Ovda Regio?*

Romeo et al. (2005) reported a major dextral *"shear belt"* comprising *"folds of different wavelength, normal faults usually forming narrow graben (ribbons), and strike-slip faults"* along the southern margin of Ovda Regio. They suggested that it was kinematically and tectonically linked with the sinistral shearing identified by Davis and Ghail (1999) and Tuckwell and Ghail (2003; cf. the dextral interpretation of Kumar, 2005). Romeo et al. (2005) compared the purported shearing deformation with known strike-slip shear zones in the terrestrial Tibetan Plateau, wherein Ovda Regio would be analogous to the Indian indentor (Fig. 42). Romeo et al. (2005) described the shear belt in two parts, each ~200 km wide and named according to its location with respect to the core of Ovda Regio (their figs. 1 and 4): "[an] *Inner Shear Belt (ISB) where the strike-slip deformation is accommodated by en échelon folds and perpendicular* [graben], *and* [an] *Outer Shear Belt (OSB) where it is accomplished by strike-slip faults and en échelon sigmoidal ridges*" (Fig. 42).

Romeo et al. (2005) made some unsupported assumptions from which they derived a kinematic interpretation of the margins of the inner shear belt: *"Assuming that the folds are pure contractional structures normal to the shortening axis … and that the* [graben] *are pure extensional structures developed along the shortening direction, it would follow that both structures are coherent with the same stress field … the folding is oblique to the margin trend showing a right-stepped en échelon pattern of the folds, a fact that implies a relative dextral movement along the plateau boundary"* (my emphases). These statements encompass several thematic errors: (i)

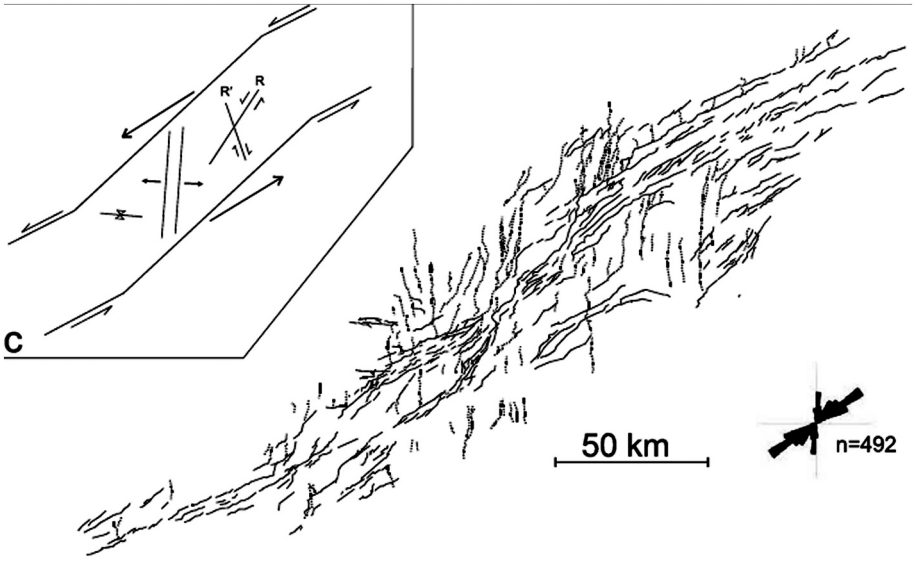

Fig. 37. Fig. 3 in Tuckwell and Ghail (2003; see Fig. 35 for location). According to these authors, structural lineaments are fault scarps, dashed lines indicate dip-slip extensional faults on Venus. Rose diagram is length weighted. Inset: schematic interpretation indicating the geometry and kinematics of the deformation zone according to a Reidel shear model (see Fig. 36). The predicted orientations of Riedel shears, extensional faults and compressive structures are shown. Discussed in the text. With permission from Elsevier. (For interpretation of the references to colour in this figure legend, the reader is referred to the web version of this article.)

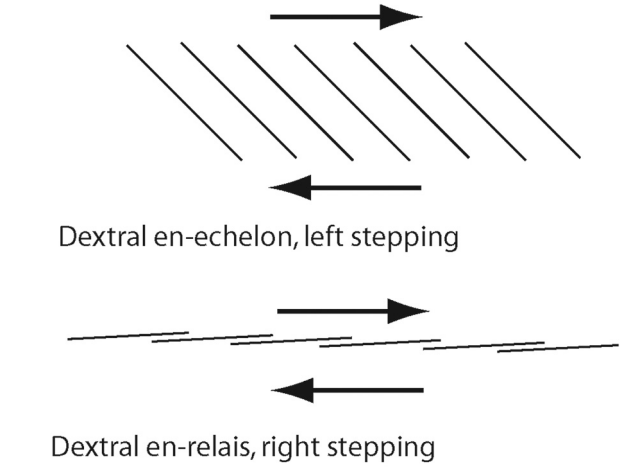

Fig. 38. Schematic illustration of the discrimination of en-echelon and en-relais fracture arrays. In dextral shear, left-stepping en-echelon fracture arrays are readily distinguished from right-stepping en-relais fracture arrays. The opposite applies in sinistral shear. Redrafted from fig. 9 in Hanmer et al. (1997).

an observed finite strain does not indicate stress orientation in natural materials (e.g. Donath, 1968; Cobbold et al., 1971); (ii) folds and graben were hypothesised to be coeval, but not shown to be so; and (iii) neither folds nor graben are sigmoidal, except at their terminations, and hence do not indicate a rotational component of the deformation or a sense of vorticity at the scale of a geologically unrealistic ~200 km wide *"shear belt"* (see their fig. 1).

Romeo et al. (2005) described the outer shear belt as a *"... dextral tectonic belt ... formed by large (>600 km) straight bright lineaments with a subparallel trend to the* [Regio] *margin ... spaced 10–30 km ... that correspond ... probably to a damage fault zone, i.e., a dense fracture swarm ...* [with] *an internal anastomosing and rhomboidal fracture pattern ... very similar to the R–P Riedel systems"*. However, in the evidence provided, the hypothesised Reidel fractures are only indicated in the inner shear belt (their fig. 1). The outer shear belt is shown with simple fractures parallel to the Regio margin, and purported folds at ~45° to the fractures. Romeo et al. (2005) concluded that the outer shear belt is a brittle deformation zone characterised by *"distributed dextral shear, most of whose displacement is being absorbed by the large strike-slip faults ... and in a lesser degree by the transpressive deformation of the inter-strike-slip fault domains"*. In effect, they interpreted the outer shear belt as a ~ 200 km wide zone of *incipient* simple shearing without significant regional-scale strain localisation. However, despite their detailed map (their fig. 4), Romeo et al. (2005) did not provide the observational evidence required to support this interpretation, either kinematically or mechanically. Nonetheless, they estimated a dextral displacement of 35–50 km across the inferred shear belts.

8.6. Planet-scale shear zone networks?

At the planet scale, Byrne et al. (2021) reported *"a globally distributed set of crustal blocks* [100-1000+ km across] *in the Venus lowlands that show evidence for having rotated and/ or moved laterally relative to one another, akin to jostling pack ice"*. Building on this, they determined that *"Lithospheric stresses calculated from interior viscous flow models consistent with long wavelength gravity and topography are sufficient to drive brittle failure in the upper Venus crust in all areas where these blocks are present, confirming that interior convective motion can provide a mechanism for driving deformation at the surface"*, a model that *"may offer parallels to interior–surface coupling on the early Earth"*.

The slipping and rotation of crustal blocks is an established geological phenomenon that can lead to the local;isation of slip along block margins (e.g. Hammond et al., 2011, their figs. 1, 10 and 12). However, the observational evidence presented by Byrne et al. (2021, their figs. 1, 2 and 3; Fig. 43), and their analytical rationale for *"jostling"*, were primarily based on the very same structural geological errors that underpinned the earlier work by Solomon et al. (1991, 1992), Koenig and Aydin (1998), Tuckwell and Ghail (2003), Kumar, 2005, Romeo et al. (2005) and Fernández et al. (2010), reviewed above. Indeed, Byrne et al. (2021) cited these papers in support of their own analysis, and derivation of 10s of kilometres of strike slip motion across the boundaries of the individual jostling blocks. The purported jostling blocks are bounded by a diverse array of features, including potentially diapiric coronae, extensional chasmata, and various strain belts (lineae, dorsae and montes), as well as the purported strike-slip crustal-scale shear zones associated with deformation belts reported by the previously published papers. However, while orthogonal strains may have been accommodated by ridge and fracture belts, observational evidence for the strike-slip motions proposed for the jostling block model is not readily apparent.

For example, Byrne et al. (2021, their fig. 1b) reported *"extensional faults curving into the main* [125 km wide deformation] *belt ... here with a right-lateral sense of slip"* (Fig. 43 and Supplemental S2a). However they

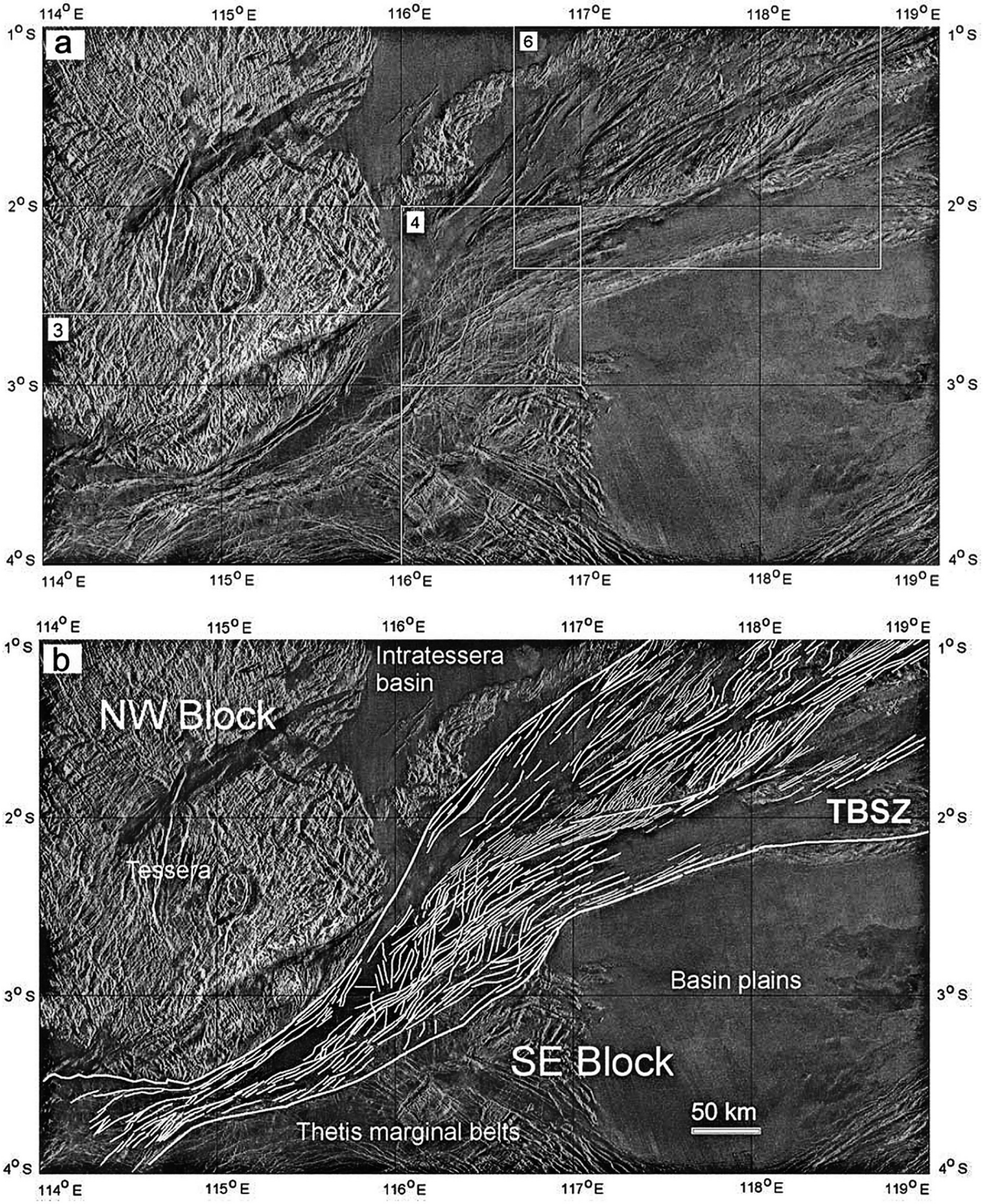

Fig. 39. Images of the Thetis boundary shear zone (TBSZ), Venus, with (lower) and without (top) overlay (see Figs. 1 and 35 for location). Fig. 2 in Kumar (2005). According to Kumar (2005) white lines mark structural lineaments that define the overall pattern of the TBSZ. The white box marked 4 is the location of Fig. 40. Discussed in the text.

did not explain why the faults are extensional, nor did they demonstrate that the observed curvature occurred with progressive strain, i.e. a strain gradient. Nor did they eliminate the possibility that the curvature is a response to initially oblique features being subjected to coaxial shortening across the deformation belt. Similarly, Byrne et al. (2021, their fig. 1c) reported slip interpreted from topographic relief (*"sigmoidal, positive-relief landforms* [that] *we interpret as right-lateral transpressive structures"*), but without kinematic justification (Fig. 43 and Supplemental S2b). In addition, the landform shown is irregular in strike, as opposed to systematically varying as a sigmoid, and oriented at a high angle to the edge of the purportedly jostled block. Nonetheless, the authors deduced a shear couple at ~45° to the landform, *and* to the block boundary. Even assuming that the landform were indeed the product of shortening, a non-coaxial interpretation of this geometry

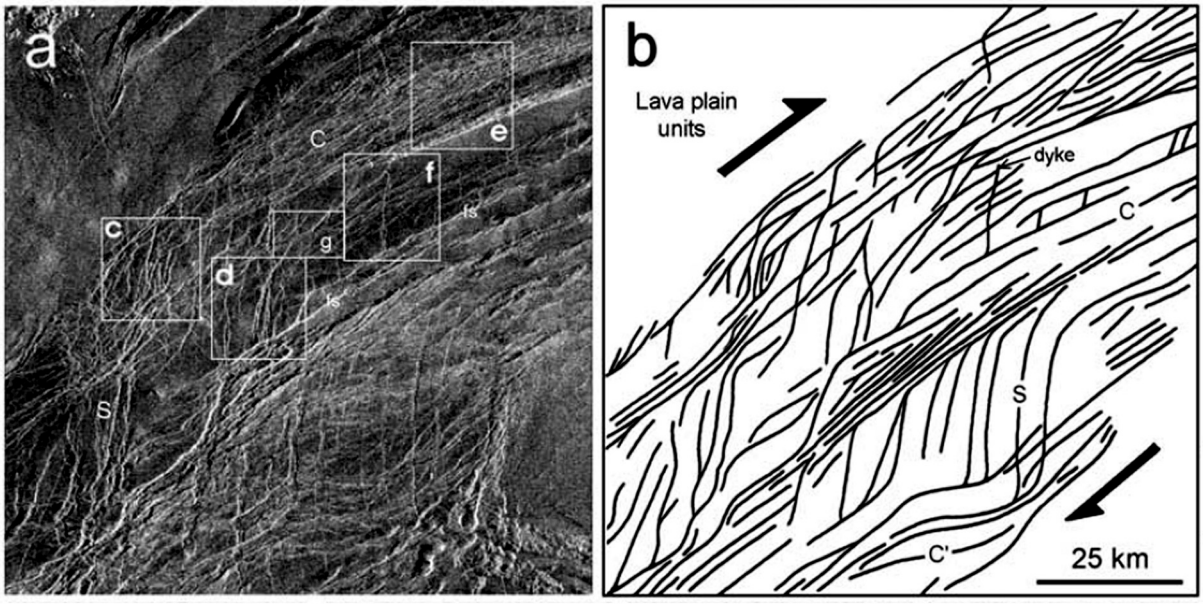

Fig. 40. Images of the Thetis boundary shear zone (TBSZ), Venus, radar (left) and interpretation of linear features (right) See Fig. 39 for location. Part of fig. 4 in Kumar (2005). According to Kumar (2005) black lines (right) mark structural lineaments that define wrinkle ridges and deformation bands. The wrinkle ridges define S bands and the deformation bands represent C and C′ bands interpreted as indicators of dextral shearing. The wrinkle ridges show sigmoidal curvature against the deformation bands. In the white box marked d, paired wrinkle ridges form single ridges. Discussed in the text.

Fig. 41. C planes (horizontal in image, discrete, periodically distributed and cm-spaced) and an S fabric (trending lower-left to upper-right) developed in a leucogranite, Wopmay fault zone, Northwest Territories, Canada. The S fabric elements are mildly sigmoid with respect to the C planes, the curvature having developed with progressive deformation and slip on the C planes, highlighted by the discrete off-sets of the quartz vein injected parallel to the S fabric. The image illustrates a dextral shear couple (see Berthe et al., 1979a for model details). Discussed in the text. (Image by the author).

would imply only incipient shearing. In addition, the authors did not address the ~45° between their shear couple and the boundaries of the purportedly jostling block. Byrne et al. (2021, their fig. 1d) further reported *"an example of sigmoidal, positive-relief ridges we regard as denoting right-lateral transpression"*, again without kinematic justification (Fig. 43 and Supplemental S2c). The ridges lie within and parallel to a ~ 200 km wide belt of ridges that bounds a purportedly jostled block. A single sigmoid ridge was used to derive the sense and orientation of the shear couple.

In none of these examples did Byrne et al. (2021) note or explain that the shear zones they were invoking were unrealistically wide (50–125+ km) compared with known terrestrial limitations on shear zone width.

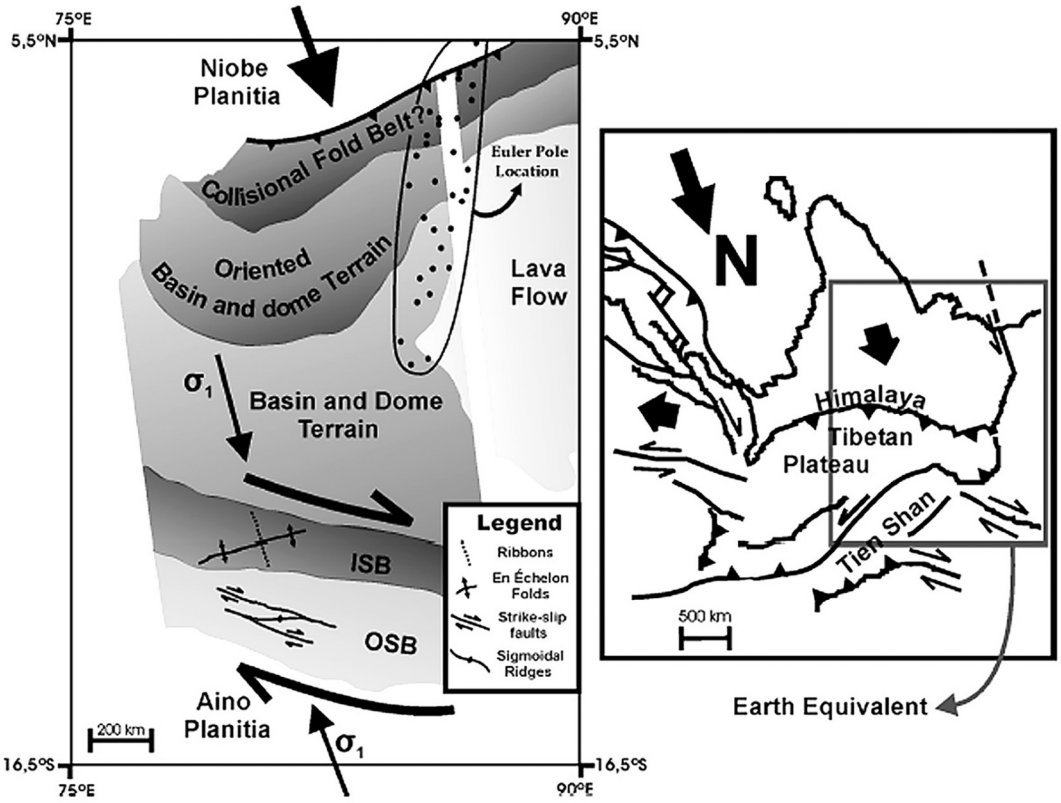

Fig. 42. Tectonic scheme of Central Ovda Regio (see Fig. 1a for location). Part of fig. 6 in Romeo et al. (2005). According to these authors, a dextral shear zone (ISB: inner shear belt; OSB: outer shear belt) located in the Southern Margin of Ovda Regio formed in a transcollisional setting in the foreland of a collisional belt on the Northern Margin. A comparative scheme of the Himalayan collision, where similar strike-slip zones appear to the North of the Tibetan Plateau, is shown on the right. Discussed in the text. With permission from Elsevier.

Nor did they comment on the absence of demonstrable strain gradients, or the lack of evidence for contemporaneity of any of the structures described with respect to a given, derived shear couple. In short they provided no observational or thematic evidence for progressive non-coaxial flow. Byrne et al. (2021, their fig. 2) further reported *"Extensional structures in the northwestern margin* [of a jostled block that] *boast a right-lateral shear fabric (i.e., transtensional deformation)"*, yet again without kinematic justification, from which they derived a viscous flow velocity vector for the jostled block (Supplemental S2d). However, it is unclear how they derived a shear couple from the angular relations of the extensional structures given the absence of an observed strain gradient (their fig. 2c). Similar issues apply to their fig. 3.

9. Discussion

Comprehensive analysis of basic terrestrial structural geology typically involves observation of multiple geometrical stages during progressive deformation of the feature in question, from which to deduce kinematic, mechanical and, eventually, dynamic development (e.g. Hanmer, 1986, 1988a, 1988b, 1990; Tikoff et al., 2013; Hobbs, 2019), even in the absence of knowledge of far-field boundary conditions (e.g. Hanmer and Greene, 2002). However, on off-world bodies of the inner Solar System, such analysis is hampered by the requirement for remote observation from orbit, even with regard to basic structural geology.

9.1. Extension, shortening and strike-slip shearing

This review raises important questions regarding what is, and is not known and understood of the basic structural geology of Venus. How robust is past and current structural geological interpretation based on satellite-borne remote observation of surface topographical morphology? How far can one take empirical information and apply it to derive geometrical, kinematic and mechanical analogues formulated on other planetary bodies? Specifically with respect to distributed extension, what known geological processes might result in the relatively simple, penetrative, periodic linear, graben "fabrics" that extend in all directions at the regional- to planet-scale on Venus, without regional strain localisation? I have recently discussed this question in detail with respect to tessera terrains on Venus (Hanmer, 2020). Therein I proposed a potential relationship between surface graben fabrics and regional-scale swarms of parallel blind dykes (see Head and Wilson, 2017; Wilson and Head, 2017 for an extensive analysis including blind dyke emplacement). In this contribution I have suggested that a similar hypothesis could apply to distributed extensional tectonic features in other parts of the second planet. In what follows, this discussion will focus on distributed shortening on Venus and elsewhere in the inner Solar System, and on venusian crustal-scale shear zones, followed by suggestions for future avenues of basic structural geological research on venusian extension, shortening and shearing..

9.1.1. Distributed shortening

Regarding distributed shortening, this contribution highlights issues directly related to satellite-based remote observation and interpretation, and emphasises the non-unique nature of the relationship between surface topographical morphology and the "hidden", subsurface, internal geometry, kinematics and mechanics of the structures involved. The historical terminology, still in use today, is equivocal and confusing. In addition, it is systematically applied across the inner Solar System to different surface topographical morphologies of linear, positive relief features that differ geometrically from one telluric body to another.

Comparison with potential analogues, both natural and simulated, can be a useful exercise, but it must be applied critically: it may illustrate

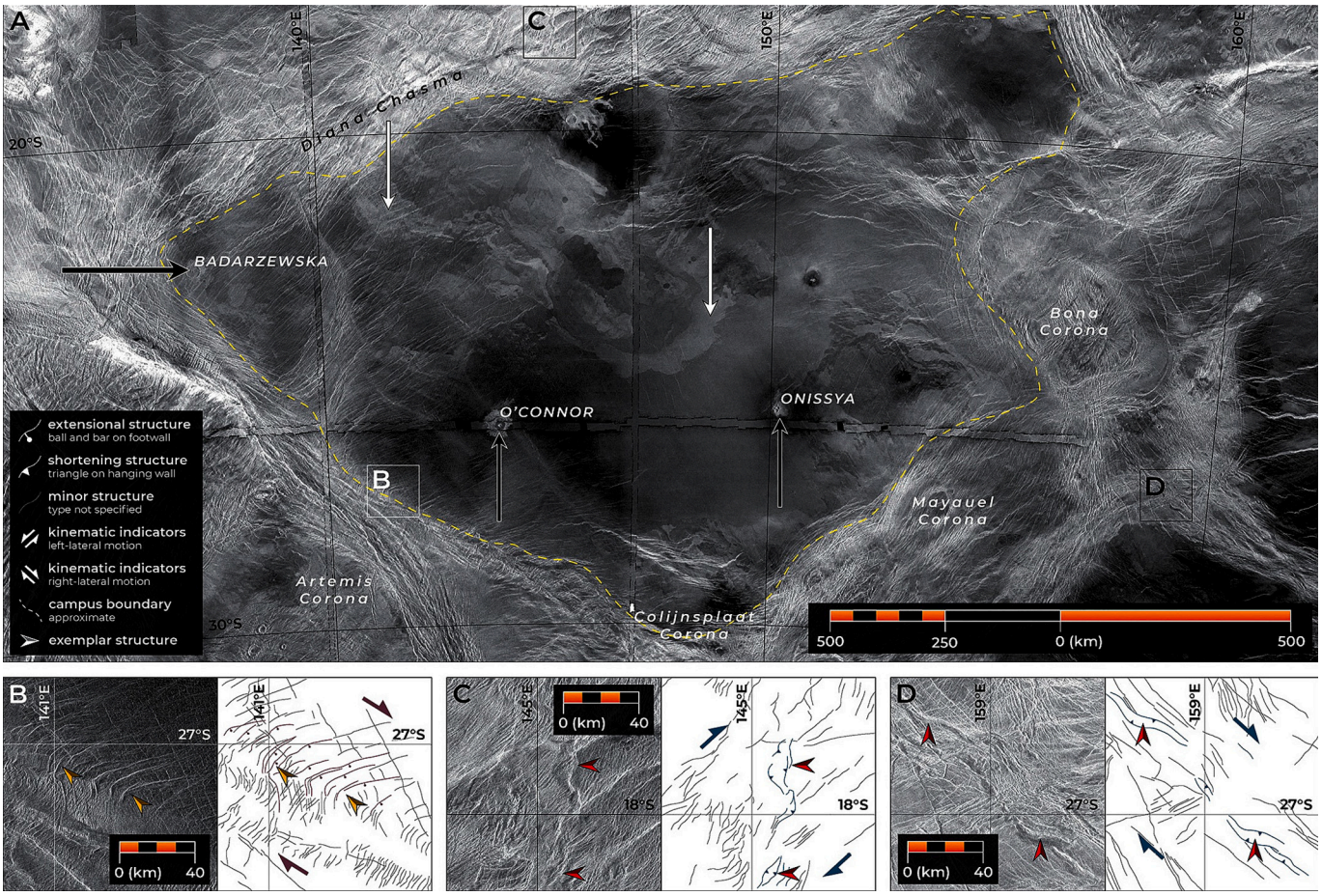

Fig. 43. Fig. 1 in Byrne et al. (2021). According to these authors, this illustrates a large crustal block in the Venus lowlands, located immediately NE of Artemis Corona (see Fig. 1a for approximate location). (A) Magellan radar image mosaic of the block. Named landforms are shown; the black and white arrows mark impact craters and prominent lava flows, respectively. The approximate outline of the block (campus) is marked by a dashed yellow line. (B) Radar image (left) and structural sketch (right) of extensional faults curving into the main groove belt that delineates the southwestern margin of this campus, here with a right-lateral sense of slip. (C) Sigmoidal, positive-relief landforms interpreted as right-lateral transpressive structures. (D) Another example of sigmoidal, positive-relief ridges regarded as denoting right-lateral transpression, with a different strike from those structures in C. Prominent extensional structures are in purple (with ball-and-bar symbols shown on example down-thrown blocks), and prominent shortening structures are in teal (with sawtooth symbols on example upper blocks). Minor and/or poorly expressed fractures of various types are shown as thin, black lines; wrinkle ridges are generally not recorded. Exemplar extensional and shortening landforms are marked with gold and red arrows, respectively. See also Supplemental S2A, S2B and S2C. Discussed in the text. With permission from Proceedings of the National Academy of Science. (For interpretation of the references to colour in this figure legend, the reader is referred to the web version of this article.)

feasibility, but not necessarily causality. However, in the case of published structural geological analyses of distributed shortening tectonic features on off-world telluric bodies of the inner Solar System, analogies have been empirically drawn with the asymmetrical *shapes* of surface topographical morphologies to support inference of the unseen, internal, present-day geometry of the underlying structure. The inferred internal geometry has then been used to construct quantitative models of the growth of the surface relief in question that have then been applied to Venus. In addition, by far the most frequent invocation of structural analogues involves uncritical acceptance of a limited number of terrestrial examples. However, detailed examination of the original terrestrial studies reveals that the only aspect that is potentially analogous is the *shape* of the surface topographical morphology, and even that is not necessarily the case. Indeed, on Venus, the surface topographical morphologies (symmetry/asymmetry) of distributed shortening tectonic features remain essentially unknown. Importantly, the far-field boundary conditions of the purported terrestrial analogues are commonly demonstrably complex, and closely linked to regional, modern-style plate tectonics unique to Earth. It is, therefore, difficult to support these examples as valid analogues of structural features on single-plate, off-world, telluric bodies of the inner Solar System, and especially Venus.

Invocation of terrestrial analogues extends beyond empirical application to individual shortening tectonic features. It has also been applied in support of the interpretation of regional- to global-scale map patterns of distributed shortening, including those that measure more than 1000 km in all directions. Some studies invoke comparison with terrestrial thin-skinned fold-and-thrust belts, while others draw parallels with terrestrial basement uplift tectonics. Such appeals to map-scale terrestrial analogues side-step major structural geological issues, including: (i) the transmission of compressive stress over vast distances, potentially in porous regolith, at very low values of distributed shortening strain; and, most importantly, (ii) the absence of extensive strain localisation, a characteristic feature of regional-scale deformation on Earth.

The source of estimations of low values of fault-related shortening strain on off-world telluric bodies of the inner Solar System is essentially two-fold: (i) quantitative, elastic, numerical modelling on the one hand; and (ii) the observation of partially occluded impact craters on the other. The former is based upon multiple assumptions and approximations regarding the geometry of the shortening tectonic feature under analysis, the elastic behaviour of the rocks containing the feature, and the implicit assumption that thrust fault daylighting, where included, is

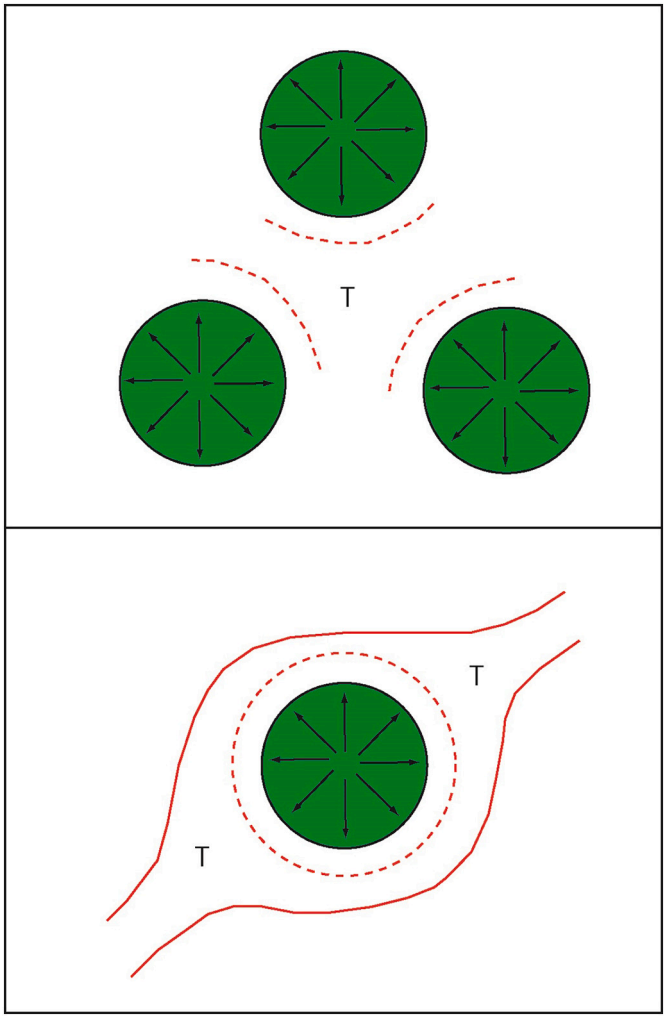

Fig. 44. Upper: Three schematic radially expanding diapiric bodies in plan view. The intersection of their local strain fields (dashed arcs = trace of the steeply dipping flattening plane) in the horizontal plane generates a triangular interference pattern cored by a steeply plunging prolate finite strain ellipsoid (T). Lower: A single expanding diapiric body emplaced during a regional shortening event, seen in plan view. The intersection of the local (dashed) and regional (solid) flattening planes in plan view results in two triangular interference patterns, each cored by a steeply plunging prolate finite strain ellipsoid (T). Discussed in the text. See Brun et al., 1976 and Hanmer et al., 1982 for model details.

incipient. The latter assumption, principally related to lobate scarps, is based on the further assumption that all impact crater occlusion is essentially structural However, the potential for mass wasting, involving sources of landslides either within or external to craters, has not been critically evaluated. Commonly, the craters cited are small, or heavily degraded, and their relationship to the local geology is equivocal. Yet studies continue to accept, present and interpret what amounts to poor observational data. These studies are then in turn uncritically cited by other studies as empirical support for their own interpretations (see Appendix for detailed review).

9.1.2. Strike-slip shearing

Regarding the purported crustal-scale strike-slip shear zones reported for Venus, this contribution emphasises that the published analyses are static. Interpretations of purported strike-slip shearing on Venus have consistently proposed models of implicit incipient deformation, even when the features concerned are 500 km to over 1000 km long, and 50 to 200 km wide. Such interpretations are geologically unrealistic on geometrical, kinematic and mechanical grounds. In contrast, modern terrestrial structural geological analysis is a dynamic, sequential paradigm that steps from observed geometries, via kinematics, to a mechanical interpretation. Recognition of strain gradients, manifested as the rotation of material planes and lines with progressive deformation, plus the localisation of strain, all observed in the correct plane (e.g. Ramsay and Graham, 1970; Berthe et al., 1979a; Díaz-Azpiroza et al., 2019), are inherent to the identification of shear zones (e.g. Fig. 25). Accordingly, reporting the present-day orientations of the traces of assumed or interpreted structural features, remotely observed on the venusian surface, does not constitute a valid kinematic analysis. In addition, it does not critically evaluate the possibility that the structural elements reported may be neither temporally or kinematically related. While mindful of Fossen et al. (2019) caution that "Uncritically defining deformation phases can easily generate a complicated discrete deformation history with no link to tectonic reality", it remains to be shown that the reported structures on Venus are *not* the products of unrelated, polyphase, deformation events that do not necessarily involve non-coaxial flow.

9.2. Basic structural geology on Venus: Future studies

What is the current state of the art regarding basic structural geology on off-world telluric bodies in the inner Solar System in general, and its applicability to understanding the surface of Venus? With respect to off-world distributed shortening in all parts of the inner Solar System, the past decade has seen the beginnings of doubts and questioning of the hitherto established consensual, but internally self-contradictory paradigms with respect to wrinkle ridges and lobate scarps, tentatively manifested in an evolving terminology: e.g. *"shortening tectonic features"*. However, this conceptual development is, as yet, limited in scope and extent. A similar questioning with respect to interpretation of distributed extension, specifically on Venus, has yet to initiate (however, see Hanmer, 2020). Regarding strike-slip shearing on Venus, the published literature has universally neglected to take account of the known geometrical, kinematic and mechanical determinants of crustal-scale shear zone development. This, despite the fact that, as this contribution demonstrates, such determinants have been well-known for the past 50 years. Given the increasing activity in inner Solar System science, both recently and for the coming decade, and especially with respect to Venus, it is essential that planetary scientists be unequivocally clear on what exactly they are proposing to map, as well as what has purportedly been mapped hitherto. What is required to go forward, to further the potential for the successful study of the basic structural geology of Venus? It goes without saying that imagery at greater resolution is always desirable. However, as this contribution shows, planetary science needs to be better grounded in a solid understanding of basic Earth-based structural geology in order to take full advantage of new and improved remote observational data and transform them into robust knowledge.

New data from upcoming missions to Venus are unlikely to be available until the mid-2030s. In the meantime, what can the planetary science community do today to better understand the basic structural geology of Venus and its significance for the tectonic evolution of the planetary surface?

This paper has critically reviewed proposed structural geological analogues, and found them wanting (Section 7). This is not surprising. A terrestrial structural geological analogue for remotely observed shortening features must be young enough that its surface topographic expression is preserved. In short, it must lie within the region of influence of very recent tectonic activity: typically, convergent continental margins. However, a terrestrial analogue for deformation on a single plate planet would be intra-plate, and sufficiently removed from the direct influence of plate tectonics. Alternatively, it could be limited in extent to a local scale, driven by local boundary conditions that are independent of plate tectonics. The former is improbable, while the latter

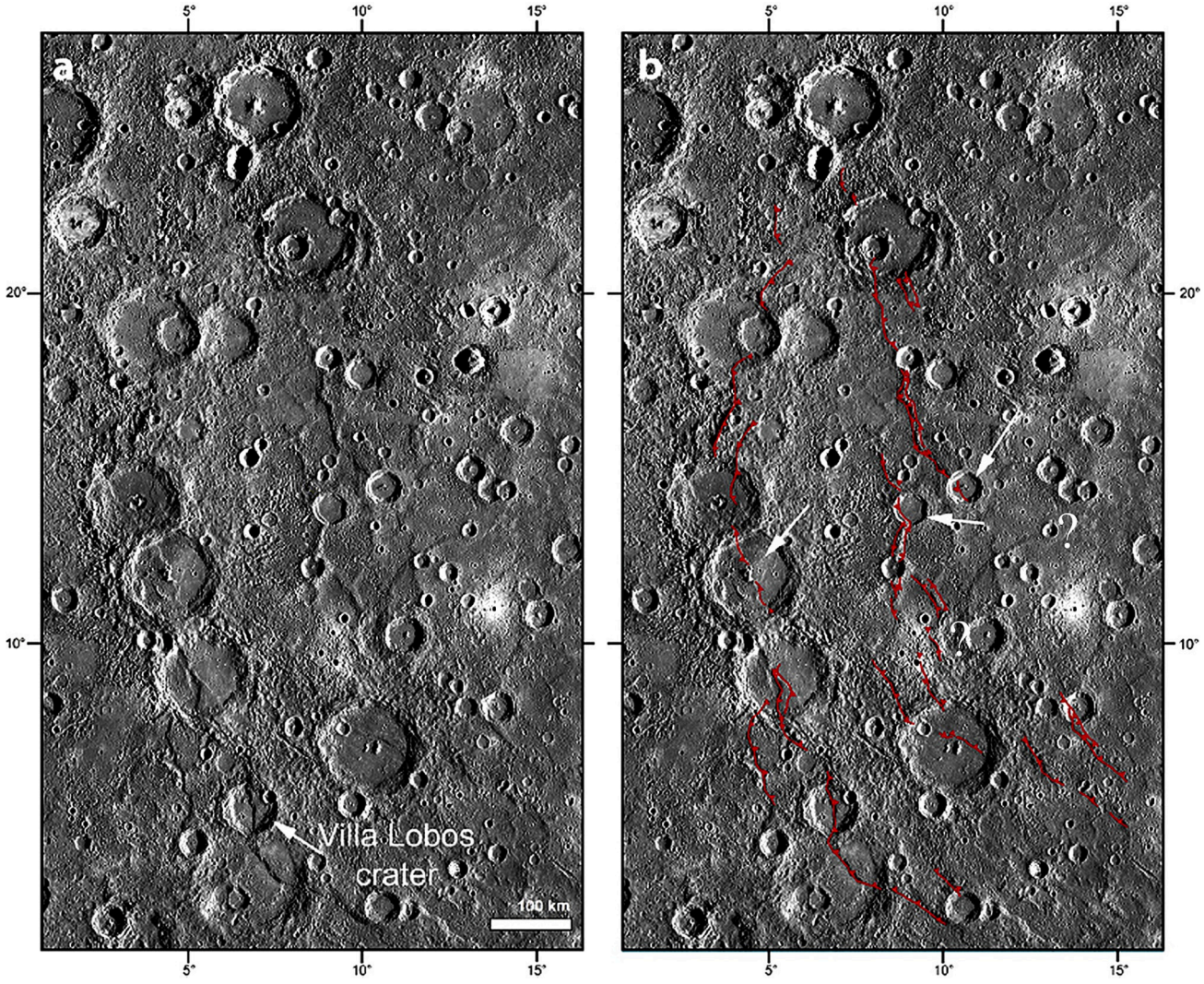

Fig. 45. Thrust system on Mercury (red). Fig. 2 in Giacomini et al. (2020). According to these authors, triangles indicate the dip direction of the thrusts, which show a NW vergence, except for four craters (white arrows) wherein the structures were interpreted to verge in the opposite direction, despite the absence of transverse accommodation faults. However, with few exceptions (e.g. Villa Lobos crater), it is not obvious that craters in this image are in fact transected. Furthermore, it is not obvious why some curvlinear ridges were identified as thrusts, but not others (e.g. between the question marks at right of centre). With permission from Geoscience Frontiers.. (For interpretation of the references to colour in this figure legend, the reader is referred to the web version of this article.)

might be found at the outcrop scale, much in the manner of the recent detailed analyses of jointing and detachment folding by Passchier et al. (2021) and Alsop et al. (2021), respectively. Unfortunately, the discovery of such key outcrops is of necessity serendipitous, and therefore unpredictable.

An obvious alternative option is modelling. On the one hand, numerical modelling has been undertaken with respect to axiomatic wrinkle ridges and lobate scarps (Section 4.4). However, it tends to be overly prescriptive. On the other hand, analogue table-top modelling is less prescriptive, and has more degrees of freedom. Note that the rheological properties of common modelling materials (e.g. Reber et al., 2020 and references therein), techniques for the creation of very fine-scale anisotropy (e.g. Dixon and Summers, 1985; see also Hanmer, 1986; Hanmer et al., 1996), and "real world" scaling of analogue models (e.g. Ramberg, 1981, p.1–6), have long been well-established. I suggest that laboratory analogue models could readily test the published hypotheses, reviewed above (e.g. Schultz, 2000), regarding the surface topographical expressions of both distributed axiomatic wrinkle ridges (i.e.. rise, ridge and wrinkle), and localised axiomatic lobate scarps.

In addition, it is apparent that, to date, the available Magellan data relevant to structural geology have not been fully exploited, despite extensive mapping. The most obvious example is the near total absence of information regarding the symmetry/asymmetry of distributed shortening tectonic features identified as wrinkle ridges on Venus (Supplemental 1). Based on their surface distribution on lowland plains about topographical and geoid highs, planet-scale geophysical modelling understandably postulates that such features are probably the product of shortening under the influence of gravity, as proposed by Sandwell et al. (1997) and Bilotti and Suppe (1999). This is a reasoned hypothesis, even though it assumes that the present-day topography, geoid and stress field applied at the time of wrinkle ridge formation. However, it does not inform us regarding the internal geometry of individual ridges, nor regarding the kinematics and mechanics of local shortening. Nor does it contribute to understanding the absence of strain localisation at the regional- to global-scales. Most importantly, given the general lack of *observational* evidence of systematic asymmetry associated with venusian features identified as wrinkle ridges, this planet-scale hypothesis is currently untestable. On the one hand, analogies have been drawn with superficially similar features on other planetary surfaces in the inner Solar System, including Earth. However, as shown in this review, off-world data and interpretations from elsewhere in the inner Solar System are not currently sufficiently robust to be directly applied

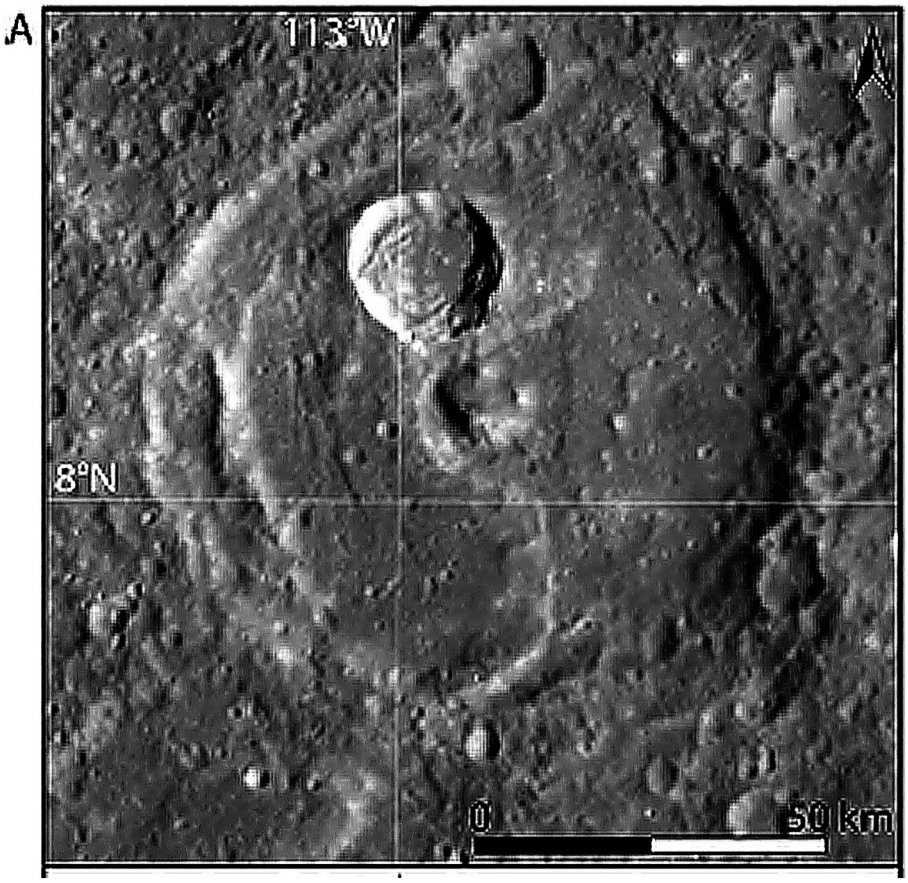

Fig. 46. Upper: Part of fig. 10 in Klimczak et al. (2019). According to these authors, this image shows a syntaxis on Mercury, formed where the central peak in an impact crater presented an obstacle to a thrust-fault-related landform. Alternatively, one might hypothesise that the lobate scarp within the crater could represent a landslide sourced in the crater wall at the left of the image. With permission from the Canadian journal of earth sciences.

on Venus in any event, and parallels drawn with terrestrial analogues are highly debatable. On the other hand, the under-utilisation of Magellan structural geological data presents an opportunity to reformulate the hypothesis to explain distributed shortening tectonic features on the second planet.

Given the absence of information regarding the symmetry/asymmetry of features identified as wrinkle ridges on Venus, one can speculate: what if such features were in fact mostly symmetrical? This could potentially eliminate the requirement for generalised reverse or thrust faulting, placing greater emphasis on periodic buckle folding (cf. Philip and Meghraoui, 1983; Crane, 2020a), and thereby diminish the requirement for significant regional-scale strain localisation. Furthermore, it might also allow that the mechanical problem of reticulate patterns could be resolved if the younger, superposed, local set of linear features were igneous (hypabyssal) in origin, similar to ridge rings (ring dykes) proposed in lunar maria by Strom (1972). Alternatively, a simple positive test of McGill (1993) suggestion that local linear patterns represent contractional wrinkle ridges developed concentric to magmatically-associated topographical highs (e.g. coronae) would be the presence of triangular strain interference patterns cored by low-strain zones, where two or more coeval sets of shortening tectonic features mutually interfere (e.g. Brun et al., 1976; Hanmer et al., 1982; Fig. 44). However, all of this is but hypothetical speculation without a fuller use of the available Magellan data. For example, basic testing of the fundamental symmetrical/asymmetrical postulate for distributed shortening tectonic features on Venus could be undertaken in a first instance by careful examination of a selection of the best quality "postage stamp" map areas in the existing Magellan data distributed across the planetary surface, where such features are, or can be, better imaged in stereo, as recently demonstrated by Knicely and Herrick (2021; see also Herrick et al., 2012; Herrick, 2018), to derive an initial, first order, statistically significant characterisation of their surface topographical morphologies. More systematic regional mapping would be undertaken in the future with higher resolution data from the planned Venus mapping missions that will be available in the 2030s.

The lack of a robust explanation for the common development of extensive, penetratively developed, distributed extensional graben "fabrics", without regional-scale strain localisation across Venus, points to the need to test alternative hypotheses, one of which envisions that graben fabrics could develop mechanically above the shallow-seated tips of hypabyssal blind magmatic intrusions in large scale dyke swarms. While there is still debate regarding the precise role of magmatic intrusion per se in developing linear dyke swarms (see Hanmer, 2020 and references therein), predictive models are available for the geometry and setting of individual graben developed above intruding dykes (e.g. Schultz et al., 2004, 2010). The diagnostic difference in vertical relief of the surface uplift adjacent to a dyke-induced graben, as opposed to the surface flanking a similar size graben generated by far-field extension, is of the order of $<$10 m to 100 m (e.g. Klimczak, 2014; however, see critical review in Martin and Watters, 2021), depending on the planetary body in question. Although currently available Magellan altimetry data do not lend themselves readily to detection of such subtle differences, careful examination of a selection of best quality "postage stamp" map areas, that are, or can be (e.g. Herrick et al., 2012; Herrick, 2018), better imaged in stereo in the Magellan data might provide a preliminary test of the hypothesis while awaiting higher resolution data due in the 2030s.

Over the past 30 years an unchallenged consensus has developed that

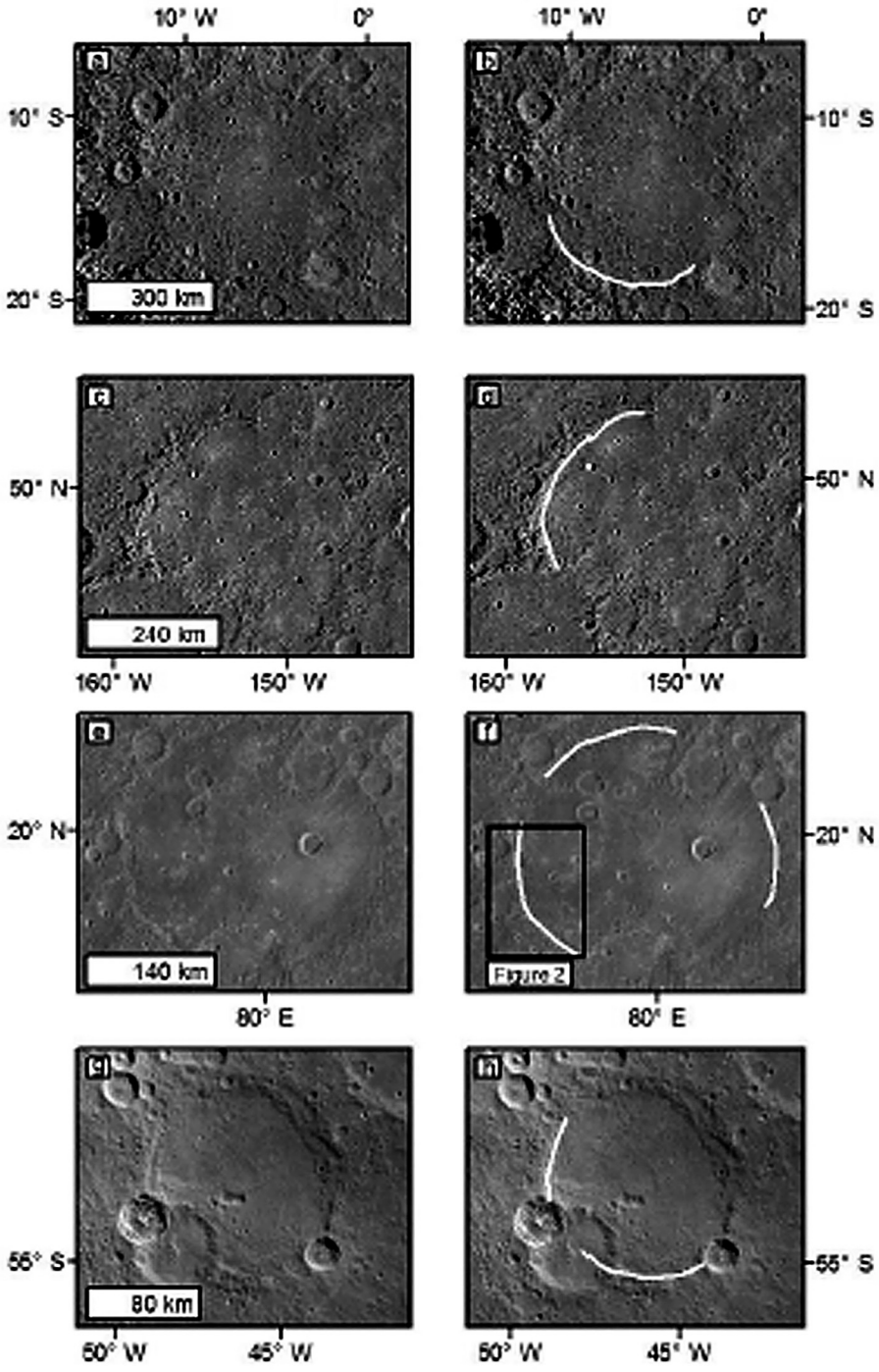

Fig. 47. Fig. 1 in Fegan et al. (2017). Examples of four basins on Mercury in which, according to these authors, the volcanic infill is part-bounded by one or more lobate scarps. White lines delineate resolvable lobate scarps where basin-fill is thrust toward or over the basin rim. However, the crater rims are so highly degraded that the presence of structural features within their rims is debatable. With permission from Elsevier.

crustal-scale strike-slip shear zones are present on Venus. However this consensus side-steps the lack of application of well-established structural geological determinants regarding the formation and development of crustal-scale shear zones that underpin criteria required to recognise and map them (see Section 8.2). Nonetheless, models of cratonic indentation and planet-scale mobile crustal / lithospheric *"jostling"* have been proposed for Venus, and extrapolated to the potential tectonic behaviour of the early Earth. The proposed crustal-scale shear zones in the venusian literature are currently testable against an Earth-based understanding of shear zone geology. For example, the current temperature at the venusian surface is ~465 °C; approximately equivalent to the thermal regime of terrestrial greenschist facies metamorphism. Setting aside the principal unknowns (e.g. the timing of deformation with respect to venusian planetary thermal evolution, the presence / absence of intra-crystalline water during venusian deformation, and the absence of experimental data for crystal-plastic behaviour of rocks at any planetary surface), the maximum width of a terrestrial greenschist mylonite zone is ~1000 m (e.g. Hanmer, 1988a; Hanmer, 1991; Hanmer et al., 1992), compared with the geologically unrealistic shear zones, up to 200 km wide, reported from Venus. Additionally, one

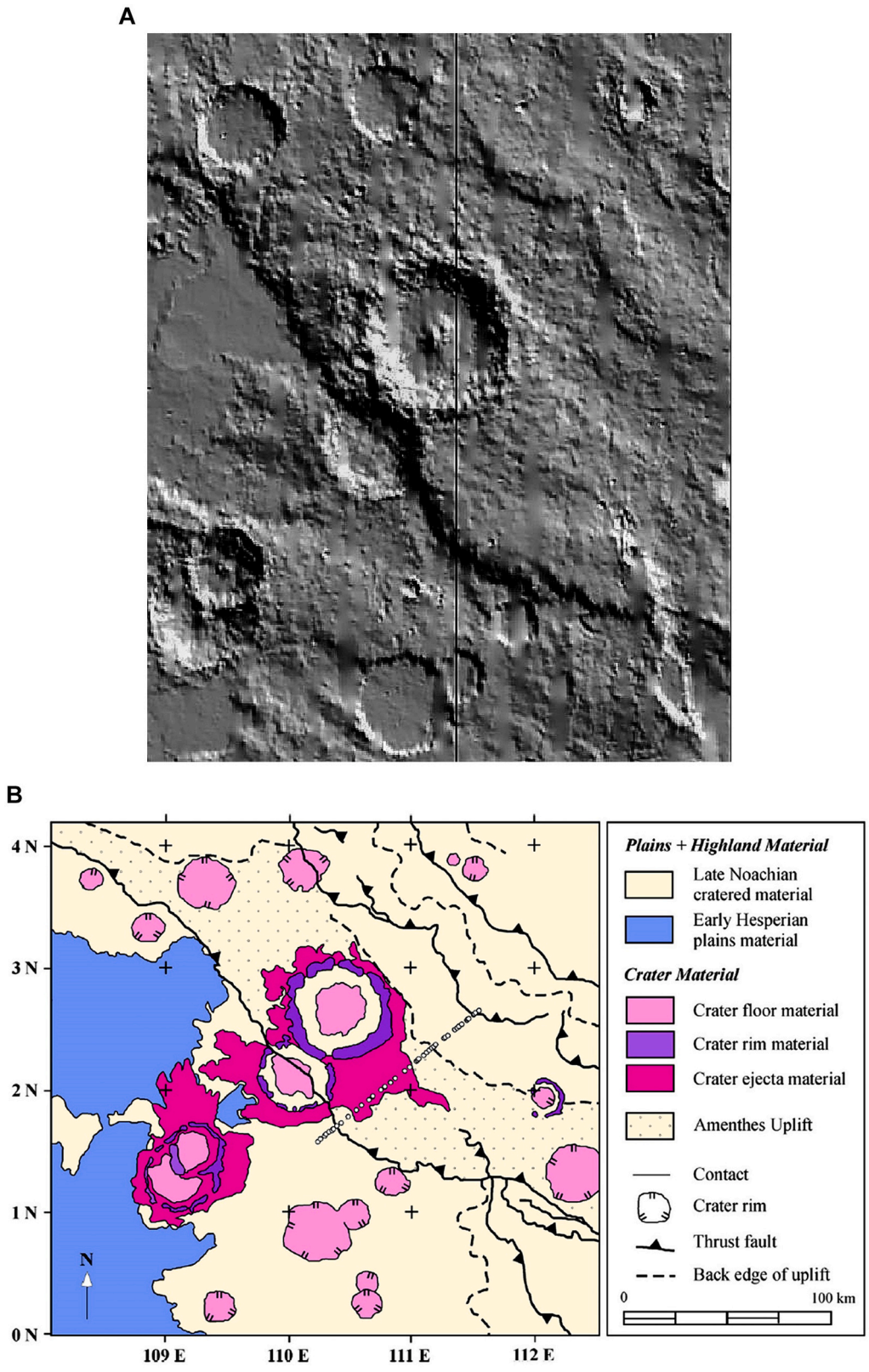

Fig. 48. (A) According to Watters (1993, his fig. 3b), Amenthes Rupes, a large-scale lobate scarp on Mars (see Fig. 5a for location) resulted from several kilometres or more of horizontal shortening, as determined from impact crater transection and occlusion. This image was sourced from JMARS (**J***ava* **M***ission-planning and* **A***nalysis for* **R***emote* **S***ensing*) at https://jmars.mars.asu.edu/.
B) Geologic map part of Amenthes Rupes, Mars, illustrating surface deposits, major thrust faults, impact craters and their ejecta. Fig. 1 in Mueller et al. (2014). With permission from Elsevier. The main Amenthes Rupes lobate scarp extends across the center of both images. Note the impact crater in the footwall at the base of the scarp), interpreted by both Watters (1993) and Mueller et al. (2014) as structurally transected, and the younger impact crater in the hanging wall immediately above it. Discussed in the text.

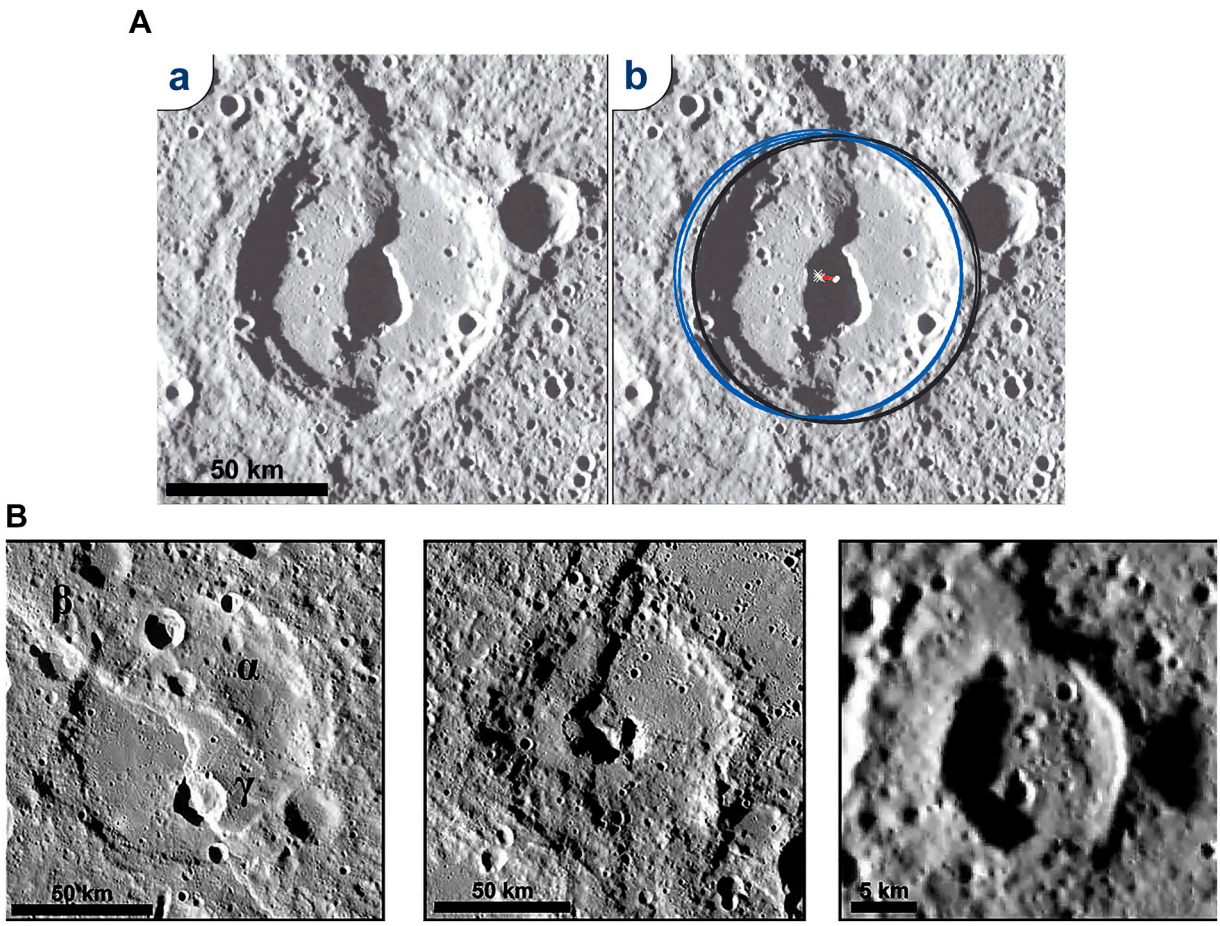

Fig. 49. (A) Crater on Mars used for measuring horizontal and vertical offsets of faulted craters: (a) image in stereographic projection centered at the crater centroid. (b) circles fitting the hanging wall part of the crater (black) versus their copies fitting the footwall part of the crater (blue). Circle centers are also shown for the hanging wall (white dot) and the footwall (white cross). The horizontal offset in the slip direction is measured along the red lines (from cross to dot). (B) Images of impact craters transected by Carnegie Rupes, Victoria Rupes, and Endeavour Rupes on Mercury (see Figs. 5b and 21 for locations) from which slip vectors and values have been reported. However, note the highly degraded nature of the crater rims. Parts of figs. 2 and 7 in Galluzzi et al. (2019). Discussed in the text. (For interpretation of the references to colour in this figure legend, the reader is referred to the web version of this article.)

can frame the basic question *"Do crustal-scale strike-slip shear zones exist on Venus?"* in terms of a series of basic structural geological inquiries. These can be addressed by careful examination of a patchwork selection of the best quality "postage stamp" map areas, locally well-imaged in stereo within the available Magellan data, initially guided by previous studies, to derive a first order, statistically significant characterisation of purported (candidate?) strike-slip crustal-scale shear zones. Such inquiries would include: can we recognise (i) strain gradients; (ii) the rotation of planes and lines with progressive deformation; (iii) the localisation of regional strain at geologically reasonable scales; and (iv) structural configurations from which to recognise a rotational component of deformation and derive a sense of vorticity of flow. Answers to these inquiries, even partial, would provide a first-order basic test of the existence of crustal-scale strike-slip shear zones, as well as hypotheses of the regional- to planet-scale tectonic behaviour of the crust and lithosphere of Venus, and their potential application to that of early Earth. More systematic regional mapping of candidate shear zones would be undertaken in the future with higher resolution data from the planned Venus mapping missions that will be available in the 2030s.

10. Conclusions

Across the inner Solar System the study of the geology of off-world telluric bodies is based on remote observation from orbit. Interpretations of basic structural geology based on satellite-borne observations of surface topographical morphology are not robust, and especially in the case of Venus. Adequate, observation-based, basic structural geological mapping of Venus has yet to be undertaken. Models of spatially extensive distributed shortening and extensional tectonic features applied to Venus side-step major structural geological issues, and are geologically unrealistic. Reports of purported strike-slip crustal-scale strike-slip shear zones on Venus do not take account of well-established Earth-based geometrical, kinematic and mechanical determinants of shear zone development. Comparisons of off-world shortening tectonic features across the inner Solar System with terrestrial analogues, and subsequently applied to Venus, are empirical and highly debatable. The formulation of regional- and global-scale tectonic models of Venus based on the current understanding of its basic structural geology, and their extrapolation to the tectonic behaviour of the early Earth is premature. Magellan data relevant to the basic structural geology of Venus are currently under-utilised. Basic structural geological questions regarding distributed shortening, extension and strike-slip shearing could be addressed today by strategic targeting and upgrading of currently available high quality stereo data from the Magellan mission, as well as analogue modelling, while awaiting higher resolution data from future Venus mapping missions expected in the 2030s.

Declaration of competing interest

The author declares that he has no known competing financial

interests or personal relationships that could have appeared to influence the work reported in this paper.

Data availability

No data was used for the research described in the article.

Acknowledgements

Alan Galley, Jim Head and Jim Thompson critically read earlier versions of this paper. I thank the journal reviewers for their input, and especially Kelsey Crane for her helpful, insightful comments. I am also grateful to Richard Ernst for unfailing bibliographical support, without which this research could not have been undertaken.

Appendix

A.1. Transected impact craters

Ubiquitous, initially circular impact crater rims are potential strain markers with which to test and calibrate structural models for transecting shortening tectonic features; principally lobate scarps. However, such deformed craters are notably rare (e.g. Conel, 1969; Sharpton and Head, 1988; Golombek et al., 1991). Nonetheless, many published studies have presented images purporting to illustrate the transection, deformation and/or partial occlusion of impact craters by linear traces at the base of shortening tectonic features on Mercury, the Moon and Mars, from which they quantitatively derive the dips and slips of proposed associated reverse or thrust faults. Indeed, such craters have been commonly used to justify the very existence of thrust and reverse faults (e.g. Head and Solomon, 1981; Sharpton and Head, 1988; Schultz and Tanaka, 1994; Mangold et al., 2000; Watters et al., 2000, 2009, 2010, 2015a; Mueller et al., 2014; Solomon et al., 2008; Galluzzi et al., 2014; Clark et al., 2017; Fegan et al., 2017; Ruj et al., 2018; Lu et al., 2019; Williams et al., 2019; Herrero-Gil et al., 2019, 2020; Giacomini et al., 2020). However, the transection relations are rarely unambiguous. This might not be unexpected for small diameter craters (< 5 km diameter; e.g. Watters et al., 2009, their fig. 9; Banks et al., 2015, their fig. 4; van der Bogert et al., 2018, their fig. 1). However, with few exceptions, commonly duplicated in multiple publications (e.g. Watters, 1993, his fig. 4b; Solomon et al., 2008, their figs. 2, 4 and 5; Byrne et al., 2014, their fig. 3; Kneissl et al., 2015, their fig. 3; Galluzzi et al., 2014, their fig. 5; Banks et al., 2015, their fig. 2e; Giacomini et al., 2020, their figs. 4, 6 and 10), it is also the case for large (>50 km) craters (e.g. Watters et al. (2009, their fig. 2a; Giacomini et al., 2020, their figs. 2 and 8; Fig. 45).

For example, many of the observations reported from Mercury, Mars and the Moon in support of structural transection or deformation of impact craters by daylighting thrusts associated with lobate scarps could equally well be interpreted in terms of mass wasting within the craters (e.g. Schultz and Tanaka, 1994, their fig. 16; Mangold et al., 2000; Watters et al., 2009, their figs. 4, 9 and 10; Watters et al., 2009, their figs. 2b, 3, and 4; Zuber et al., 2010, their fig. 1b; Watters et al., 2010, their fig. 4; Rothery and Massironi, 2010, their fig. 3; Byrne et al., 2014, their figs. 3 and S1c; Banks et al., 2015, their figs. 2, 3b and 3d; Fegan et al., 2017, their figs. 1 and 3; Ruj et al., 2018, their figs. 1, 3 and 6; Williams et al., 2019, their fig. 9; Klimczak et al., 2019, their fig. 11a; Herrero-Gil et al., 2020, their fig. 2; Giacomini et al., 2020, their fig. 2). By way of illustration, on Mercury, a scarp, confined to ~75% of the floor of a circular, ~80 km diameter impact crater, that diverges about the crater's central peak, was interpreted by Klimczak et al. (2019) as a *"syntaxis … a thrust-related landform"* (Fig. 46). However, it could equally be interpreted as a divergent landslide. Similarly, most of the craters presented by Fegan et al. (2017) are so highly degraded that the presence of tectonic features within their rims is debatable (Fig. 47).

In a detailed study, Watters, 1993, his fig. 3b; see also Watters and Robinson, 1999, their fig. 2a; Watters et al., 2000, their fig. 1b; Watters, 2003, his fig. 3) presented Amenthes Rupes, Mars (see Fig. 5a for location), as underlain by a simple thrust that partially occludes a ~ 30 km impact crater located in the footwall at the base of the scarp (Fig. 48). Watters (1993) used the observed occlusion to estimate the amount of slip (several km) on the thrust fault. A ~ 40 km impact crater located at the rim of the scarp, immediately above the occluded crater, was described as undisturbed. However, referring to the same two impact craters, Mueller et al. (2014) acknowledged a major complication regarding this example: *" … about 40% of the crater rim* [beneath] *the hanging wall of the thrust has been modified by an ejecta blanket produced by a subsequent large impact located immediately* [in the hangingwall]*"*. One might ask how one separates structural occlusion from impact ejecta occlusion of the crater in the footwall in this example.

A.2. Quantitative estimates of fault vectors, dips and slips

In a study of Discovery Rupes, the largest individual shortening tectonic feature on Mercury (Fig. 9; see Fig. 5b for location), Watters et al., 1998, their figs. 1 and 3) were very clear. Even though Discovery Rupes cuts the 60 km diameter Rameau crater diametrically*"… there is no significant difference in the diameter of Rameau crater, the larger of two craters cut by Discovery Rupes, regardless of the azimuthal orientation of the measured diameter. These measurements indicate that overthrusting is not a significant component of total horizontal shortening"* (see also Byrne et al., 2014, their figs. 1b and 3). Taken at face value, the reported observations imply that this regional-scale thrust fault, >500 km in strike length, only breaks the planetary surface incipiently. On its own, this would be geologically remarkable. However, this is not an isolated occurrence: *"It is important to note that these estimates assume there has been no significant translation of the fault block over the fault ramp onto the flat"* (Watters et al., 1998; see also Antoniadi Dorsa in Watters et al., 2015a, their fig. 2b; Fegan et al., 2017, their figs. 3 and 9). Similarly, again regarding Discovery Rupes, Head and Solomon (1981) reported that *"The lobate scarps on Mercury have been interpreted as thrust or reverse faults on the basis of morphology, transection relations, and the foreshortening of at least one crater cut by a younger scarp"*, yet the illustration provided (their fig. 6) shows two apparently circular, diametrically transected craters. One obvious hypothetical explanation for these observations is that these impact craters post-date most of the fault movement, and only record very minor post-impact fault reactivation (e.g. Galluzzi et al., 2014). If valid, this would imply that the impact crater shape per se provides little or no constraint on the total slip accumulated on the fault in question.

Galluzzi et al., 2014, their figs. 3 and 5; Galluzzi et al., 2019, their fig. 2; Fig. 49) derived fault slip values and vectors by fitting circles to the purportedly displaced rims of what they reasonably assumed to be originally circular impact craters preserved in the hangingwalls and footwalls of transecting lobate scarps on Mercury. However, the highly degraded state of the craters analysed makes it difficult to observe the original crater plan-forms for the purpose of fitting circles (see also Galluzzi et al., 2019, their fig. 7; *"The large uncertainty is due to its irregular and degraded rim that can be fitted by different set* [sic] *of circles"*). Nonetheless, Galluzzi et al. (2014) determined slip values of less than a kilometer for the lobate scarps studied. However, they noted that some of their results had to be treated with caution because measurements on different transected impact craters associated with the same lobate scarp yielded internally inconsistent thrust dip values (31–53°), and slip values that differed by a factor of ~3 between the craters.

A.3. Tectonic occlusion or mass wasting?

According to the cited studies of impact crater occlusion (Appendix A.2), off-world lobate scarps of the inner Solar System represent either universally minor reverse/thrust fault slip, or fault slip that coincidentally attenuates to near zero at planetary surfaces. Either way, this is a mechanical conundrum for scarps 100 s of kilometres in strike length,

which has not been explicitly addressed in the published literature. Is there an alternative hypothesis? In addition to the possibility that associated impact craters may post-date most of the fault movement (see Appendix A.2), and only record minor post-impact fault reactivation, the inner walls of many impact craters show features that could be interpreted as slumping (mass wasting). Combined with the highly lobate nature of the linear trace of the scarp that transects the crater in question, plus the absence of detectable shortening of the circular crater plan-form, it is not unreasonable to ask whether some "transected" impact craters might simply post-date structural activity associated with the adjacent lobate scarp. Could some impact craters, located adjacent to the foot of a lobate scarp, contain landslide run-outs on their floors and, thereby, not furnish any constraints whatsoever on the geometry, kinematics, mechanics or strain associated with a fault that may underlie the adjacent lobate scarp? On the Moon, Binder and Gunga (1985), Clark et al. (2017), van der Bogert et al. (2018), and Williams et al. (2019) acknowledged a potential role for mass wasting in the modification of small impact craters at the base of lunar lobate scarps (see also Banks et al., 2015). However, none of these studies considered the possibility that mass wasting might lead to partial crater occlusion. Most importantly, they only considered mass wasting generated by local faulting, as opposed to shaking of potentially far-field origin (seismic or impact; see Melosh, 1979 for detailed analysis).

The examples cited in the foregoing sections (Appendix A.1 and A.2) point to multiple occurrences of scarps confined to all or part of an impact crater floor, either with (i) no external extensions; (ii) external extensions only on one side of the crater; or (iii) a lack of direct linkage between the scarp within the crater and the scarp(s) outside. Some scarps within mildly elliptical craters trend parallel to kinematically upstream slump scars located in the impact crater walls that are responsible for the crater's non-circular plan-form, such that both slump scars and scarps lie perpendicular to the long semi-axis of the crater (Zuber et al., 2010, their fig. 1b). Clearly this configuration is inconsistent with the concept of shortening of the crater along a vector perpendicular to the purported internal trace of a lobate scarp.

Taken together, potential reinterpretation of the evidence reviewed in this Appendix opens the possibility that (i) some topographical scarps within craters might reflect mass wasting of impact crater walls; (ii) some crater occlusions may record a combination of structural and mass wasting effects, or no structural effect at all; (iii) some "transections" could reflect localised mass wasting from an adjacent topographical high into a lower lying, younger impact crater; and (iv) some occluded impact craters may thereby postdate the adjacent, external topographical scarps in question. Whatever the correct interpretations, the purported tectonic transecting relationships, if real, are not without ambiguity that warrants further, critical evaluation.

References

Alsop, G.I., Weinberger, R., Marco, S., Levi, T., 2021. Detachment fold duplexes within gravity-driven fold and thrust systems. J. Struct. Geol. 142, 104207.

Andrews-Hanna, J.C., 2020. The tectonic architecture of wrinkle ridges on Mars. Icarus 351 (2020), 113937.

Arvidson, R.E., Greeley, R., Malin, M.C., Saunders, R.S., Izenberg, N., Plaut, J.J., Stofan, E.R., Shepard, M.K., 1992. Surface modification of Venus as inferred from Magellan observations of plains. J. Geophys. Res. 97, 13303–13317.

Aubele, J.C., 1989. Morphologic Components And Patterns In Wrinkle Ridges: Kinematic Implications. Lunar Planet. Sci. MEVTV Workshop on Tectonic Features on Mars, pp. 13–15.

Bak, J., Korstgard, J., Sorensen, K., 1975. A major shear zone within the Nagssugtoqidian of West Greenland. Tectonophysics 27, 191–209.

Banerdt, W.B., Sammis, C.G., 1992. Small-scale fracture patterns on the volcanic plains of Venus. J. Geophys. Res. 97, 16,149-16,166.

Banerdt, W.B., McGill, G.E., Zuber, M.T., 1997. Plains tectonics on Venus. In: Bougher, S. W., et al. (Eds.), Venus II. The University of Arizona Press, ISBN 0816518300, pp. 901–930.

Banks, M.E., Watters, T.R., Robinson, M.S., Tornabene, L.L., Tran, T., Ojha, L., Williams, N.R., 2012. Morphometric analysis of small-scale lobate scarps on the Moon using data from the Lunar Reconnaissance Orbiter. J. Geophys. Res. 117, E00h11. https://doi.org/10.1029/2011je003907.

Banks, M.B., Xiao, Z., Watters, T.R., Strom, R.G., Braden, S.E., Chapman, C.R., Solomon, S.C., Klimczak, C., Byrne, P.K., 2015. Duration of activity on lobate-scarp thrust faults on Mercury. J. Geophys. Res. Planets 120, 1751–1762. https://doi.org/10.1002/2015JE004828.

Barrash, W., Bond, J., Venkatakrishnan, V., 1983. Structural evolution of the Columbia Plateau Washington and Oregon. Am. J. Sci. 183, 897–935.

Basilevsky, A.T., 1994. Concentric wrinkle ridge pattern around Sif and Gula. Proc. Lunar Planet. Sci. Lunar Planet. Inst. 25, 63–64.

Basilevsky, A.T., Head, J.W., 1998. The geologic history of Venus: a stratigraphic view. J. Geophys. Res. 103, 8531–8544.

Basilevsky, A.T., Head, J.W., 2003. The surface of Venus. Rep. Prog. Phys. 66, 1699–1734.

Bell, T.H., 1981. Foliation development - the contribution, geometry and significance of progressive, bulk, inhomogeneous shortening. Tectonophysics 75, 273–296.

Bell, T.H., 1985. Deformation partitioning and porphyroblast rotation in metamorphic rocks: a radical reinterpretation. J. Metamorph. Geol. 3, 109–118.

Bell, T.H., Hammond, R.L., 1984. On the internal geometry of mylonite zones. J. Geol. 3, 109–118.

Berthe, D., Choukroune, P., Jegouzo, P., 1979a. Orthogneiss, mylonite and non coaxial deformation of granites: the example of the South Armorican Shear Zone. J. Struct. Geol. 1, 31–42.

Berthe, D., Choukroune, P., Gapais, D., 1979b. Orientations preferentielles du quartz et orthogneissification progressive en regime cisaillant: l'exemple du cisaillement sud-armoricain. Bull. Soc. Fr. Minéral. Cristallogr. 102, 265–272.

Bethell, E.M., Ernst, R.E., Samson, C., 2022. Analysis of Venusian wrinkle ridge morphometry using stereo-derived topography: a case study from Southern Eistla Regio. J Geophys. Res.: Planets 127. https://doi.org/10.1029/2021JE006879 e2021JE006879.

Bilotti, F., Suppe, J., 1999. The global distribution of wrinkle ridges on Venus. Icarus 139, 137–157.

Binder, A.B., Gunga, H.C., 1985. Young thrust-fault scarps in the highlands: Evidence for an initially totally molten Moon. Icarus 6, 421–441.

Bindschadler, D.L., Head, J.W., 1991. Tessera terrain, Venus: characterization and models for origin and evolution. J. Geophys. Res. 96, 5889–5907.

Bindschadler, D.L., Schubert, G., Kaula, W.M., 1992. Coldspots or hotspots? The origin of plateau-shaped highlands on Venus. J. Geophys. Res. 97, 13459–13532.

Biot, M.A., 1961. Theory of folding of stratified viscoelastic media and its implications in tectonics and orogenesis. Geol. Soc. Am. Bull. 72, 1595–1620.

Bjonnes, E.E., Hansen, V.L., Swenson, J.B., 2012. Equilibrium resurfacing of Venus: results from new Monte Carlo modeling and implications for Venus surface histories. Icarus 217, 451–461. https://doi.org/10.1016/j.icarus.2011.03.033.

Blakely, R.J., Sherrod, B.L., Weaver, C.S., Wells, R.E., Rohay, A.C., Barnett, E.A., Knepprath, Nichole E., 2011. Connecting the Yakima fold and thrust belt to active faults in the Puget Lowland, Washington. J. Geophys. Res. 116, B07105. https://doi.org/10.1029/2010JB008091.

Boyer, S.E., 1986. Styles of folding within thrust sheets: examples from the Appalachian and Rocky Mountains of the USA and Canada. J. Struct. Geol. 8, 325–339.

Boyer, S.E., Elliott, D., 1982. Thrust systems: Am. Assoc. Petrol. Geol. Bull. 66, 1196–1230.

Brun, J.P., Le Corre, C., Le Theoff, B., 1976. Schistosite et diapirisme: un exemple, les "mantled gneiss domes" de Kuopio (Finlande). Bull. Soc. Geol. Fr. 7 (18), 143–1459.

Buchan, K.L., Ernst, R.E., 2019. Giant circumferential dyke swarms: catalogue and characteristics. In: Srivastava, R.K., et al. (Eds.), Dyke Swarms of the World: A Modern Perspective. Springer Geology. https://doi.org/10.1007/978-981-13-1666-1_1.

Butler, R.W.H., 1986. Thrust tectonics, deep structure and crustal subduction in the Alps and Himalayas. J. Geol. Soc. Lond. 143, 857–873. https://doi.org/10.1144/gsjgs.143.6.0857.

Butler, R.W.H., 1992. Evolution of Alpine fold–thrust complexes: a linked kinematic approach. In: Mitra, S., Fisher, G. (Eds.), Structural Geology of Fold and Thrust Belts. Johns Hopkins University Press, Baltimore, MD, pp. 29–44.

Butler, R.W.H., Bond, C.E., Cooper, M.A., Watkins, H.M., 2018. Interpreting structural geometry in fold– thrust belts: why style matters. J. Struct. Geol. 114, 251–273.

Butler, R.W.H., Bond, C.E., Cooper, M.A., Watkins, H., 2020. Fold–thrust structures – where have all the buckles gone? In: Bond, C.E., Lebit, H.D. (Eds.), Folding and Fracturing of Rocks: 50 Years of Research since the Seminal Text Book of J. G. Ramsay. Geol. Soc. Lon. Sp. Pub, 487, pp. 21–44. https://doi.org/10.1144/SP487.7.

Byrne, P.K., Klimczak, C., Celâl Sengör, A.M., Solomon, S.C., Watters, T.R., Hauck, S.A., 2014. Mercury's global contraction much greater than earlier estimates. Nat. Geosci. https://doi.org/10.1038/NGEO2097.

Byrne, P.K., Klimczak, C., McGovern, P.J., Mazarico, E., James, P.B., Neumann, G.A., Zuber, M., Solomon, S.C., 2015. Deep-seated thrust faults bound the Mare Crisium lunar mascon. Earth Planet. Sci. Lett. 427, 183–190.

Byrne, P.K., Ghail, R.C., Gilmore, M.S., Şengör, A.M., Klimczak, C., Senske, D.A., Whitten, J.L., Khawja, S., Ernst, R.E., Solomon, S.C., 2020. Venus tesserae feature layered, folded, and eroded rocks. Geology 49, 81–85.

Byrne, P.K., Ghail, R.C., Celâl Sengör, A.M., James, P.B., Klimczak, C., Solomon, S.C., 2021. A globally fragmented and mobile lithosphere on Venus., 2021. PNAS 118 (26). https://doi.org/10.1073/pnas.2025919118 e2025919118.

Catchings, R., 1994. Upper-crustal structure beneath the Columbia River Basalt Group, Washington: Gravity interpretation controlled by borehole and seismic studies: discussion. Geol. Soc. Am. Bull. 106, 1096-1011.

Catchings, R., Mooney, W.D., 1988. Crustal structure of the Columbia Plateau: evidence for continental rifting. J. Geophys. Res. 93, 459–474.

Cawood, A.J., Bond, C.E., 2020. Broadhaven revisited: a new look at models of fault–fold interaction, 2020. In: Bond, C.E., Lebit, H.D. (Eds.), Folding and Fracturing of Rocks:

50 Years of Research since the Seminal Text Book of J. G. Ramsay. Geol. Soc. London Sp. Pub, 487, pp. 105–126. https://doi.org/10.1144/SP487.11.
Chapple, W.M., 1978. Mechanics of thin-skinned fold-and-thrust belts. Geol. Soc. Am. Bull. 89, 1189–1198.
Chemenda, A.I., 2022. Bed thickness-dependent fracturing and inter-bed coupling define the nonlinear fracture spacing-bed thickness relationship in layered rocks: numerical modeling. J. Struct. Geol. 165 https://doi.org/10.1016/j.jsg.2022.104741.
Chemenda, A.I., Lamarche, J., Matonti, C., Bazalgette, L., Richard, P., 2021. Origin of strong nonlinear dependence of fracture (joint) spacing on bed thickness in layered rocks: Mechanical analysis and modeling. J. Geophys. Res. Solid Earth 126. https://doi.org/10.1029/2020JB020656 e2020JB020656.
Chicarro, A.F., Schultz, P.H., Masson, P., 1985. Global and regional ridge patterns on Mars. Icarus 63, 153–174.
Chinnery, M.J., 1966. Secondary faulting. Can. J. Earth Sci. 3, 163–190.
Christie-Blick, N., Biddle, K.T., 1985. Deformation and basin formation along strike-slip faults. *In* Strike-slip deformation, basin formation, and sedimentation. In: Biddle, K. T., Christie-Blick, N. (Eds.), Soc,. Econ. Paleontol. Mineral. Sp. Pub, 37, pp. 1–34.
Clark, J.D., Hurtado, J.M., Hiesinger, H., van der Bogert, C.H., Bernhardt, H., 2017. Investigation of newly discovered lobate scarps: implications for the tectonic and thermal evolution of the Moon. Icarus 298, 78–88.
Cobbold, P.R., Cosgrove, J.W., Summers, J.M., 1971. Development of internal structures in deformed anisotropic rocks. Tectononophysics 12, 23–53.
Cole, H.M., Andrews-Hanna, J.C., 2017. The anatomy of a wrinkle ridge revealed in the wall of Melas Chasma, Mars 2017. J. Geophys. Res.: Planets 122 (5), 889.
Conel, J., 1969. Structural features relating to the origin of lunar wrinkle ridges. Jet Prop. Lab. Space Prog. Sum. 37-56 (11), 58–63.
Connors, C.D., Hughes, A.N., Ball, S.M., 2021. Forward kinematic modeling of fault-bend folding. J. Struct. Geol. 143, 104252.
Cooke, M.L., Pollard, D.D., 1997. Bedding-plane slip in initial stages of fault-related folding. J. Struct. Geol. 19, 567–581.
Corti, G., 2005. Dynamics of periodic instabilities during stretching of the continental lithosphere: view from centrifuge models and comparison with natural examples. Tectonics 24. https://doi.org/10.1029/2004TC001739. TC2008.
Coward, M.P., 1976. Strain within ductile shear zones. Tectonophysics 34, 181–197.
Coward, M.P., Kim, J.H., 1981. Strain within thrust sheets. In: McClay, K., Price, N.J. (Eds.), Thrust and Nappe Tectonics: Geol. Soc. Lond. Sp. Pub, 9, pp. 275–292.
Crane, K., 2020a. Structural interpretation of thrust fault-related landforms on Mercury using Earth analogue fault models. Geomorphology 369 (2020). 107366.
Crane, K., 2020b. Approach and application of industry software to structural investigations in the subsurface of Mercury's thrust fault-related landforms. J. Struct. Geol. 141, 104218.
Crane, K.T., Klimczak, C., 2019. Tectonic patterns of shortening landforms in Mercury's northern smooth plains. Icarus 317, 66–80.
Dahlstrom, C.D.A., 1970. Structural geology in the eastern margin of the Canadian Rocky Mountains. Bull. Can. Petrol. Geol. 18, 332–406.
Davidson, A., 1984. Identification of ductile shear zones in the southwestern Grenville Province of the Candian Shield. In: Kroner, A., Greiling, R. (Eds.), Precambrian Tectonic Illustrated, E. Int. Un. Geol. Sci. Comm Tectonics. Schweizerbart'sche Verlagsbuchhandlung, Stuttgart, pp. 263–280.
Davis, A.M., Ghail, R.C., 1999. An extended strike-slip zone in Aphrodite Terra. In: Lunar Planet. Sci. XXI, Lunar Planet. Inst. Conf. XXX, p. 1330.
Davis, G.A., Lister, G.S., 1988. Detachment faulting in continental extension: perspectives from the southwestern U.S. Cordillera. In: John Rodgers symposium volume: Geol. Soc. Am. Sp. Pap, 218, pp. 133–159.
DeShon, H.R., Young, D.A., Hansen, V.L., 2000. Geologic evolution of southern Rusalka Planitia, Venus. J. Geophys. Res. 105, 6983–6995.
Díaz-Azpiroza, M., Fernández, C., Czeckc, D.M., 2019. Are we studying deformed rocks in the right sections? Best practices in the kinematic analysis of 3D deformation zones. J. Struct. Geol. 125, 218–225.
Dixon, J.M., Summers, J.M., 1985. Recent developments in centrifuge modelling of tectonic processes: equipment, model construction techniques and rheology of model materials. J. Struct. Geol. 7, 83–102.
Donath, F.A., 1968. Experimental study of kink-band development. In: Baer, A.J., Norris, D.K. (Eds.), Proc. Conf. Res. Tectonics, pp. 255–292. Geol. Surv Canada. Pap. 68, 52.
Elliott, D., 1976. The energy balance and deformation mechanisms of thrust sheets. Phil. Trans. Roy. Soc. Lond. A283, 289–312. https://doi.org/10.1098/rsta.1976.0086.
Ernst, R.E., Head, J.W., Parfitt, E., Grosfils, E., Wilson, L., 1995. Giant radiating dyke swarms on Earth and Venus. Earth Sci. Rev. 39 (1–58), 1995.
Ernst, R.E., Grosfils, E.B., Mège, D., 2001. Giant dyke swarms: Earth, Venus and Mars. Annu. Rev. Earth Planet. Sci. 29, 489–534.
Ernst, R.E., Desnoyers, D.W., Head, J.W., Grosfils, E.B., 2003. Grabens-fissure systems in Guinevere Planitia and Beta Regio (264°–312°E, 24°–60°N), Venus, and implications for regional stratigraphy and mantle plumes. Icarus 164, 282–316.
Ernst, R.E., Buchan, K.L., Desnoyers, D.W., 2007. Plumes and plume clusters on Earth and Venus: evidence from Large Igneous Provinces (LIPS). In: Yuen, D.A., Maruyama, S., Karato, S.I., Windley, B.F. (Eds.), Superplumes: Beyond Plate Tectonics. Springer, Dordrecht. https://doi.org/10.1007/978-1-4020-5750-2_18.
Escher, A., Sorensen, K., Zeck, H.P., 1976. Nagssugtoqidian mobile belt in West Greenland. In: Escher, A., Watterson, J. (Eds.), Geology of Greenland. Geological Survey of Greenland, Copenhagen, pp. 76–95.
Fagereng, A., Biggs, J., 2019. New perspectives on 'geological strain rates' calculated from both naturally deformed and actively deforming rocks. J. Struct. Geol. 125, 100–110.
Fegan, E.R., Rothery, D.A., Marchi, S., Massironi, M., Conway, S., Anand, M., 2017. Late movement of basin-edge lobate scarps on Mercury. Icarus 288, 226–234. https://doi.org/10.1016/j.icarus.2017.01.005. hal-02271712.
Fernández, C., Anguita, F., Ruiz, J., Romeo, I., Martín-Herrero, A.I., Rodríguez, A., Pimentel, C., 2010. Structural evolution of Lavinia Planitia, Venus: implications for the tectonics of the lowland plains. Icarus. 206, 210–228.
Ford, J.P., Plaut, J.J., Weitz, C.M., Farr, T.G., Senske, D.A., Stofan, E.R., Michaels, G., Parker, T.J., 1993. Guide to Magellan image interpretation, JPL Publ. 93-24, Jet Propul. Lab., Pasadena, Calif.
Fossen, H., Cavalcante, G.C.G., 2017. Shear zones - a review. Earth Sci. Rev. 17, 434–455.
Fossen, H., Cavalcante, G.C.G., Vizeu, R., Pinheiroc, L., Archanjod, C.J., 2019. Deformation – progressive or multiphase? J. Struct. Geol. 125, 82–99.
Fossen, H., Harris, L.B., Cavalcante, C., Archanjo, C.J., Avila, C.F., 2022. The Patos-Pernambuco shear system of NE Brazil: partitioned intracontinental transcurrent deformation revealed by enhanced aeromagnetic data. J. Struct. Geol. 158 https://doi.org/10.1016/j.jsg.2022.104573.
Frank, S.L., Head, J.W., 1990. Ridge belts on Venus: Morphology and origin: Earth, Moon and Planets, 50/51, pp. 421–470.
Galluzzi, V., Di Achille, G., Ferranti, L., Popa, C., Palumbo, P., 2014. Faulted craters as indicators for thrust motions on Mercury. In: Platz, T., Massironi, M., Byrne, P.K., Hiesinger, H. (Eds.), Volcanism and Tectonism Across the Inner Solar System. Geol. Soc. Lon.Sp. Pub. 401. https://doi.org/10.1144/SP401.17.
Galluzzi, V., Ferranti, L., Massironi, M., Giacomini, L., Guzzetta, L., Palumbo, P., 2019. Structural analysis of the Victoria Quadrangle Fault Systems on Mercury: timing, geometries, kinematics, and relationship with the high-Mg region. J. Geophys. Res. Planets 124. https://doi.org/10.1029/2019JE005953.
Gerya, T.V., 2014. Plume induced crustal convection: 3D thermomechanical model and implications for the origin of novae and coronae on Venus. Earth Planet. Sci. Lett. 391, 183–192.
Ghail, R.C., 2002. Structure and evolution of southeast Thetis Regio. J. Geophys. Res. 107, 5060. https://doi.org/10.1029/2001JE001514.
Ghent, R., Hansen, V., 1999. Structural and kinematic analysis of eastern Ovda Regio, Venus: implications for crustal plateau formation. Icarus 139, 116–136.
Giacomini, L., Massironi, M., Galluzzi, V., Ferrari, S., Palumbo, P., 2020. Dating long thrust systems on Mercury: new clues on the thermal evolution of the planet. Geosci. Front. 11, 855–870.
Gilmore, M.S., Head, J.W., 2018. Morphology and deformational history of Tellus Regio, Venus: evidence for assembly and collision. Planet. Space Sci. 154, 5–20.
Gilmore, M.S., Collins, G.C., Ivanov, M.A., Marinageli, L., Head, J.W., 1998. Style and sequence of extensional structures in tessera terrain, Venus. J. Geophys. Res. 103, 16,813-16,840.
Golombek, M.P., 1985. Fault type predictions from stress distributions on planetary surfaces: importance of fault initiation depth. J. Geophys. Res. 90, 3065–3074.
Golombek, M.P., Suppe, J., Narr, W., Plescia, J., Banerdt, B., 1990. Does wrinkle ridge formation on Mars involve most of the lithosphere?. In: Lunar Planet. Sci. XXI, Lunar Planet. Inst, pp. 421–422.
Golombek, M.P., Plescia, J.B., Franklin, B.J., 1991. Faulting and folding in the formation of planetary wrinkle ridges. Proc. Lunar Planet. Sci., Lunar Planet. Inst. 21, 679–693.
Golombek, M.P., Anderson, F.S., Zuber, M.T., 2001. Martian wrinkle ridge topography' evidence for subsurface faults from MOLA. J. Geophys. Res. 106, 23811–23821.
Gordon, F.R., Lewis, J.D., 1980. Yje Meckering and Calingiri earthquakes October 1968 and March 1970. Geol. Surv. W. Australia, Bulletin 126, 229 p.
Graff, J.R., Ernst, R.E., Samson, C., 2018. Evidence for triple-junction rifting focussed on local magmatic centres along Parga Chasma, Venus. Icarus 306, 122–138.
Guseva, E.N., Ivanov, M.A., 2019. Spatiotemporal relationships of the groove belts, coronal structures, and rift zones of Venus. Sol. Syst. Res. 53, 411–422.
Hagood, M.C., 1985. Structure-and Evolution of the Horse Heaven Hills in South-Central Washington. Unpublished MSc thesis. Portland State University, p. 201p.
Hamilton, W.B., 2005. Plumeless Venus has ancient impact-accretionary surface. In: Foulger, G.R. (Ed.), Plates, Plumes, and Paradigms, 388, pp. 781–814. Spec. Pap. Geol. Soc. Am.
Hamilton, W.B., 2019. Toward a myth-free geodynamic history of Earth and its neighbors. Earth Sci. Rev. 198 https://doi.org/10.1016/j.earscirev.2019.102905.
Hammond, W.C., Blewitt, G., Kreemer, C., 2011. Block modeling of crustal deformation of the northern Walker Lane and Basin and Range from GPS velocities. J. Geophys. Res. 116, B04402. https://doi.org/10.1029/2010JB007817.
Hanmer, S., Le Corre, C., Berthe, D., 1982. The role of Hercynian granites in the deformation and metamorphism of Brioverian and Palaeozoic rocks of Central Brittany. J. Geol. Soc. Lond. 139, 85–93.
Hanmer, S., 1986. Asymmetrical pull-aparts and foliation fish as kinematic indicators. J. Struct. Geol. 8, 111–122.
Hanmer, S., 1988a. Great Slave Lake Shear Zone, Canadian Shield: reconstructed vertical profile of a crustal-scale fault zone. Tectonophysics 149, 245–264.
Hanmer, S., 1988b. Ductile thrusting at mid-crustal level, southwestern Grenville Province. Can. J. Earth Sci. 25, 1049–1059.
Hanmer, S., 1989. Initiation of cataclastic flow in a mylonite zone. J. Struct. Geol. 11, 751–762.
Hanmer, S., 1990. Natural rotated inclusions in non-ideal shear. Tectonophysics 176, 245–255.
Hanmer, S., 1991. Geology, Great Slave Lake Shear Zone, District of Mackenzie, Northwest Territories. Geological Survey of Canada Map 1740A, scale 1:150,000.
Hanmer, S., 2020. Tessera terrain ribbon fabrics on Venus reviewed: Could they be dyke swarms? Earth Sci. Rev. 201, 103077.
Hanmer, S., Greene, D.C., 2002. A modern structural regime in the Paleoarchean (~3.64 Ga); Isua Greenstone Belt, southern West Greenland. Tectonophysics 346, 201–222.

Hanmer, S., McEachern, S., 1992. Kinematical and rheological evolution of a crustal-scale ductile thrust zone, Central Metasedimentary Belt, Grenville Orogen, Ontario. Can. J. Earth Sci. 29, 1779–1790.
Hanmer, S., Passchier, C.W., 1991. Shear Sense Indicators: A Review: Geol. Surv. Can. Paper, 90-17, 72 p.
Hanmer, S., Williams, M., Kopf, C., 1995. Modest movements, spectacular fabrics in an intracontinental deep-crustal strike-slip fault: striding-Atbabasca Mylonite Zone, NW Canadian Shield. J. Struct. Geol. 17, 493 to 507.
Hanmer, S., Bowring, S., van Breemen, O., Parrish, R., 1992. Great Lake shear zone, NW Canada: mylonitic record of Early Proterozoic continental convergence, collision and indentation. J. Struct. Geol. 14, 757–773.
Hanmer, S., Corrigan, D., Ganas, A., 1996. Orientation of nucleating faults in anisotropic media: insights from three-dimensional deformation experiments. Tectonophysics 267, 275–290.
Hanmer, S., Mengel, F., Connelly, J., Van Gool, J., 1997. Significance of crustal-scale shear zones and synkinematic dykes in the Nagssugtoqidian oroegen, SW Greenland: a reexamination. J. Struct. Geol. 19, 59–75.
Hanmer, S., Tella, S., Ryan, J.J., Sandeman, H.A., Berman, R.G., 2006. Late Neoarchean thick-skinned thrusting and Paleoproterozoic reworking in the MacQuoid supracrustal belt and Cross Bay plutonic complex, western Churchill Province, Nunavut, Canada. Precambrian Res. 144, 126–139.
Hansen, V.L., 2006. Geologic constraints on crustal plateau surface histories, Venus: the lava pond and bolide impact hypotheses. J. Geophys. Res. 111, E11010. https://doi.org/10.1029/2006JE002714.
Hansen, V.L., 2007. Venus: a thin-lithosphere analogue for early Earth? In: van Kranendonk, M.J., Smithies, R.H., Bennett, V.C. (Eds.), Earth's Oldest Rocks, 15. Elsevier, p. 987. Developments in Precambrian Geology.
Hansen, V.L., 2018. Global tectonic evolution of Venus, from exogenic to endogenic over time, and implications for early Earth processes. Philos. Transac. Royal Soc. Soc. A 376. https://doi.org/10.1098/rsta.2017.0412.
Hansen, V.L., López, I., 2010. Venus records a rich early history. Geology 38 (4), 311–314. https://doi.org/10.1130/G30587.1.
Hansen, V.L., López, I., 2018. Mapping of geologic structures in the Niobe-Aphrodite map area of Venus: unraveling the history of tectonic regime change. J. Geophys. Res. 123 https://doi.org/10.1029/2018JE005566.
Hansen, V.L., Olive, A., 2010. Artemis, Venus: The largest tectonomagmatic feature in the solar system? Geology 38, 467–470. https://doi.org/10.1130/G30643.1.
Hansen, V.L., Willis, J.J., 1996. Structural analysis of a sampling of tesserae: implications for Venus geodynamics. Icarus 123, 296–312.
Hansen, V.L., Willis, J.J., 1998. Ribbon terrain formation, Southwestern Fortuna tessera, Venus: implications for lithosphere evolution. Icarus 132, 321–343.
Hansen, V.L., Young, D.A., 2007. Venus's evolution: a synthesis. In: Cloos, M., Carlson, W.D., Gilbert, M.C., Liou, J.G., Sorensen, S.S. (Eds.), Convergent Margin Terranes and Associated Regions: A Tribute to W.G. Ernst, pp. 255–273. https://doi.org/10.1130/2006. 2419. Geol. Soc. Am. Sp. Paper 419.
Hansen, V.L., Banks, B.K., Ghent, R.R., 1999. Tessera terrain and crustal plateaus, Venus. Geol. 27, 1071–1074.
Hansen, V.L., Phillips, R.J., Willis, J.J., Ghent, R.R., 2000. Structures in tessera terrain, Venus: issues and answers. J. Geophys. Res. 105, 4135–4152.
Harris, L.B., Bédard, J.H., 2014a. Interactions between continent-like 'drift', rifting and mantle flow on Venus: gravity interpretations and Earth analogues. In: Platz, T., Massironi, M., Byrne, P.K., Hiesinger, H. (Eds.), Volcanism and Tectonism Across the Inner Solar System. 401 Geol. Soc. London. https://doi.org/10.1144/SP401.9. Special Publications.
Harris, L.B., Bédard, J.H., 2014b. Crustal evolution and deformation in a non-plate tectonic Archaean Earth: comparisons with Venus. In: Dilek, Y., Furnes, H. (Eds.), Evolution of Archean Crust and Early Life Modern Approaches in Solid Earth Sciences. 7, pp. 215–291.
Head, J.W., 1990. Formation of mountain belts on Venus: Evidence for large-scale convergence, underthrusting, and crustal imbrication in Freyja Montes, Ishtar Terra. Geology 18, 99–102.
Head, J.W., Solomon, S.C., 1981. Tectonic evolution of the terrestrial planets. Science 213, 62–76. http://www.jstor.org/stable/1687006.
Head, J.W., Wilson, L., 2017. Generation, ascent and eruption of magma on the Moon: New insights into source depths, magma supply, intrusions and effusive/explosive eruptions (Part 2: Predicted emplacement processes and observations). Icarus 283, 176–223.
Herrero-Gil, A., Egea-Gonzalez, I., Ruiz, J., Romeo, I., 2019. Structural modeling of lobate scarps in the NW margin of Argyre impact basin, Mars. Icarus 319, 367–380.
Herrero-Gil, A., Ruiz, J., Romeo, I., 2020. 3D modeling of planetary lobate scarps: the case of Ogygis Rupes. Mars. Earth Planet. Sci. Lett. 532, 116004.
Herrick, R., 2018. Using stereo-derived topography for venus to search for new craters in the tessera and to re-evaluate tectonic destruction of craters. 49th Lunar Planet. Sci. Conf., 1740.
Herrick, R., Stahlke, D.L., Sharpton, 2012. Fine-scale Venusian Topography from Magellan stereo data. EOS 93, 125–126.
Hobbs, B.E., 2019. The development of structural geology and the historical context of the journal of structural geology: a reflection by Bruce Hobbs. J. Struct. Geol. 125, 3–19.
Hobbs, B.E., Mohlhaus, H.B., Ord, A., 2015. Instability, softening and localization of deformation. In: Knipe, R.J., Rutter, E.H. (Eds.), 1990, Deformation Mechanisms, Rheology and Tectonics. Geol. Soc. Sp. Pub. No, 54, pp. 143–165.
Howard, K.A., Muehlburger, W.R., 1973. Lunar thrust faults in the Taurus-Littrow region. In: Apollo 17 Preliminary Science Report, 31-22 - 31-25.
Hubbert, M.K., Rubey, W.W., 1959. Role of fluid pressures in mechanics of overthrust faulting: I. Mechanics of fluid-filled porous solids and its application to overthrust faulting. Geol. Soc. Am. Bull. 70, 115–166.
Ivanov, M.A., Head, J.W., 1996. Tessera terrain on Venus: a survey of the global distribution, characteristics, and relation to surrounding units from Magellan data. J. Geophys. Res. 101, 14861–14908.
Ivanov, M.A., Head, J.W., 2010. The Lada Terra rise and Quetzalpetlatl Corona: A region of long-lived mantle upwelling and recent volcanic activity on Venus. Planet. Space Sci. 58, 2010 1880–1894.
Ivanov, M.A., Head, J.W., 2011. Global geological map of Venus. Planet. Space Sci. 59, 1559–1600.
Ivanov, M.A., Head, J.W., 2013. The history of volcanism on Venus. Planet. Space Sci. 84, 66–92.
Ivanov, M.A., Head, J.W., 2015. The history of tectonism on Venus: a stratigraphic analysis. Planet. Space Sci. 113–114, 10–32.
Izquierdo, K., Sori, M.M., Soderblom, J.M., Johnson, B.C., Wiggins, S.E., 2021. Lunar megaregolith structure revealed by GRAIL gravity data. Geophys. Res. Lett. https://doi.org/10.1029/2021GL095978.
Johnston, J.F., White, S.R., 2018. Understanding the Meckering earthquake: Western Australia, 14 October 1968: Geol. Surv. W. Australia, 26p.
Jurdy, D.M., Stoddard, P.R., 2007. The coronae of Venus: Impact, plume, or other origin? In: Fulger, G.R., Jurdy, D.M. (Eds.), Plates, Plumes and Planetary Processes, Geol. Soc. Am. Sp. Paper, 430. https://doi.org/10.1130/SPE430.
Karagoz, O., Kenkmann, T., Wulf, G., 2022. Circum-Tharsis wrinkle ridges at Lunae Planum: Morphometry, formation, and crustal implications. Icarus 374, 114808. https://doi.org/10.1016/j.icarus.2021.114808.
Keep, M., Hansen, V.L., 1994. Structural history of Maxwell Montes, Venus: implications for Venusian mountain belt formation. J. Geophys. Res. 99, 26015–26028.
Kelsey, H.M., Ladinsky, T.C., Staisch, L., Sherrod, B.L., Blakely, R.J., Pratt, T.L., Stephenson, W.J., Odum, J.K., Wan, E., 2017. The story of a Yakima Fold and how it informs Late Neogene and Quaternary Backarc deformation in the Cascadia Subduction Zone, Manastash Anticline, Washington, USA. Tectonics 36, 2085–2107. https://doi.org/10.1002/2017TC004558.
Khawja, S., Ernst, R.E., Samson, C., Byrne, P.K., Ghail, R.C., MacLellan, L., 2020. Tesserae on Venus may preserve evidence of fluvial erosion. Nat. Commun. 11, 5789 |. https://doi.org/10.1038/s41467-020-19336-1.
Klimczak, C., 2014. Geomorphology of lunar grabens requires igneous dikes at depth. Geology 42, 963–966. Data Repository item 2014341. https://doi.org/10.1130/G35984.1.
Klimczak, C., Byrne, P.K., Solomon, S.C., 2015. A rock-mechanical assessment of Mercury's global tectonic fabric. Earth Planet. Sci. Lett. 416, 82–90.
Klimczak, C., Kling, C.L., Byrne, P.K., 2018. Topographic expressions of Large Thrust Faults on Mars. J. Geophys. Res. Planets. 1123, 1973–1995. https://doi.org/10.1029/2017JE005448.
Klimczak, C., Byrne, P.K., Sengor, A.M.C., Solomon, S.C., 2019. Principles of structural geology on rocky planets. Can. J. Earth Sci. 56, 1437–1457.
Kneissl, T., Michael, G.G., Platz, T., Walter, S.H.G., 2015. Age determination of linear surface features using the Buffered Crater Counting approach – case studies of the Sirenum and Fortuna Fossae graben systems on Mars. Icarus 250, 384–394.
Knicely, J.J.C., Herrick, R.R., 2021. Survey of mid-sized Venusian volcanoes using stereo-derived topography. Icarus. https://doi.org/10.1016/j.icarus.2021.114577.
Koenig, E., Aydin, A., 1998. Evidence for large-scale strike-slip faulting on Venus. Geology 26 (6), 551–554. June 1998.
Kolzenberg, S., Kubanek, J., Dirscherl, M., Hamilton, C.W., Hauber, E., Scheidt, S.P., Munzer, U., 2022. Solid as a rock: tectonic control of graben extension and dike propagation. Geology 50, 260–265. https://doi.org/10.1130/G49406.1.
Kreslavsky, M.A., Basilevsky, A.T., 1998. Morphometry of wrinkle ridges on Venus: comparison with other planets. J. Geophys. Res. 103, 11103–11111.
Kreslavsky, M.A., Ivanov, M.A., Head, J.W., 2015. The resurfacing history of Venus: constraints from buffered crater densities. Icarus 250, 438–450.
Kryuchkov, V.P., 1990. Ridge belts: ate they Compressional or Extensional Structures? Earth Moon Planet. 50 (51), 47–491.
Kumar, P.S., 2005. An alternative kinematic interpretation of Thetis Boundary Shear Zone, Venus: evidence for strike-slip ductile duplexes. J. Geophys. Res. 110, E07001. https://doi.org/10.1029/2004JE002387.
Langevin, Y., 1997. The regolith of Mercury: present knowledge and implications for the Mercury Orbiter mission. Planet. Space Sci. 45 (1), 31–37. https://doi.org/10.1016/S0032-0633(96)00098-0.
Li, B., Linga, Z., Zhanga, J., Chena, J., Nia, Y., Liu, C., 2018. Displacement-length ratios and contractional strains of lunar wrinkle ridges in Mare Serenitatis and Mare Tranquillitatis. J. Struct. Geol. 109, 27–37.
Lin, M.L., Lu, C.Y., Kuo-Jen Chang, K.J., Jeng, F.S., Lee, C.J., 2005. Sandbox experiments of plate convergence - scale effect and associated mechanisms. Terrestrial Atmos. Ocean. Sci. J. 16, 595–620.
Lister, G.S., Davis, G.A., 1989. The origin of metamorphic core complexes and detachment faults formed during Tertiary continental extension in the northern Colorado River region, U.S.A. J. Struct. Geol. 11, 65–94.
Lister, G.S., Williams, P.F., 1983. The partitioning of deformation in flowing rock masses. Tectonophysics 92, 1–33.
Lu, Y., Wu, Y., Michael, G.G., Basilevsky, A.T., Li, C., 2019. Young wrinkle ridges in Mare Imbrium: evidence for very recent compressional tectonism. Icarus 329, 24–33.
Lucchitta, B.A., 1976. Mare ridges and related highland scarps - result of vertical tectonism? Proc. Lunar Sci. Conf. 7th, 2761–2782.
Malavielle, J., 1984. Modelisations experimentales des chevauchememnts imbriques: applications au chaines de montagnes. Bull. Soc. Geol. Fr. XXVI, 129–138.

Mandl, G., 1987. Tectonic deformation by rotating parallel faults: the "bookshelf" mechanism. Tectonophysics 141, 277–316.
Mangold, N., Allemand, P., Thomas, P., 1998. Wrinkle ridges of Mars : structural analysis and evidence for shallow deformation controlled by ice-rich deollements. Planet. Space Sci. 46, 345–356.
Mangold, N., Allemand, P., Thomas, P., Vidal, G., 2000. Chronology of compressional deformation on Mars: evidence for a single and global origin. Planet. Space Sci. 48, 1201–1211.
Martin, E.S., Watters, T.R., 2021. Topography of nearside mare graben: implications for dike-induced or passive extension formation. Icarus 354. https://doi.org/10.1016/j.icarus.2020.114039.
Matsuyama, I., Keane, J.T., Trinh, A., Beulthe, M., Watters, T.R., 2021. Global tectonic patterns of the Moon. Icarus 358. https://doi.org/10.1016/j.icarus.2020.114202.
Maxwell, T.A., Phillips, R.J., 1978. Stratigraphic correlation of the radar-detected subsurface interface in Mare Crisium. Geophys. Res. Lett. 5, 811–814.
Maxwell, T.A., El-Baz, F., Ward, S.H., 1975. Distribution, morphology, and origin of ridges and arches in mare Serenitatis. Geol. Soc. Am. Bull. 86, 1273–1278.
McClay, K.R., Dooley, T., Whitehouse, P., Mills, M., 2002. 4-D evolution of rift systems: Insights from scaled physical models. Am. Assoc. Pet. Geol. Bull. 86, 935–959.
McGill, G.E., 1993. Wrinkle ridges, stress domains, and kinematics of venusian plains. Geophys. Res. Lett. 20, 2407–2410.
McGill, G.E., Stofan, E.R., Smrekar, S.E., 2010. Venus tectonics. In: Watters, T.R., Schultz, R.A. (Eds.), Planetary Tectonics. Cambridge University Press, pp. 81–120.
Means, W.D., Hobbs, B.E., Lister, G.S., Williams, P.F., 1980. Vorticity and non-coxiality in progressive deformations. J. Struct. Geol. 2, 371–378.
Mège, D., Ernst, R.E., 2001. Contractional effects of mantle plumes on Earth, Mars, and Venus. In: Ernst, R.E., Buchan, K.L. (Eds.), Mantle Plumes: Their Identification Through Time: Boulder, Colorado, Geol. Soc. Am. Spec. Pap, 352, pp. 103–140.
Mège, D., Masson, P., 1996a. Stress models for Tharsis formation. Mars. Planet. Space Sci. 44, 1471–1497.
Mège, D., Masson, P., 1996b. A plume tectonics model for the Tharsis province. Mars. Planet. Space Sci. 44, 1499–1546.
Mege, D., Reidel, S.P., 2001. A method for estimating 2D wrinkle ridge strain from application of fault displacement scaling to the Yakima folds, Washington. Geophys. Res. Lett. 28, 3545–3548.
Melosh, H.J., 1979. Acoustic fluidization: a new geologic process. J. Geophys. Res. 84, 7513–7520.
Melosh, J., McKinnon, W., 1988. The tectonics of Mercury. In: Mercury (A89-43751 19-91). University of Arizona Press, Tucson, AZ, pp. 374–400.
Montesi, G.J., Zuber, M.T., 2003. Clues to the lithospheric structure of Mars from wrinkle ridge sets and localization instability. J. Geophys. Res. 108 https://doi.org/10.1029/2002JE001974.
Mueller, K., Golombek, M., 2004. Compressional structures on Mars. Annu. Rev. Earth Planet. Sci. 2004 (32), 435–464. https://doi.org/10.1146/annurev.earth.32.101802.120553.
Mueller, K., Vidal, A., Robbins, S., Golombek, M., West, C., 2014. Fault and fold growth of the Amenthes uplift: Implications for Late Noachian crustal rheology and heat flow on Mars. Earth Planet. Sci. Lett. 408, 100–109.
Nadeau, L., Hanmer, S., 1992. Deep-crustal break-back stacking and slow exhumation of the continental footwall beneath a thrusted marginal basin, Grenville orogen, Canada. Tectonophysjcs 210 (1992), 215–233.
Nino, F., Philip, H., Chery, J., 1998. The role of bed-parallel slip in the formation of blind thrust faults. J. Struct. Geol. 20, 503–516.
Okubo, C.H., Schultz, R.A., 2004. Mechanical stratigraphy in the western equatorial region of Mars based on thrust fault–related fold topography and implications for near-surface volatile reservoirs. Geol. Soc. Am. Bull. 116, 594–605. https://doi.org/10.1130/B25361.1.
Orme, D.A., 2020. New timing constraints for the onset of laramide deformation in Southwest Montana challenge our understanding of the development of a thick-skinned structural style during flat-slab subduction. Tectonics 39. https://doi.org/10.1029/2020TC006193 e2020TC006193.
Passchier, M., Passchier, C.W., Weismuller, C., Urai, J.L., 2021. The joint sets on the Lilstock Benches, UK. Observations based on mapping a full resolution UAV-based image. J. Struct. Geol. 147, 104332.
Peterson, G.A., Johnson, C.L., Byrne, P.K., Phillips, R.J., 2020. Fault structure and origin of compressional tectonic features within the smooth plains on Mercury. J. Geophys. Res.: Planets 125. https://doi.org/10.1029/2019JE006183 e2019JE006183.
Pettengill, G.H., Campbell, B.A., Campbell, D.B., Simpson, R.A., 1997. Surface scattering and dielectric properties. In: Bougher, S.W., Hunten, D.M., Phillips, R.J. (Eds.), Venus II—Geology, Geophysics, Atmosphere and Solar Wind Environment. Univ. of Ariz. Press, Tucson, pp. 527–546.
Pfiffner, O.A., 2014. Geology of the Alps. WILEY Blackwell, Chichester, UK, 376p.
Pfiffner, O.A., 2017. Thick-skinned and thin-skinned tectonics: a global perspective. Geosciences 7, 71. https://doi.org/10.3390/geosciences7030071.
Pfiffner, O.A., Ramsay, J.G., 1982. Constraints on geological strain rates; arguments from finite strain states of naturally deformed rocks. J. Geophys. Res. 87, 311–321. https://doi.org/10.1029/JB087iB01p00311.
Philip, H., Meghraoui, M., 1983. Structural analysis and interpretation of the surface deformations of the El Asnam Earthquake of October 10, 1980. Tectonics 2, 17–49.
Piskorz, D., Elkins-Tanton, L.T., Smrekar, S.E., 2014. Coronae formation on Venus via extension and lithospheric instability. J. Geophys. Res. Planets 119, 2568–2582. https://doi.org/10.1002/2014JE004636.
Plescia, J.B., Golombek, M.P., 1986. Origin of planetary wrinkle ridges based on the study of terrestrial analogues. Geol. Soc. Am. Bull. 97, 1289–1299.
Plescia, J.B., Roth, L.E., Saunders, R.S., 1980. Tectonic features of Southeast Tharsis. Lunar Planet. Sci. Xi 891–893.
Plotek, B., Guzman, C., Cristallini, E., Yagupsky, D., 2021. Analysis of fault bend folding kinematic models and comparison with an analog experiment. J. Struct. Geol. 146, 104316.
Poirier, J.P., 1980. Shear localisation and shear instability in materials in the ductile field. J. Struct. Geol. 2, 135–142.
Pollard, D.D., Aydin, A., 1988. Progress in understanding jointing over the past century. Geol. Soc. Am. Bull. 100, 1181–1204.
Pollard, D., Segall, P., 1987. Theoretical displacements and stresses near fractures in rock: With applications to faults, joints, veins, dikes, and solution surfaces. In: Atkinson, B.K. (Ed.), Fracture Mechanics of Rock. Academic Press, London, pp. 277–349.
Pollard, D.D., Delaney, P.T., Duffield, W.A., Endo, E.T., Okamura, A.T., 1983. Surface deformation in volcanic rift zones. In: Morgan, P., Baker, B.H. (Eds.), Processes of Continental Rifting, Tectonophysics, 94, pp. 541–584.
Pratt, T.L., 2012. Large-scale splay faults on a strike-slip fault system: The Yakima Folds, Washington State. Geochem. Geophys. Geosyst. 13, Q11004. https://doi.org/10.1029/2012GC004405.
Price, R.A., 1981. The Cordilleran foreland fold and thrust belt in the southern Canadian Rocky Mountains. In: McClay, K.R., Price, N.J. (Eds.), Thrust and Nappe Tectonics, Geol. Soc. London Sp. Pub., 9, pp. 427–448.
Raitala, J., 1988. Superposed ridges of the Hesperia Planum area on Mars. Earth Moon Planet. 40, 71–99.
Ramberg, H., 1962. Contact strain and folding instability of a multilayered body under compression. Geol. Rundsch. 51, 405–439.
Ramberg, H., 1963. Evolution of drag folds. Geol. Mag. 100, 97–196.
Ramberg, H., 1964. Selective buckling of composite layers with contrasted rheological properties: a theory for simultaneous formation of several orders of folds. Tectonophysics 1, 307–341.
Ramberg, H., 1981. Gravity, Deformation and the Earth's Crust. Academic Press, 452 p.
Ramsay, J.G., 1967. Folding and Fracturing of Rocks. McGraw-Hill, 568 p.
Ramsay, J.G., 1980. Shear zone geometry: a review. J. Struct. Geol. 2, 83–99.
Ramsay, J.G., Graham, R.H., 1970. Strain variation in shear belts. Can. J. Earth Sci. 7, 786–813.
Reber, J.E., Cooke, M.L., Dooley, T.P., 2020. What model material to use? A review on rock analogs for structural geology and tectonics. Earth Sci. Rev. 202, 103107.
Reidel, S.P., Campbell, N.P., Fecht, K.R., Lindsey, K.A., 1994. Late Cenozoic structure and stratigraphy of south-central Washington. Wash. Div. Geol. Earth Res. Bull. 80, 159–180.
Reidel, S.P., Fecht, K.R., Hutter (Harrold), I.L., Tolan, T.L., Chamness, M.A., 2021. The Olympic-Wallowa lineament: a new look at an old controversy. Geol. Soc. Am. Bull. 133, 115–133. https://doi.org/10.1130/B35454.1.
Roering, J., Cooke, M.L., Pollard, D.D., 1997. Why blind thrust faults do not propagate to the Earth's surface: numerical modeling of coseismic deformation associated with thrust-related anticlines. J. Geophys. Res. 102, 11901–119112.
Roggon, L., Hetzel, R., Hiesinger, H., Clark, J.D., Hampel, A., van der Bogert, C.H., 2017. Length-displacement scaling of thrust faults on the Moon and the formation of uphill-facing scarps. Icarus 292, 111–124.
Romeo, I., 2013. Monte Carlo models of the interaction between impact cratering and volcanic resurfacing on Venus: the effect of the Beta-Atla-Themis anomaly. Planet. Space Sci. 87, 157–172.
Romeo, I., Capote, R., Anguita, F., 2005. Tectonic and kinematic study of a strike-slip zone along the southern margin of Central Ovda Regio, Venus: geodynamical implications for crustal plateaux formation and evolution. Icarus 175, 320–334.
Rosenberg, E., McGill, G.E., 2001. Geologic Map of the Pandrosos Dorsa Quadrangle V–5, Venus: U.S. Geological Survey, Geologic Investigations Series I-2721, scale 1: 5,000,000.
Rothery, D.A., Massironi, M., 2010. Beagle Rupes - evidence for a basal decollement of regional extent in Mercury's lithosphere. Icarus 209, 256–261.
Ruiz, J., 2007. The heat flow during the formation of ribbon terrains on Venus. Planet. Space Sci. 55, 2063–2070. https://doi.org/10.1016/j.pss.2007.05.003.
Ruiz, J., López, V., Dohm, J.M., Fernández, C., 2012. Structural control of scarps in the Rembrandt region of Mercury. Icarus 219, 511–514.
Ruj, T., Komatsua, G., Pondrellia, M., Di Pietroa, I., Pozzobon, R., 2018. Morphometric analysis of a Hesperian aged Martian lobate scarp using high resolution data. J. Struct. Geol. 113, 1–9.
Saha, P., Santanu Bose, S., Mandal, N., 2013. Varying frontal thrust spacing in mono-vergent wedges: an insight from analogue models. J. Earth Syst. Sci. 122, 699–714.
Saltus, R., 1994. Upper-crustal structure beneath the Columbia River Basalt Group, Washington: gravity interpretation controlled by borehole and seismic studies: discussion. Geol. Soc. Am. Bull. 106, 1102–1105.
Sandwell, D.T., Johnson, C.L., Bilotti, F., Suppe, J., 1997. Driving Forces for Limited Tectonics on Venus. Icarus 129, 232–244.
Saylor, J.R., Rudolph, K.W., Sundell, K.E., van Wijk, J., 2020. Laramide orogenesis driven by late cretaceous weakening of the North American lithosphere. J. Geophys. Res. Solid Earth 125. https://doi.org/10.1029/2020JB019570 e2020JB019570.
Schultz, R.A., 2000. Localization of bedding plane slip and Backthrust Faults above Blind Thrust Faults: keys To wrinkle ridge structure. J. Geophys. Res. 105, 12035–12052.
Schultz, R.A., Tanaka, K.L., 1994. Lithospheric-Scale buckling and thrust structures on Mars: the coprates rise and South Tharsis Ridge Belt. J. Geophys. Res. 99, 8371–8385.
Schultz, R.A., Watters, T.R., 2001. Forward mechanical modeling of the Amenthes Rupes thrust fault on Mars. Geophys. Res. Lett. 28, 4659–4662.
Schultz, R.A., Okubo, C.H., Goudy, C.L., Wilkins, S.J., 2004. Igneous dikes on Mars revealed by Mars Orbiter Laser Altimeter topography. Geology 32, 889–892. https://doi.org/10.1130/G20548.1.

Schultz, R.A., Moore, J.M., Grosfils, E.B., Tanaka, K.L., Mege, D., 2007. Canyonlands model for planetary grabens: Revised physical basis and implications. In: Chapman, M.G. (Ed.), The Geology of Mars: Evidence from Earth-Based Analogues. Cambridge University Press, pp. 371–399.
Schultz, R.A., Soliva, R., Okubo, C.H., Mege, D., 2010. Fault populations. In: Watters, T. R., Schultz, R.A. (Eds.), Planetary Tectonics. Cambridge University Press, pp. 457–510.
Sharpton, V.L., Head, J.W., 1982. Stratigraphy and structural evolution of southern mare serenitatis: a reinterpretation based on Apollo lunar sounder experiment data. J. Geophys. Res. 87, 10983–10998.
Sharpton, V.L., Head, J.W., 1988. Lunar mare ridges: analysis of ridge-crater intersections and implications for the tectonic origin of Mare ridges. In: Lunar and Planetary Science Conference, 18th, Houston, TX, Mar. 16-20, 1987, Proceedings (A89-10851 01-91). Cambridge University Press/Lunar and Planetary Institute, Cambridge and New York/Houston, TX, pp. 307–317.
Simpson, C., De Paor, D.G., 1993. Strain and kinematic analysis in general shear zones. J. Struct. Geol. 15, 1–20.
Simpson, C., Schmidt, S.M., 1983. An evaluation of criteria to deduce the sense of movement in sheared rocks. Geol. Soc. Am. Bull. 94, 1281–1288, 10.1130/0016-HYPERLINK "doi:10.1130/0016-7606(1983)94%3C1281:AEOCTD%3E2.0.CO;2" \t "_blank" 7606(1983)94<1281:AEOCTD>2.0.CO;2.
Smithson, S.B., Brewer, J.A., Kaufman, S., Oliver, J.E., Hurich, C.A., 1979. Structure of the Laramide Wind River Uplift, Wyoming, From COCORP Deep Reflection Data and From Gravity Data. J. Geophys. Res. 84, 5955–5972.
Solomon, S.C., Head, J.W., Kaula, W.M., Mckenzie, D., Parsons, B., Phillips, R.J., Schubert, G., Talwani, M., 1991. Venus tectonics: initial analysis from Magellan. Science 252, 291–312.
Solomon, S.C., Smrekar, S.E., Bindschadler, D.L., Grimm, R.E., Kaula, W., McGill, G.E., Phillips, R.J., Saunders, R.S., Schubert, G., Squyres, S.W., Stofan, E.R., 1992. Venus tectonics: an overview of magellan observations. J. Geophys. Res. 97, 13199–13255.
Solomon, S.C., McNutt, R.L., Watters, T.R., Lawrence, D.J., Feldman, W.C., Head, J.W., Krimigis, S.M., Murchie, S.L., Phillips, R.J., Slavin, J.A., Zuber, M.T., 2008. Return to mercury: a global perspective on MESSENGER's first Mercury flyby. Science. 321, 59–62.
Spencer, J.E., 2001. Possible giant metamorphic core complex at the center of Artemis Corona, Venus. Geol. Soc. Am. Bull. 113, 333–345.
Squyres, S.W., Jankowski, D.G., Simons, M., Solomon, S.C., Hager, B.H., McGill, G.E., 1992. Plains tectonism on Venus: the deformation belts of Lavinia Planitia. J. Geophys. Res. 97, 13579–13599.
Stofan, E.R., Senske, D., Michaels, G., 1993. Tectonic features in Magellan data. In: Ford, J.P., Plaut, J.J., Weitz, C.M., Farr, T.G., Senske, D.A., Stofan, E.R., Michaels, G., Parker, T.J. (Eds.), Guide to Magellan Image Interpretation, JPL Publ. 93-24. Jet Propul. Lab, Pasadena, Calif.
Strom, R.G., 1972. Lunar mare ridges, rings and volcanic ring complexes. In: The Moon, Urey and Runcorn (eds). International Astronomical Union, pp. 187–215.
Strom, R.G., Trask, N.J., Guest, J.E., 1975. Tectonism and volcanism on Mercury. J. Geophys. Res. 80, 2478–2507.
Studd, D., Ernst, R.E., Samson, C., 2011. Radiating grabens-fissure systems in the Ulfrun Regio area, Venus. Icarus 215, 279–291.
Suppe, J., 1983. Geometry and kinematics of fault-bend folding. Am. J. Sci. 283, 684–721. https://doi.org/10.2475/ajs.283.7.684.
Suppe, J., Connors, C., 1992. Critical taper wedge mechanics of fold-and-thrust belts on Venus' initial results from Magellan. J. Geophys. Res. 97, 13545–13561.
Suppe, J., Medwedeff, D.A., 1990. Geometry and kinematics of fault-propagation folding. Eclogae Geol. Helv. 83 (3), 409–454.
Sylvester, A.G., 1988. Strike-slip faults. Geol. Soc. Am. Bull. 100, 1666–1703.
Tchalenko, J.S., 1970. Similarities between shear zones of different magnitudes. Geol. Soc. Am. Bull. 81, 1625–1640.
Tikoff, B., Blenkinsop, T., Kruckenberg, S.C., Morgan, Sven, Newman, J., Wojtal, S., 2013. A perspective on the emergence of modern structural geology: Celebrating the feedbacks between historical-based and process-based approaches. In: Bickford, M.E. (Ed.), The Web of Geological Sciences: Advances, Impacts, and Interactions. Geol. Soc. Am. Sp. Pap, 500, pp. 65–119. https://doi.org/10.1130/2013.250003.
Treagus, S.H., 1983. A theory of of stress and strain variations in viscous layers, and its bearing on cleavage refraction. J. Struct. Geol. 5, 351–368.
Treagus, S.H., 1988. Strain refraction in layered systems. J. Struct. Geol. 10, 517–527. https://doi.org/10.1016/0191-8141(88)90038-7.
Tuckwell, G.W., Ghail, R.C., 2003. A 400-km-scale strike-slip zone near the boundary of Thetis Regio, Venus. Earth Planet. Sci. Lett. 211, 45–55.
van der Bogert, C.H., Clark, J.D., Hiesinger, H., Banks, M.E., Watters, T.R., Robinson, M. S., 2018. How old are lunar lobate scarps? 1. Seismic resetting of crater size-frequency distributions. Icarus 306, 225–242.
Vorder Bruegge, R.W., Head, J.W., Campbell, D.B., 1990. Orogeny and large-scale strike-slip faulting on venus' tectonic evolution of Maxwell Montes. J. Geophys. Res. 95, 8357–8381.
Wallace, W.K., Homza, T.X., 2004. Detachment folds versus fault-propagation folds, and their truncation by thrust faults. In: McClay, K.R. (Ed.), Thrust tectonics and hydrocarbon systems: Am, Assoc. Petrol. Geol. Memoir, 82, pp. 324–355.
Watters, T.R., 1988. Wrinkle ridge assemblages on the terrestrial planets. J. Geophys. Res. 93, 10236–10254.
Watters, T.R., 1989. Periodically spaced anticlines of the Columbia Plateau. In: Reidel, S. P., Hooper, P.R. (Eds.), Volcanism and Tectonism in the Columbia River Flood-Basalt Province. https://doi.org/10.1130/SPE239-p289. Geol. Soc. Am. Sp. Pap. 239.
Watters, T.R., 1991. Origin of periodically spaced wrinkle ridges on the Tharsis Plateau of Mars. J. Geophys. Res. 96, 15599–15616.
Watters, T.R., 1992. System of tectonic features common to Earth, Mars, and Venus. Geology 20, 609–612.
Watters, T.R., 1993. Compressional tectonism on Mars. J. Geophys. Res. 98, 17049–17060.
Watters, T.R., 2003. Thrust faults along the dichotomy boundary in the eastern hemisphere of Mars. J. Geophys. Res. 108 https://doi.org/10.1029/2002JE001934.
Watters, T.R., 2004. Elastic dislocation modeling of wrinkle ridges on Mars. Icarus 171, 284–294.
Watters, T.R., 2021. A case for limited global contraction of Mercury. Commun. Earth Environ. | (2021) 2, 9. https://doi.org/10.1038/s43247-020-00076-5. www.nature.com/commsenv.
Watters, T.R., Chadwick, 1989. Crosscutting periodcally spaced first-order ridges in the ridged plains of Hesperia Planum: Another case for a buckling model. Lunar Planet. Sci. MEVTV Workshop on Tectonic Features on Mars, pp. 68–70.
Watters, T.R., Johnson, C.L., 2010. Lunar tectonics. In: Watters, T.R., Schultz, R.A. (Eds.), Planetary Tectonics. Cambridge University Press, pp. 121–182.
Watters, T.R., Robinson, M.S., 1997. Radar and photoclinometric studies of wrinkle ridges on Mars. J. Geophys. Res. 102, 10889–10903.
Watters, T.R., Robinson, M.S., 1999. Lobate scarps and the Martian crustal dichotomy. J. Geophys. Res. 104, 18981–18990.
Watters, T.R., Schultz, R.A., 2002. The Fault Geometry of Planetary Lobate Scarps: Listric versus Planar. Lunar Planet. Sci. Conf. XXXIII, p. 1668.
Watters, T.R., Robinson, M.S., Cook, A.C., 1998. Topography of lobate scarps on Mercury: new constraints on the planet's contraction. Geology. 26, 991–994.
Watters, T.R., Schultz, R.A., Robinson, M.S., 2000. Displacement-length relations of thrust faults associated with lobate scarps on Mercury and Mars: comparison with terrestrial faults. Geophys. Res. Lett. 27, 3659–3662.
Watters, T.R., Schultz, R.A., Robinson, M.S., Cook, A.C., 2002a. The mechanical and thermal structure of Mercury's early lithosphere. Geophys. Res. Lett. 29, 11, 37-1-37-4. https://doi.org/10.1029/2001GL014308.
Watters, T.R., Schultz, R.A., Robinson, M.S., Cook, A.C., 2002b. Displacement-length relations of thrust faults associated with lobate scarps on Mercury and Mars: comparison with terrestrial faults. Geophys. Res. Lett. 22, 3659–3662.
Watters, T.R., Robinson, M.S., Bina, C.R., Spudis, P.D., 2004. Thrust faults and the global contraction Mercury. Geophys. Res. Lett. 31, L04701. https://doi.org/10.1029/2003GL019171.
Watters, T.R., Solomon, S.C., Robinson, M.S., Head, J.W., André, S.L., Hauck, S.A., Murchie, S.L., 2009. The tectonics of Mercury: the view after MESSENGER's first flyby. Earth Planet. Sci. Lett. 285 (2009), 283–296.
Watters, T.R., Robinson, M.S., Beyer, R.A., Banks, M.E., Bell, J.F., Pritchard, M.E., Hiesinger, H., van der Bogert, C.H., Thomas, P.C., Turtle, E.P., Williams, N.R., 2010. Evidence of recent Thrust Faulting on the Moon revealed by the Lunar Reconnaissance Orbiter Camera. Science 329, 936–940.
Watters, T.R., Robinson, M.S., Banks, M.E., Tran, T., Denevi, B.W., 2012. Recent extensional tectonics on the Moon revealed by the Lunar Reconnaissance Orbiter Camera. Nat. Geosci. 5, 181–185.
Watters, T.R., Selvans, M.S., Banks, M.E., Hauck, S.A., Becker, K.J., Robinson, M.S., 2015a. Distribution of large-scale contractional tectonic landforms on Mercury: implications for the origin of global stresses. Geophys. Res. Lett. 42, 3755–3763. https://doi.org/10.1002/2015GL063570.
Watters, T.R., Robinson, M.S., Collins, G.C., Banks, M.E., Daud, K., Williams, N.R., Selvans, M., 2015b. Global thrust faulting on the Moon and the influence of tidal stresses. Geology 43, 851–854.
Way, M.J., Del Genio, A.D., 2020. Venusian habitable climate scenarios: modeling Venus through time and applications to slowly rotating Venus-Like Exoplanets. J. Geophys. Res. Planets. 125 e2019JE006276.
Wernicke, B., 1981. Low-angle normal faults in the Basin and Range Province: Nappe tectonics in an extending orogeny. Nature 291, 645–648. https://doi.org/10.1038/291645a0.
Wernicke, B., 1985. Uniform-sense normal simple shear of the continental lithosphere. Can. J. Earth Sci. 22, 108–125.
Wheeler, J.O., Hoffman, P.F., Card, K.D., Davidson, A., Sanford, B.V., Okulitch, A.V., Roest, W.R., 1996. Geological Survey of Canada, "A" Series Map 1860A, 1996, 3 sheets; 1 CD-ROM. https://doi.org/10.4095/208175.
White, S.H., 1976. The effects of strain on microstructures, fabrics and deformation mechanisms in quartzites. Phil. Trans. Roy. Soc. Lond. A283, 69–86.
White, S.H., Burrows, S.E., Carreras, J., Shaw, N.D., Humphreys, F.J., 1980. On mylonites in ductile shear zones. J. Struct. Geol. 2, 175–188.
Wilcox, R.E., Harding, T.P., Seely, D.R., 1973. Basic wrench tectonics. Am. Assoc. Pet. Geol. Bull. 57, 74–96.
Willett, S., Beaumont, C., Fullsack, P., 1993. Mechanical model for the tectonics of doubly vergent compressional orogens. Geology 21, 371–374.
Williams, N.R., Watters, T.R., Pritchard, M.E., Banks, M.E., Bell, J.F., 2013. Fault dislocation modeled structure of lobate scarps from Lunar Reconnaissance Orbiter Camera digital terrain models. J. Geophys. Res.: Planets 118, 224–233. https://doi.org/10.1002/Jgre.20051.
Williams, N.R., Bell, J.F., Watters, T.R., Banks, M.E., Daud, K., French, R.A., 2019. Evidence for recent and ancient faulting at Mare Frigoris and implications for lunar tectonic evolution. Icarus 326, 151–161.
Wilson, L., Head, J.W., 2017. Generation, ascent and eruption of magma on the Moon: new insights into source depths, magma supply, intrusions and effusive/explosive eruptions (Part 1: Theory). Icarus 283, 146–175.
Wu, H., Pollard, D.D., 1991. Fracture spacing, density and distribution in layered rock masses: results from a new experimental technique. In: Roegiers (Ed.), Rock Mechanics as a Multidisciplinary Science. Balkema, Rotterdam. ISBN90 6191 194 X.

Wu, H., Pollard, D.D., 1992. Propagation of a set of opening-mode fractures in layered brittle materials under uniaxial strain cycling. J. Geophys. Res. 97, 3381–3396.
Xue, Z., Lin, W., Chu, Y., Faure, M., Chen, Y., Ji, W., Qiu, H., 2021. An intracontinental orogen exhumed by basement-slice imbrication in the Longmenshan Thrust Belt of the Eastern Tibetan Plateau. Geol. Soc. Am. Bull. 134, 15–38. https://doi.org/10.1130/B35826.1.
Young, D.A., Hansen, V.L., 2005. Poludnista Dorsa, Venus: history and context of a deformation belt. J. Geophys. Res. 110, E03001. https://doi.org/10.1029/2004je002280.
Yue, Z., Li, W., Di, K., Liu, Z., Liu, J., 2015. Global mapping and analysis of lunar wrinkle ridges. J. Geophys. Res. Planet. 120, 978–994. https://doi.org/10.1002/2014JE004777.
Zhu, T., Zhang, J., Lin, Y., 2021. Ultra-thick paleoregolith layer detected by Lunar penetrating radar: implication for Fast Regolith Formation between 3.6 and 2.35 Ga. Geophys. Res. Lett. https://doi.org/10.1029/2021GL095282.
Zuber, M.T., 1987. Constraints on the Lithospheric structure of Venus from mechanical models and tectonic surface features. Proceedings Of The Seventeenth Lunar And Planetary Science Conference, Part 2. J. Geophys. Res. 92, E541–E551.
Zuber, M.T., Aist, L.L., 1990. The Shallow Structure of the Martian Lithosphere in the Vicinity of the Ridged Plains. J. Geophys. Res. 95, 14215–14230.
Zuber, M.T., Montési, L.G.J., Farmer, G.T., Hauck, S.A., Ritzer, J.A., Phillips, R.J., Solomon, S.C., Smith, D.E., Talpe, M.J., Head, J.W., Neumann, G.A., Watters, Thomas R., Johnson, C.L., 2010. Accommodation of lithospheric shortening on Mercury from altimetric profiles of ridges and lobate scarps measured during MESSENGER flybys 1 and 2. Icarus 209, 247–255.